A&A 582, A81 (2015)
DOI: 10.1051/0004-6361/201526604

Astronomy & Astrophysics

Gaia FGK benchmark stars: abundances of α and iron-peak elements⋆,⋆⋆

P. Jofré[1], U. Heiter[2], C. Soubiran[3], S. Blanco-Cuaresma[3,4], T. Masseron[1], T. Nordlander[2], L. Chemin[3], C. C. Worley[1], S. Van Eck[5], A. Hourihane[1], G. Gilmore[1], V. Adibekyan[6], M. Bergemann[1,7], T. Cantat-Gaudin[8], E. Delgado-Mena[6], J. I. González Hernández[15,16], G. Guiglion[9], C. Lardo[10], P. de Laverny[9], K. Lind[2], L. Magrini[11], S. Mikolaitis[9,12], D. Montes[15], E. Pancino[13,14], A. Recio-Blanco[9], R. Sordo[8], S. Sousa[6], H. M. Tabernero[15], and A. Vallenari[8]

[1] Institute of Astronomy, University of Cambridge, Madingley Road, Cambridge CB3 0HA, UK
e-mail: pjofre@ast.cam.ac.uk
[2] Department of Physics and Astronomy, Uppsala University, Box 516, 75120 Uppsala, Sweden
[3] Univ. Bordeaux, CNRS, Laboratoire d'Astrophysique de Bordeaux (UMR 5804), 33270 Floirac, France
[4] Observatoire de Genève, Université de Genève, 1290 Versoix, Switzerland
[5] Institut d'Astronomie et d'Astrophysique, U. Libre de Bruxelles, CP 226, Boulevard du Triomphe, 1050 Bruxelles, Belgium
[6] Instituto de Astrofísica e Ciências do Espaço, Universidade do Porto, CAUP, rua das Estrelas, 4150-762 Porto, Portugal
[7] Max-Planck Institute for Astronomy, 69117 Heidelberg, Germany
[8] INAF, Osservatorio di Padova, Università di Padova, Vicolo Osservatorio 5, Padova 35122, Italy
[9] Laboratoire Lagrange (UMR 7293), Univ. Nice Sophia Antipolis, CNRS, Observatoire de la Côte d'Azur, 06304 Nice, France
[10] Astrophysics Research Institute, Liverpool John Moores University, 146 Brownlow Hill, Liverpool L3 5RF, UK
[11] INAF/Osservatorio Astrofisico di Arcetri, Largo Enrico Fermi 5, 50125 Firenze, Italy
[12] Institute of Theoretical Physics and Astronomy, Vilnius University, A. Goštauto 12, 01108 Vilnius, Lithuania
[13] INAF–Osservatorio Astronomico di Bologna, via Ranzani 1, 40127 Bologna, Italy
[14] ASI Science Data Center, via del Politecnico s/n, 00133 Roma, Italy
[15] Dpto. Astrofísica, Facultad de CC. Físicas, Universidad Complutense de Madrid, 28040 Madrid, Spain
[16] Instituto de Astrofísica de Canarias, 38205 La Laguna, Tenerife, Spain

Received 26 May 2015 / Accepted 29 June 2015

ABSTRACT

Context. In the current era of large spectroscopic surveys of the Milky Way, reference stars for calibrating astrophysical parameters and chemical abundances are of paramount importance.
Aims. We determine elemental abundances of Mg, Si, Ca, Sc, Ti, V, Cr, Mn, Co, and Ni for our predefined set of *Gaia* FGK benchmark stars.
Methods. By analysing high-resolution spectra with a high signal-to-noise ratio taken from several archive datasets, we combined results of eight different methods to determine abundances on a line-by-line basis. We performed a detailed homogeneous analysis of the systematic uncertainties, such as differential versus absolute abundance analysis. We also assessed errors that are due to non-local thermal equilibrium and the stellar parameters in our final abundances.
Results. Our results are provided by listing final abundances and the different sources of uncertainties, as well as line-by-line and method-by-method abundances.
Conclusions. The atmospheric parameters of the *Gaia* FGK benchmark stars are already being widely used for calibration of several pipelines that are applied to different surveys. With the added reference abundances of ten elements, this set is very suitable for calibrating the chemical abundances obtained by these pipelines.

Key words. methods: data analysis – stars: atmospheres – Galaxy: abundances

1. Introduction

Much of our understanding of the structure and evolution of the Milky Way today comes from the analysis of large stellar spectroscopic surveys. After the low-resolution spectra from SDSS data (see Ivezić et al. 2012, for a review) revolutionised Galactic science, new surveys are on-going. They have a much higher resolution than SDSS, allowing to determine not only the stellar parameters of the stars more precisely, but also the chemical abundances of several individual elements. Examples of such projects are the *Gaia*-ESO Survey (GES; Gilmore et al. 2012; Randich et al. 2013), RAVE (Steinmetz et al. 2006), APOGEE (Allende Prieto et al. 2008), GALAH (De Silva et al. 2015), and the future billion of stars from the Radial Velocity Spectrograph (RVS) from *Gaia*. Furthermore, several groups have collected large samples of stars over the years, creating independent surveys for the same purpose of unraveling the structure and chemical enrichment history of our Galaxy (e.g. Fuhrmann 2011; Adibekyan et al. 2012; Ramírez et al. 2013; Bensby et al. 2014, and references therein).

⋆ Based on NARVAL and HARPS data obtained within the *Gaia* DPAC (Data Processing and Analysis Consortium) and coordinated by the GBOG (Ground-Based Observations for *Gaia*) working group and on data retrieved from the ESO-ADP database.
⋆⋆ Tables C.1–C.35 are only available at the CDS via anonymous ftp to cdsarc.u-strasbg.fr (130.79.128.5) or via http://cdsarc.u-strasbg.fr/viz-bin/qcat?J/A+A/582/A81

To parametrise these data properly in an automatic way and to link the data between the different surveys in a consistent way, good standard calibrators are needed. To this aim, we have defined a sample, the *Gaia* FGK benchmark stars (GBS), which includes 34 FGK stars of a wide range of metallicities and gravities. These stars are deemed to be representative of the different FGK stellar populations of the Galaxy. The sample is presented in Heiter et al. (2015a, hereafter Paper I), who determined effective temperature and surface gravity. Briefly, the GBS were chosen such that the angular diameter, bolometric flux, and distance of the stars are known. Angular diameters are known from interferometric observations for most of the stars with accuracies better than 1%; bolometric fluxes are known from integrations of the observed spectral energy distribution for most of the stars with accuracies better than 5%; and distances are known from parallaxes with accuracies better than 2%. The source and value for each star can be found in Paper I. This information allowed us to directly determine the temperature from the Stefan-Boltzmann relation. With $T_{\rm eff}$ and luminosity, the mass was determined homogeneously from stellar evolution models, and then the surface gravity using Newton's law of gravity (see Paper I for details).

The third main atmospheric parameter for the characterisation of stellar spectra is the metallicity, [Fe/H], which was determined from a spectroscopic analysis. Since the GBS are located in the northern and southern hemispheres, we built a spectral library collecting spectra with high resolution and high signal-to-noise ratio (S/N) (Blanco-Cuaresma et al. 2014b, hereafter Paper II). Using this spectral library, we determined the metallicity from iron lines (Jofré et al. 2014b, hereafter Paper III). In Paper III we combined the results of six different methods that used the same input atmosphere models and line list. Several studies in the literature report metallicities for the GBS, but as pointed out in Paper III, they have a large scatter that is due to the different methods and input data employed in the analyses. We determined the metallicity homogeneously, such that the [Fe/H] values for all stars can be used as reference in the same way. In addition to a final [Fe/H] value, we provided the results of each method for each star and spectral line. This makes the GBS excellent reference material when particular methods or spectral regions are being investigated. A summary of this series of papers and the parameters of the GBS can be also found in Jofré et al. (2014a).

The material of the GBS is already being used to evaluate and calibrate several methods to determine parameters. One example is the GES pipeline (Smiljanic et al. 2014; Recio-Blanco et al., in prep.), where the spectra of the GBS have been observed by the survey for this purpose (see also Pancino et al., in prep.; Randich et al. 2013, for calibration strategy of GES). In addition, De Pascale et al. (2014) recently used the GBS parameters to show consistency. This was part of the AMBRE project (de Laverny et al. 2013), which consists of determining stellar parameters of the ESO archive spectra. With the tools described in Paper II, we furthermore created GBS spectral libraries to render them in an SDSS-like data format; they were analysed by Schönrich & Bergemann (2014). We also created libraries to reproduce RAVE-like data, which helps to improve the analysis of metal-rich stars of the RAVE sample (Kordopatis 2014) and GALAH-like spectra, which were initially used to develop its pipeline. Some GBS have recently begun to be observed for GALAH with its own instrument (De Silva et al. 2015). In summary, the GBS are showing the potential to be excellent stars on which to cross-calibrate different survey data.

In this paper we present the next step in our analysis, which is the determination of individual abundances. The motivation for this is that high-resolution spectroscopic surveys determine not only the main stellar parameters automatically, but also individual abundances. Thus, a reference value for these abundances is needed. Since the GBS are well known, there is an extensive list of previous works that have measured individual abundances, but none of them have done it for the whole sample. Under the same argument as in Paper III (inhomogeneity in the literature), we determined the abundances in an homogeneous way for all the GBS.

We focus in this article on the abundance determination of the α elements Mg, Si, Ca, and Ti and the iron-peak elements Sc, V, Cr, Mn, Co, and Ni. There are two main reasons for starting with these elements. The first one is a practical reason: the data contain at least 12 spectral lines for each of the elements, which allow us to follow a similar procedure as in Paper III for deriving the iron abundances. The second reason is that α and iron-peak element are widely used for Galactic chemo-dynamical studies (see e.g. Bensby et al. 2014; Boeche et al. 2014; Jackson-Jones et al. 2014; Mikolaitis et al. 2014; Nidever et al. 2014, and references therein).

This article is organised as follows. In Sect. 2 we describe the data used in this work, which includes a brief description of the updates of our library and the atomic data considered for our analysis. In Sect. 3 we explain the methods and strategy employed in our work, that is, we describe the different methods used to determine the abundances considered here, as well as the analysis procedure employed by the methods. The analysis of our results and the abundance determination is explained in Sect. 4, while the several sources of systematic errors are described in Sect. 5, such as departures from non-local thermal equilibrium (NLTE) and uncertainties of the atmospheric parameters. We proceed in the article with a detailed discussion of our results for each individual element in Sect. 6. In Sect. 7 we summarise and conclude this work.

2. Spectroscopic data and input material

In this section we describe the data we employed in this analysis. By data we refer to the spectra (described in Sect. 2.1), the list of spectral lines (described in Sect. 2.2), and the atomic data and atmospheric models (described in Sect. 2.3).

2.1. Spectral library

As in our previous work on the subject, we built a library of high-resolution spectra of the GBS, using our own observations on the NARVAL spectrograph at Pic du Midi in addition to archived data. The different spectra were processed with the tools described in Paper II[1] and in Blanco-Cuaresma et al. (2014a). Briefly, the spectra were normalised, convolved to a common resolution, corrected for radial velocity, and re-sampled. The final library employed here differs from the 70 k library used in Paper III in the following aspects:

– *A new source of spectra*: ESPaDOnS spectra were retrieved from the PolarBase (Petit et al. 2014). They were ingested in our library in the same fashion as the standard spectra from HARPS, UVES, and NARVAL. The advantage of ESPaDOnS spectra is that the original spectra cover a very

[1] The spectral library can be downloaded from http://www.blancocuaresma.com/s/benchmarkstars/

wide wavelength range like those of NARVAL (they are the same spectrographs) and have high resolution and high S/N. Furthermore, we added the spectra from the atlas of Hinkle et al. (2000) for the Sun and Arcturus. Although the atlases were part of our library published in Paper II, they became available after the analysis of Paper III was carried out.

- *New processed spectra*: since the analysis of Paper III, the UVES advanced data archive has provided newly reduced spectra of all archive data in a homogenous fashion. We have updated our spectra considering this. In addition, new spectra of GBS have been taken with UVES over the past year, which we ingested in our library. In particular, the spectrum of α Cen A was kindly provided by Svetlana Hubrig before they were published in the ESO archives.
- *Wavelength coverage*: the spectral range of the HR21 Giraffe setup (~848–875 nm) was included in addition to the standard UVES 580 (~480–680 nm). The reason was that we wished to provide reference spectra and abundances in the wavelength range covered by the *Gaia*-RVS spectrograph and with Milky Way field targets of GES observed with Giraffe.
- *Telluric free:* The telluric lines in the HR21 range were removed from the spectra (R. Sordo, priv. comm.).
- *Resolution*: the data for this study at all wavelength ranges have a resolving power of $R = 65\,000$. This limit was set according to the ESPaDONs spectra, which have that resolution.
- *Normalisation:* The spectra were normalised using the newest normalisation routines of iSpec as described in Blanco-Cuaresma et al. (2014a).

The source of the spectrum used for each star is summarised in Table 1. For some stars we were unable to find a high-resolution spectrum in the HR21 range. As in Paper III, we selected our "favourite" spectra for each star based on visual criteria that in turn were based on continuum placement and telluric contamination. For the UVES-580 wavelength range, we took two spectra (UVES1 and UVES2 in Table 1) except for those cases where we had only one spectrum per star. There were three main reasons for choosing two spectra: (1) to cover the wavelength gap of the red and blue CCD of the UVES-580 setup with data of other spectrographs; (2) to determine abundances in telluric regions with more confidence; (3) as validation check for repeated lines, which must give same abundances regardless of the instrument. We chose only one spectrum per star in the red RVS wavelength range (HR21 in Table 1) because there are fewer high-resolution spectra available in this wavelength range. Furthermore, we note that the Sun as observed by HARPS has no date of observation. This spectrum is the co-addition of the three spectra of asteroids in the HARPS archive (see Paper II for details). For the star HD 84937 we used the UVES and the UVES-POP spectra, which were taken on the same night. This means that we analysed the same spectrum reduced with two different pipelines.

Table 1. Spectral source used for each star.

Star	UVES1	UVES2	HR21
18Sco	E (2005-06-20)	N (2012-03-10)	E (2005-06-20)
61 Cyg A	N (2009-10-16)	–	N (2009-10-16)
61 Cyg B	N (2009-10-13)	–	N (2009-10-13)
α Cen A	H (2005-04-19)	U (2000-04-11)	U (2012-01-20)
α Cen B	H (2005-04-08)	–	–
α Cet	U (2003-08-11)	N (2009-12-09)	N (2009-12-09)
α Tau	U (2004-09-24)	H (2007-10-22)	N (2009-10-26)
Arcturus	N (2009-12-11)	A (2000-01-01)	A (2000-01-01)
β Ara	H (2007-09-29)	–	–
β Gem	H (2007-11-06)	U (2008-02-25)	E (2007-12-29)
β Hyi	P (2001-07-25)	H (2005-11-13)	P (2001-07-25)
β Vir	E (2005-12-15)	H (2009-04-10)	E (2005-12-15)
δ Eri	P (2001-11-28)	–	P (2001-11-28)
ϵ Eri	H (2005-12-28)	P (2002-10-11)	P (2002-10-11)
ϵ For	H (2007-10-22)	–	–
ϵ Vir	E (2996-02-15)	H (2008-02-24)	N (2009-11-27)
η Boo	N (2009-12-11)	H (2008-02-24)	N (2009-12-11)
γ Sge	N (2011-09-30)	–	N(2011-09-30)
Gmb 1830	N (2012-01-09)	–	N (2012-01-09)
HD 107328	H (2007-10-22)	N (2009-11-26)	N (2009-11-26)
HD 122563	E (2006-02-16)	U (2002-02-19)	E (2006-02-16)
HD 140283	E (2011-06-12)	N (2012-01-09)	E (2011-06-12)
HD 220009	N (2009-10-16)	H (2007-10-22)	N (2009-10-16)
HD 22879	H (2007-10-22)	N (2009-11-27)	N (2009-11-27)
HD 49933	E (2005-12-18)	H (2011-01-05)	E (2005-12-18)
HD 84937	U (2002-11-28)	P (2002-11-28)	N (2012-01-08)
ξ Hya	E (2005-09-21)	H (2008-02-24)	E (2005-09-21)
μ Ara	H (2004-06-08)	U (2003-09-05)	U (2011-04-12)
μ Cas	N (2009-11-26)	–	N (2009-11-26)
μ Leo	E (2006-02-17)	N (2011-12-10)	E (2006-02-17)
Procyon	E (2005-12-14)	H (2007-11-06)	E (2005-12-14)
ψ Phe	H (2007-09-30)	U (2003-02-08)	–
Sun	H (–)	A (2000-01-01)	A (2000-01-01)
τ Cet	E (2005-09-21)	H (2008-09-09)	E (2005-09-21)

Notes. In parenthesis we list the observation date of the spectra, except for when the spectrum was the product of stacked spectra taken in different nights. N: Narval, U: UVES, E: ESPaDOnS, H: HARPS, P: UVES.POP, A: Atlas.

2.2. Line list

The elements to analyse were selected by the Porto and the Epinarbo methods (see Sects. 3.3.3 and 3.3.5, respectively), as described below. From the lines of the GES v4 line list (Heiter et al. 2015b), we rejected all those lines whose flag related to the atomic data quality was "N" (meaning that the transition probabilities are expected to have low accuracy and that the usage of these lines is not recommended). However, we allowed for lines for which the synthesis profile in the Sun and Arcturus were flagged with "N" (meaning that the line is strongly blended with line(s) of different species in both stars) since we work with stars that are different form the Sun and Arcturus, for which this line could have a better synthesis profile. For details of such flags, see Heiter et al. (2015b). In this article we focused on the ten α and iron-peak elements that have at least 12 spectral lines. The elements and numbers of initial lines are listed in Table 2. Table C.35 (available at the CDS) also contains the wavelength and atomic data of these lines.

2.2.1. Selection of lines in the 480–680 nm UVES range

The lines in this range were selected by the Epinarbo method (see Sect. 3.3.5) mainly on the basis of a statistical analysis of the DR1 UVES sample of the *Gaia*-ESO Survey (e.g. Magrini et al. 2014), which included 421 stars with recommended parameters (see Smiljanic et al. 2014). Equivalent widths (EWs) were measured in a homogeneous way with an automatic version of Daospec (DOOp, Cantat-Gaudin et al. 2014), and the

Table 2. Number of initially selected lines for each element.

Element	Atom	N lines
Mg	12	12
Si	14	15
Ca	20	25
Sc	21	17
Ti	22	68
V	23	30
Cr	24	25
Mn	25	13
Co	27	22
Ni	28	25

abundances were determined with the method FAMA (Magrini et al. 2013) for lines in the EW range of 15–100 mÅ. This range helps to avoid saturated lines and faint lines affected by noise. Then, the distribution of the deviations from the averaged abundance of each element were computed in all 421 stars. Finally, lines with a standard deviation within the corresponding 68.2% percentile were selected.

2.2.2. Selection of lines in the 848–875 nm HR21 range

This selection was made with the Porto method (see Sect. 3.3.3) where a selection of strong lines ($\log gf > -4$) was taken. We only considered unblended lines whose equivalent widths (EW) were potentially measurable by the ARES code (Sousa et al. 2007). Then, abundances were determined for these lines using a subset of GBS spectra in the HR21 wavelength range using the method described in Sect. 3.3.3 and the stellar parameters indicated in Paper III. The deviation for all the lines was calculated by comparing with the mean abundance. We rejected the lines that on average (for all the stars) gave abundances that differed from the mean abundance (derived by all the lines) by ±0.3 dex.

2.3. Atomic data and atmospheric models

The atomic data were taken from the fourth version of the line list created for the *Gaia*-ESO survey (Heiter et al. 2015b). Likewise, the atmospheric models are those employed by the analysis of the spectra in the *Gaia*-ESO survey. These are the MARCS models (Gustafsson et al. 2008), which are computed under the 1D-LTE assumption and assume the standard composition for α-enhancement with respect to iron abundance.

3. Analysis strategy

To determine individual abundances we employed a similar strategy as we used in Paper III, namely fixing the stellar parameters and using a pre-selection of lines that were analysed by different methods determining the abundances. The results were then combined on a line-by-line basis, and we finally computed the departures from NLTE.

3.1. Stellar parameters

The idea is to use the effective temperature and surface gravity from Paper I and the metallicity from Paper III as well as the averaged value for micro turbulence obtained by the different methods. The initial value of the macro turbulence was set to zero. The rotational velocity is the same value as we used in Paper III, which comes from the literature. To assess systematic errors we ran the same procedure several times, considering the uncertainties on the stellar parameters. These parameters are listed in Table 3.

It is important to mention here that [Fe/H], $T_{\rm eff}$ and $\log g$ are not entirely consistent between Papers I and III and this work because we are continuously improving them. The metallicity was determined in Paper III using a line list version for GES different from that used here. This probably does not significantly affect our results because changes between v3 and v4 of the GES line list have not been made for atomic data of iron. For β Ara, HD 140283, and HD 220009, new angular diameter measurements became available (by Creevey et al. 2015, for HD 140283; and by Thévenin et al., in prep. for β Ara and HD 220009) after the abundance results by the different methods (see Sect. 3.3) were provided, which explains the the differences in $T_{\rm eff}$ for these stars. However, as discussed in Paper I, the resulting $T_{\rm eff}$ values are still considered uncertain and were not recommended as reference values. Other stars with uncertain parameters were μ Ara, ψ Phe, and Gmb 1830. For HD 84937, a new parallax was published (VandenBerg et al. 2014) since the abundance results by the different methods were provided, explaining the difference in $\log g$. For Arcturus, the recommended $\log g$ is 1.6 ± 0.2, that is, the $\log g$ uncertainty is twice as large as what we considered here. Stars with uncertain $\log g$ values are ϵ For, μ Cas, τ Cet, HD 220009, β Ara, ψ Phe (see discussions in Paper I). Although the parameters slightly evolve throughout Papers I–III, the values employed are still within the errors, which is taken into account in our spectral analyses (see below). For consistency with Papers I–III, we here analyse the whole initial GBS sample, regardless of how uncertain the stellar parameters are and regardless of our suggestions made in Paper I to which stars should be treated as reference and which should not.

3.2. Runs

The different analysis runs were identical except for the input parameters. For each run we fixed all parameters ($T_{\rm eff}$, $\log g$, [Fe/H], $v_{\rm mic}$, $v \sin i$), as indicated in Table 3. Macroturbulence was determined together with the abundances for the analyses that make on-the-fly syntheses. Some methods re-normalised and shifted the spectra in radial velocity to improve their results. The different analysis runs are described below:

- *Run – all*: main run: determination of individual abundances of all lines and all spectra using the main stellar parameters of the input table.
- *Run – LTE*: like before, but using the metallicity value obtained before NLTE corrections (i.e. the input of [Fe/H] – LTE, see Table 3). This run allowed us to quantify this effect in the abundances.
- *Run–errors*: as *Run–all,* but considering the error on the stellar parameters as determined for the metallicity in Paper III.

3.3. Methods for determining the abundances

Eight methods were used to determine the abundances and are briefly described in this section. Most of the methods were employed in the metallicity determination of Paper III and in the determination of $T_{\rm eff}$, $\log g$, and abundances within the *Gaia*-ESO Survey for the UVES data (WG11 pipeline, see Smiljanic et al. 2014, for details). A summary of the methods can be found in Table 4, and they are briefly explained below.

Table 3. Values of stellar and broadening parameters considered for the abundance determination.

Star	$T_{\rm eff} \pm \Delta T_{\rm eff}$ [K]	$\log g \pm \Delta \log g$ (dex)	[Fe/H] $\pm$ Δ[Fe/H] (dex)	$v_{\rm mic} \pm \Delta v_{\rm mic}$ [km s^{-1}]	[Fe/H]$_{\rm LTE}$ (dex)	$v \sin i$ [km s^{-1}]
18 Sco	5810 ± 80	4.44 ± 0.03	0.03 ± 0.03	1.07 ± 0.20	0.01	2.2
61 Cyg A	4374 ± 22	4.63 ± 0.04	–0.33 ± 0.38	1.07 ± 0.04	–0.33	0.0
61 Cyg B	4044 ± 32	4.67 ± 0.04	–0.38 ± 0.03	1.27 ± 0.36	–0.38	1.7
α Cen A	5792 ± 16	4.30 ± 0.01	0.26 ± 0.08	1.20 ± 0.07	0.24	1.9
α Cen B	5231 ± 20	4.53 ± 0.03	0.22 ± 0.10	0.99 ± 0.31	0.22	1.0
α Cet	3796 ± 65	0.68 ± 0.29	–0.45 ± 0.47	1.77 ± 0.40	–0.45	3.0
α Tau	3927 ± 40	1.11 ± 0.15	–0.37 ± 0.17	1.63 ± 0.30	–0.37	5.0
Arcturus	4286 ± 35	1.64 ± 0.06	–0.52 ± 0.08	1.58 ± 0.12	–0.53	3.8
β Ara	4173 ± 64	1.04 ± 0.15	–0.05 ± 0.39	1.88 ± 0.46	–0.05	5.4
β Gem	4858 ± 60	2.90 ± 0.06	0.13 ± 0.16	1.28 ± 0.21	0.12	2.0
β Hyi	5873 ± 45	3.98 ± 0.02	–0.04 ± 0.06	1.26 ± 0.05	–0.07	3.3
β Vir	6083 ± 41	4.10 ± 0.02	0.24 ± 0.07	1.33 ± 0.09	0.21	2.0
δ Eri	4954 ± 26	3.75 ± 0.02	0.06 ± 0.05	1.10 ± 0.22	0.06	0.7
ϵ Eri	5076 ± 30	4.60 ± 0.03	–0.09 ± 0.06	1.14 ± 0.05	–0.10	2.4
ϵ For	5123 ± 78	3.52 ± 0.07	–0.60 ± 0.10	1.04 ± 0.13	–0.62	4.2
ϵ Vir	4983 ± 61	2.77 ± 0.02	0.15 ± 0.16	1.39 ± 0.25	0.13	2.0
η Boo	6099 ± 28	3.80 ± 0.02	0.32 ± 0.08	1.52 ± 0.19	0.30	12.7
γ Sge	3807 ± 49	1.05 ± 0.34	–0.17 ± 0.39	1.67 ± 0.34	–0.16	6.0
Gmb 1830	4827 ± 55	4.60 ± 0.03	–1.46 ± 0.39	1.11 ± 0.57	–1.46	0.5
HD 107328	4496 ± 59	2.09 ± 0.14	–0.33 ± 0.16	1.65 ± 0.26	–0.34	1.9
HD 122563	4587 ± 60	1.61 ± 0.07	–2.64 ± 0.22	1.92 ± 0.11	–2.74	5.0
HD 140283	5514 ± 120	3.57 ± 0.12	–2.36 ± 0.10	1.56 ± 0.20	–2.43	5.0
HD 220009	4275 ± 54	1.47 ± 0.14	–0.74 ± 0.13	1.49 ± 0.14	–0.75	1.0
HD 22879	5868 ± 89	4.27 ± 0.03	–0.86 ± 0.05	1.05 ± 0.19	–0.88	4.4
HD 49933	6635 ± 91	4.20 ± 0.03	–0.41 ± 0.08	1.46 ± 0.35	–0.46	10.0
HD 84937	6356 ± 97	4.15 ± 0.06	–2.03 ± 0.08	1.39 ± 0.24	–2.09	5.2
ξ Hya	5044 ± 38	2.87 ± 0.02	0.16 ± 0.20	1.40 ± 0.32	0.14	2.4
μ Ara	5902 ± 66	4.30 ± 0.03	0.35 ± 0.13	1.17 ± 0.13	0.33	2.2
μ Cas	5308 ± 29	4.41 ± 0.01	–0.81 ± 0.03	0.96 ± 0.29	–0.82	0.0
μ Leo	4474 ± 60	2.51 ± 0.09	0.25 ± 0.15	1.28 ± 0.26	0.26	5.1
Procyon	6554 ± 84	3.99 ± 0.02	0.01 ± 0.08	1.66 ± 0.11	–0.04	2.8
ψ Phe	3472 ± 92	0.51 ± 0.18	–1.24 ± 0.39	1.75 ± 0.33	–1.23	3.0
Sun	5777 ± 1	4.44 ± 0.00	0.0300 ± 0.05	1.06 ± 0.18	0.02	1.6
τ Cet	5414 ± 21	4.49 ± 0.01	–0.49 ± 0.03	0.89 ± 0.28	–0.50	0.4

Notes. Effective temperature and surface gravity is derived from fundamental laws (see Paper I for details). Metallicity and microturbulence velocity were derived consistent with these parameters in Paper III. [Fe/H] uncertainties were obtained by quadratically summing all σ and Δ columns in Table 3 of Paper III. In addition, we list the metallicity value before the correction for NLTE effects, which is used in one of the analysis runs (see Sect. 3.2). The rotational velocity is taken from the literature (see Paper III for the corresponding references).

Table 4. Summary of methods employed to determine the abundances in this work.

Name	Approach	Radiative transfer code	Wrapper
iSpec	synth	SPECTRUM	iSpec
ULB	synth/EW	Turbospectrum	BACCHUS
Porto	EW	MOOG	
Bologna	EW	SYNTHE	GALA
Epinarbo	EW	MOOG	FAMA
GAUGUIN	synth	Turbospectrum	
Synspec	synth	Turbospectrum	
UCM	EW	MOOG	StePar

Notes. The name of the method, the approach (EW: equivalent width, synth: synthesis), the radiative transfer code employed and the wrapper code that uses the radiative transfer code (if applicable) are indicated.

3.3.1. iSpec

iSpec (Blanco-Cuaresma et al. 2014a) is a spectroscopic framework that implements routines for the determination of chemical abundances by using the spectral fitting technique. Given a set of atmospheric parameters, atomic data, and wavelength ranges, iSpec generates synthetic spectra on the fly and minimises the difference with the observed spectra by applying a least-squares algorithm.

We developed a completely automatic pipeline to analyse the GBS. Each absorption line of each spectrum was analysed separately by the same homogeneous process. Even though iSpec includes routines for identifying unreliable or doubtful solutions, we did not apply any automatic filtering to facilitate the comparison with the rest of the methods.

3.3.2. ULB

The Brussels Automatic Code for Characterising High accUracy Spectra (BACCHUS) consists of three different modules that are designed to derive EWs, stellar parameters, and abundances. For the purpose of this paper, only the modules for measuring abundances and EWs were used. The current version relies on the radiative transfer code Turbospectrum (Alvarez & Plez 1998; Plez 2012). This method has been employed in Paper III and for the WG11 pipeline.

With fixed stellar parameters, the first step consists of determining average line-broadening parameters (i.e. macroturbulence parameter in the present case) using a selection of clean

Fe lines. For each element and each line, the abundance determination module then proceeds in the following way: (i) a spectrum synthesis, using the full set of (atomic and molecular) lines, is used to find the local continuum level (correcting for a possible spectrum slope); (ii) cosmic and telluric rejections are performed; (iii) the local S/N is estimated; (iv) a series of flux points contributing to a given absorption line is selected. Abundances are then derived by comparing the observed spectrum with a set of convolved synthetic spectra characterised by different abundances. Four different diagnostics are used: line-profile fitting, core line intensity comparison, global goodness-of-fit estimate, and EW comparison. Each diagnostic yields validation flags. Based on these flags, a decision tree then rejects the line or accepts it, keeping the best-fit abundance.

One supplementary asset of the code is that it computes EWs. They are computed not directly on the observed spectrum, but internally from the synthetic spectrum with the best-fit abundance. This way, we have access to the information about the contribution of blending lines, allowing a clean computation of the equivalent width of the line of interest.

3.3.3. Porto

Porto employes ARES (Sousa et al. 2007) to measure EWs (automatically normalising the spectra) and MOOG (Sneden 1973) to derive abundances. For refractory element abundances (from Na to Ni), the fast rotator η Boo and stars with $T_{\rm eff} < 4200$ K were rejected (the EWs computed with ARES for these stars usually are poor). This method has been employed in Paper III and for the WG11 pipeline.

3.3.4. Bologna

The Bologna analysis is based on the same method as in Paper III. It has also been used in the WG11 pipeline. In particular, we ran DAOSPEC (Stetson & Pancino 2008) to measure EWs through DOOp (Cantat-Gaudin et al. 2014) until the input and output FWHM of the absorption lines agreed within 3%. The abundance analysis was carried out with GALA (Mucciarelli et al. 2013), an automatic program for determining atmospheric parameter and chemical abundance from atomic lines based on the SYNTHE code (Kurucz 2005). To provide measurements for all the selected lines, discrepant lines with respect to the fits of the slopes of Fe abundance versus EW, excitation potential, and wavelength were rejected with a very large 5σ cut. All stars and elements were analysed in this fashion.

3.3.5. Epinarbo

This method is based on EWs from DOOp, which are measured in a way similar to the Bologna method (see above). The abundance is determined with the code FAMA (Magrini et al. 2013), which is based on MOOG. This method has been employed in Paper III and for the WG11 pipeline.

FAMA can determine the stellar parameter or work with fixed parameters and return elemental abundances. In this analysis all parameters were kept fixed, including the microturbulent velocity. We provided abundances for all the selected lines that were detected. No abundance was returned if the line was detected but its EW was smaller than 5 mÅ or larger than 140 mÅ to avoid measurement errors associated with very weak or very strong lines.

3.3.6. Nice/GAUGUIN

For a given benchmark star, we first assumed an [α/Fe] enrichment consistent with the typical properties of Milky Way stars. We then normalised the observed spectrum by (i) linearly interpolating a synthetic spectrum in the GES synthetic spectra grid[2]; (ii) estimating a ratio between the synthetic flux and the observed one over a spectral range of 20 Å, centred on the interested line; and (iii) by fitting this ratio by a polynomial function. Finally, the observed spectra were divided by the polynomial fit to adjust its continuum.

The individual chemical abundances were then derived as follows: (i) 1D synthetic spectra grids for each stars were built from the initial 4D GES grid. These grids in the searched chemical abundances were cut around the analysed spectral line. To derive the iron-peak species, in practice we linearly interpolated the GES grid on $T_{\rm eff}$, $\log g$, and [α/Fe]. For the α element cases, we linearly interpolated this grid on $T_{\rm eff}$, $\log g$, and [M/H]. (ii) Then, we determined the smallest difference between the observed spectrum and the 1D synthetic spectra grids. (iii) The solution was finally refined with the Gauss-Newton algorithm GAUGUIN (Bijaoui et al. 2012).

3.3.7. Nice/Synspec

We adopted the recent version (v12.1.1) of the spectrum synthesis code Turbospectrum (Plez 2012). This pipeline determines the continuum in two steps. First, it takes the normalised spectra from the library. Second, it locally adjusts the continuum in the region (±5 Å) around every line of interest. This was done by selecting the possible line-free zones of the synthetic spectrum, defined as regions where the intensity of the synthetic spectrum is depressed by less than 0.02. If the possible line-free zones were too narrow or did not exist, we iteratively searched for the possible less contaminated zones in the synthetic spectrum. We finally determined abundances with the method described in Mikolaitis et al. (2014). This method has been employed in the WG11 pipeline.

3.3.8. UCM

This method is based on EWs, has been used in Paper III, and is part of the WG11 GES pipeline. Different line selections were considered for different stars. The division of stars was based on metallicity and surface gravity. Metallicity was divided into metal-rich ([Fe/H] ≥ -0.30), metal-poor ($-0.30 <$ [Fe/H] ≥ -1.50), and very metal-poor ([Fe/H] < -1.50). Surface gravity was divided into giants ($\log g < 4.00$) and dwarfs ($\log g \geq 4.00$). However, we decided to merge the very metal poor stars ([Fe/H] < -1.50) into one single region. The EWs were measured using TAME (Kang & Lee 2012). We followed the approach of Kang & Lee (2012) to adjust the *rejt* parameter of TAME according to the S/N of each spectrum. The abundance analysis was carried out using a wrapper program for MOOG to take care of the elemental abundances automatically; the program is based on StePar (see Tabernero et al. 2012). We also rejected outliers for lines that deviated by more than three of the standard deviation.

[2] Synthesised with the GES v4 line list and convolved to the observed resolution and to the rotational velocity of the star, more details on the grid computation are provided in de Laverny et al. (2012).

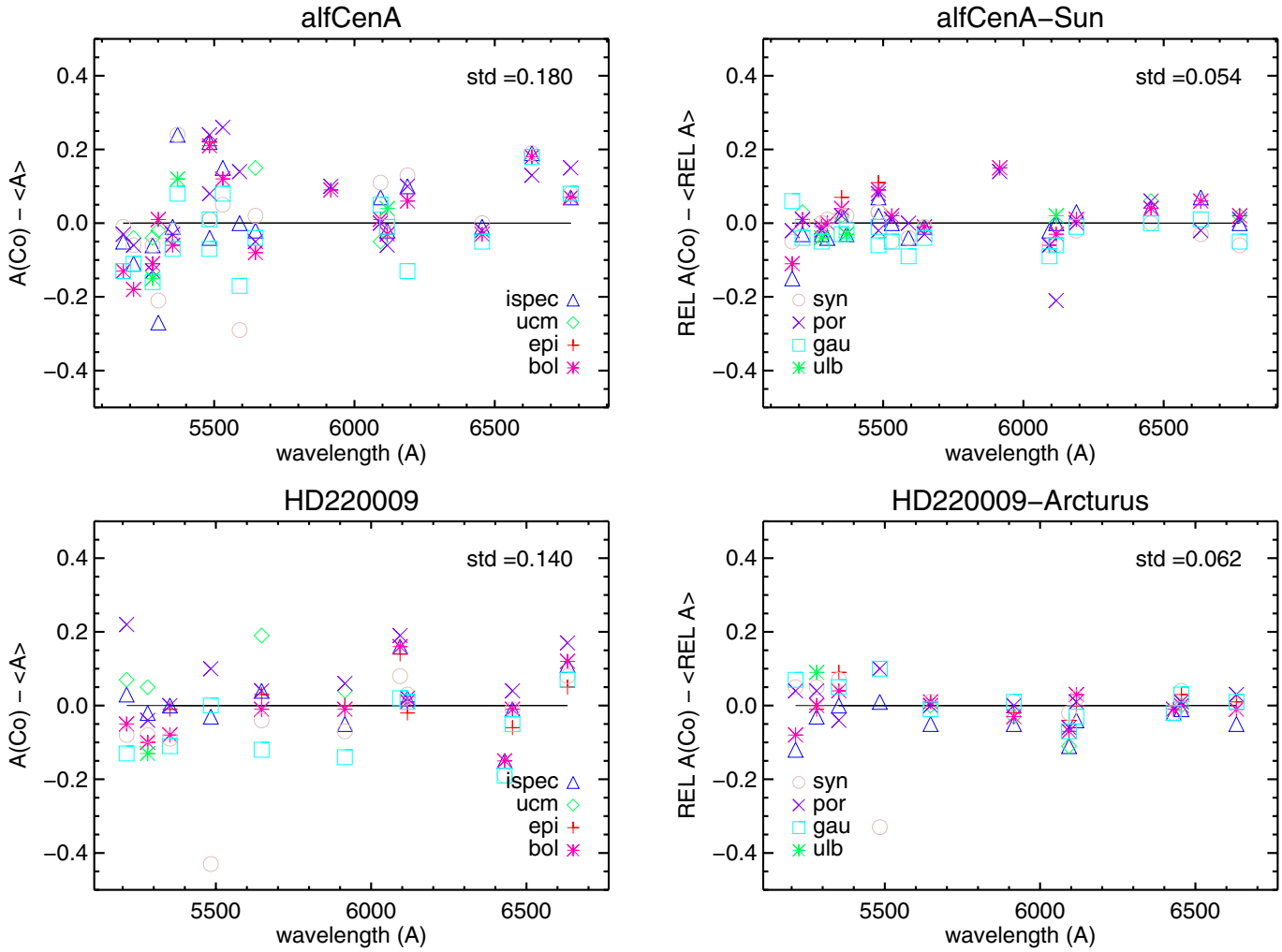

Fig. 1. Abundances of Co on a line-by-line and method-by-method basis as a function of wavelength. Colours and symbols represent the different methods, which are indicated in the legend. *Top panels*: absolute abundance (*left*) and abundance relative to the Sun (*right*) of the star α Cen A. *Bottom panels*: absolute abundance (*left*) and abundance relative to Arcturus (*right*) of the star HD 220009. The horizontal line represents the mean of all abundances with its standard deviation indicated at the *top right* of each panel.

4. Elemental abundances determination

Following Paper III, we firstly selected only lines with $-6.0 < \log(EW/\lambda) < -4.8$ (which helps to avoid very weak lines or saturated lines) and grouped the stars into metal-poor, FG-dwarfs[3], FGK-giants, M-giants, and K-dwarfs. Furthermore, to avoid effects due to normalisation or bad employment of atomic data, we performed a differential abundance analysis. For this, we chose one reference star in each of the groups, which were HD 22879, the Sun, Arcturus, α Tau, and 61 Cyg A, respectively. We searched for the lines in the allowed EW range analysed by each method for the reference star and then selected common lines for that method in the rest of the stars in that group. This provided differential abundances for each individual method, which we then combined with a much lower dispersion on a line-by-line and method-by-method basis instead of using absolute abundances. The advantage of using differential abundances for Milky Way studies with elemental abundances has been discussed for instance in Smiljanic et al. (2007), Ramírez & Allende Prieto (2011) and Feltzing & Chiba (2013).

[3] The subgiants (cf. Paper I) are included in the group of FG-dwarfs in this work.

One example of differential abundance results obtained on a line-by-line and method-by-method basis is shown in Fig. 1. We plot the results of individual line abundances of Co as a function of wavelength for all methods in different colours and symbols. For better visualisation of the symbol definition in the figure, the legend is split in the two panels. The top panels illustrate an example of an FG-dwarf star, α Cen A, which has the Sun as reference star. The bottom panels illustrate an example of an FGK-giant star, HD 220009, which has Arcturus as reference star. The left panels show the absolute abundances minus the mean of all abundances, while the right panels show the relative abundance with respect to the reference minus its mean. The standard deviation of this mean is indicated at the top right side of each panel. We only plot these relative abundances with respect to the mean for illustration purposes, aiming at keeping the same scale in both cases. This allows us to focus on the dispersion of each case. The scatter of different methods for individual lines considerably decreases from absolute to relative abundances. This mostly reflects on the removal of method-to-method systematic errors such as the approaches to normalise the data. In addition, we note that some absolute abundances agree well between methods, but deviate significantly from the mean. One example

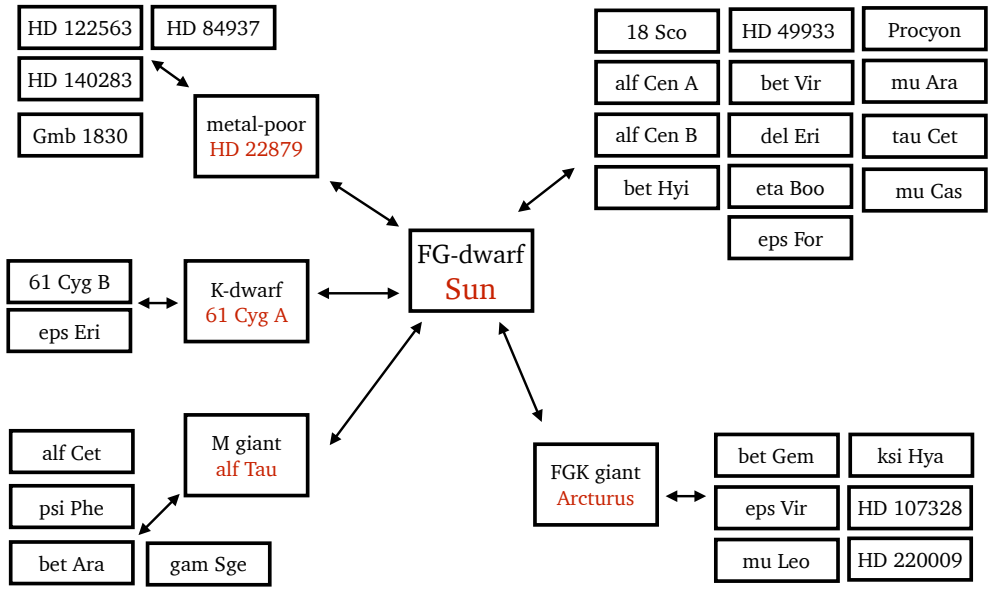

Fig. 2. Schematic picture of how the GBS are differentiated against each other. Stars are associated in five different groups according to their spectral type. One star is chosen as a reference for each group (in red). The rest of the stars in that group is analysed with respect to the reference star, and are connected with arrows. The reference stars are finally analysed with respect to the Sun, which is the zero point.

is the reddest Co line, which for both stars yields higher absolute abundances than the mean. This would suggest a revision of the atomic data, in particular of $\log gf$. When using differential abundances, this line yields abundances that agree better with the mean.

Since our abundances are relative to a reference star in each group, we needed to determine the abundances of these reference stars separately. This was also done in a differential way with respect to the Sun. This implies that not all available lines were used, but only those for which reliable EWs could be measured in the spectra of both the reference star and the Sun. This strategy is extensively discussed in the following section.

We show a scheme of the differential analysis we employed in Fig. 2. The zero point is the Sun, for which we determined absolute abundances. The lines and atomic data for the Sun were carefully inspected, as discussed in Heiter et al. (2015b). The first group of FG-dwarfs was analysed with respect to the Sun by differentiating the abundances obtained by each method for each line. This group contains the stars indicated at the top right of the scheme. The other reference stars, which are depicted in red in the large boxes in the figure, were also analysed by differentiating between common lines with respect to the Sun in the same way as all the stars from the FG-dwarfs group. Finally, the rest of the stars were analysed with respect to the reference stars of each of the groups. In summary, all groups of stars except for the FG-dwarfs were analysed in a two-step approach, differentiating the stars with respect to a representative reference star, which was then analysed with respect to the Sun.

4.1. Analysis of reference stars

The Sun and the rest of the reference stars are very different from each other, which meant that there were very few common lines in some cases. This issue is of crucial importance for our final results. To achieve the best homogeneity, having the Sun for zero point and employing a differential analysis in steps for the rest of the stars is the best way to proceed. In this section we compare this approach with the direct determination of absolute abundances for the reference stars. We show that similar mean abundances are derived and that the homogeneous/differential approach, although with significant loss of lines in some cases, is the best possible one for our purpose.

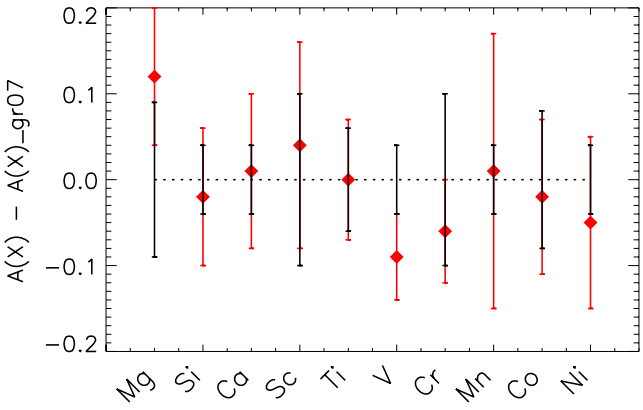

Fig. 3. Difference between abundances of the Sun obtained by us and by Grevesse et al. (2007), displayed with a red diamond. The red error bars correspond to our line-to-line scatter, while the black error bars are the uncertainties listed in Table 1 of Grevesse et al. (2007).

4.1.1. Solar abundances

We defined the Sun as our zero point, for which we needed to determine the abundances in an absolute way. For this, we used all lines with $-6.0 < \log(EW/\lambda) < -4.8$ from all methods and defined the final abundance to be the median of all abundances, after $1.5\sigma-$clipping of all abundances. This rejects less than 10% of the total measurements in most cases.

The comparison of our abundances including the line-to-line standard deviation and the solar abundance of Grevesse et al. (2007) is displayed in Fig. 3. We compare our abundances with the solar abundances of Grevesse et al. (2007) because these are the solar abundances employed for the chemical analyses of the *Gaia*-ESO Survey (see e.g. Smiljanic et al. 2014). In the figure, we plot the difference of our results from the values of Grevesse et al. (2007) with red diamonds, while in black we plot only

Table 5. Final absolute abundances for the Sun obtained in this work (here), where the standard deviation on a line-by-line basis is indicated as σ.

Element	$\log \epsilon_{\rm here}$	$\sigma_{\rm here}$	$\log \epsilon_{\rm G07}$	$\sigma_{\rm G07}$
Mg	7.65	0.08	7.53	0.09
Si	7.49	0.08	7.51	0.04
Ca	6.32	0.09	6.31	0.04
Ti	4.90	0.07	4.90	0.06
Sc	3.22	0.14	3.17	0.10
V	3.93	0.04	4.00	0.04
Cr	5.58	0.06	5.64	0.10
Mn	5.30	0.09	5.39	0.04
Co	4.89	0.09	4.92	0.08
Ni	6.18	0.10	6.23	0.04

Notes. For comparison, we list the abundances of Grevesse et al. (2007, G07) with their reported error in the last two columns.

the errors of Grevesse et al. (2007). Our values were obtained under LTE, which might cause some of the slight discrepancies seen in the figure. Within the errors, our abundances agree well with those of Grevesse et al. (2007) except for vanadium. But our results for V agree well with Battistini & Bensby (2015). As extensively discussed for example in Lawler et al. (2014), the optical lines of V I are among the weakest lines produced by Fe-peak elements in the Sun (most of them with $\log(EW/\lambda) < -6$) partly because of the slight underabundance of V with respect to other Fe-peak elements in the Sun.

The line-to-line scatter of some elements is quite large. The odd-Z elements V, Sc, Mn, and Co are affected by hyperfine structure splitting (hfs; for a recent discussion see Battistini & Bensby 2015). None of the EW methods considered hfs in the abundance determination, which could be translated into greater abundances from the derived EW in some lines. The synthesis methods ULB, GAUGUIN, and Synspec considered hfs in the line modelling, while iSpec did not. If only methods that consider hfs are taken into account, the Mn abundance of the Sun decreases from 5.43 to 5.30. The latter value differs more strongly from the value of Grevesse et al. (2007) and subsequent papers on solar abundances, such as Asplund et al. (2009) and Scott et al. (2015), which derived 0.09 dex higher, but it agrees well with Battistini & Bensby (2015). Our values and those of Battistini & Bensby (2015) were derived under LTE considerations, whereas Grevesse et al. (2007), Asplund et al. (2009), and Scott et al. (2015) consider NLTE. An extensive discussion of the effects of hfs is found in Sect. 4.3.

Figure 3 also shows a large scatter of Sc. Based on the discussion in Sect. 4.3, we cannot attribute this to a hfs effect. The scatter in this case instead probably comes from an NLTE effect, which can produce departures of up to 0.2 dex in the abundances obtained for the Sun from neutral and ionised lines (Zhang et al. 2008). We used both ionisation stages to determine the abundances of Sc. Each element is discussed extensively in Sect. 6.

The final absolute abundances for the Sun are listed in Table 5. The horizontal line divides the α elements (top) and the iron-peak elements (bottom). The measurements of individual lines can be found Table C.33 (available at the CDS) for the Sun. The values listed for Sc, V, Mn, and Co only consider the results from ULB, GAUGUIN, and Synspec, which is diffferent from the values plotted in Fig. 3 for the discussion, which consider the measurements of all methods.

4.1.2. Differential vs. absolute approach of reference stars

Employing the differential strategy of reference stars with respect to the Sun meant that a considerable number of lines had to be discarded in some cases. The few lines left were carefully checked to have a few, but reliable lines for the differential abundance of the reference stars. We studied the effects of our differential analysis of stars that have very different spectra, such as the reference stars with respect to what would be the "standard" analysis, namely the abundance determination considering the direct measurements of all methods. In this case, we relaxed our line-strength criterion to enhance the number of overlapping lines between the reference stars. We selected lines with a reduced equivalent width of $-6.5 < \log(EW/\lambda) < -4.7$, that is, we allowed for slightly weaker and slightly stronger lines than for the differential analysis of one group of stars. For Mn we even allowed for stronger lines ($\log(EW/\lambda) < -4.6$) to have more lines to analyse. The standard abundances were calculated using 1.5σ clipping of all measurements of all methods, in the same fashion as for the Sun.

The comparison of abundances for both approaches (standard v/s differential) is displayed in Fig. 4 for all reference stars and elements. To obtain the absolute abundances with the differential approach, we added the results obtained for the Sun listed in Table 5 to the final differential abundances. The error bars in black around the zero line represent the standard deviation of the line-by-line scatter of the standard measurements of all methods (std in the figure). The difference between the standard and the differential (dif in the figure) final abundances is indicated with red diamonds in the figure, with the error bar corresponding to the line-by-line scatter. Each element is indicated at the bottom of the panel, and each panel represents one reference star, with its name and its group indicated as title. At the top of each panel we plot two sequences with numbers. They correspond to the number of lines used to determine the abundances in each approach. The upper sequence indicates the number of lines used for the standard approach, while the lower sequence indicates the number of lines used for the differential approach.

From Fig. 4 we can see that the line-by-line dispersion significantly decreases when the differential approach is used to determine the final abundances. The differences of the final values in both approaches is also within the errors. This suggests that the differential approach provides reliable final abundances while improving the internal precision due to systematic uncertainties in the methods and the atomic data.

The number of lines used in the differential approach drops in almost every case, as expected because the allowed strength of the line needs to be satisfied in both the Sun and the reference star. For Arcturus, 61 Cyg A, and HD 22879, the number of lines lost with the differential analysis is minimal in most cases, whereas for α Tau the loss can be significant. This is expected because spectra of cool giants are extremely different from the solar spectrum.

4.1.3. Summary

To summarise, the differential approach in two steps for FGK-giants, K-dwarfs and metal-poor, namely one differential step with respect to Arcturus, 61 Cyg A and HD 22879, respectively, and a second one with respect to the Sun, is better than the standard approach of taking all absolute abundances and performing σ clipping. This is because without loosing too many lines, we are able to retrieve abundances with the same absolute value yet better precision.

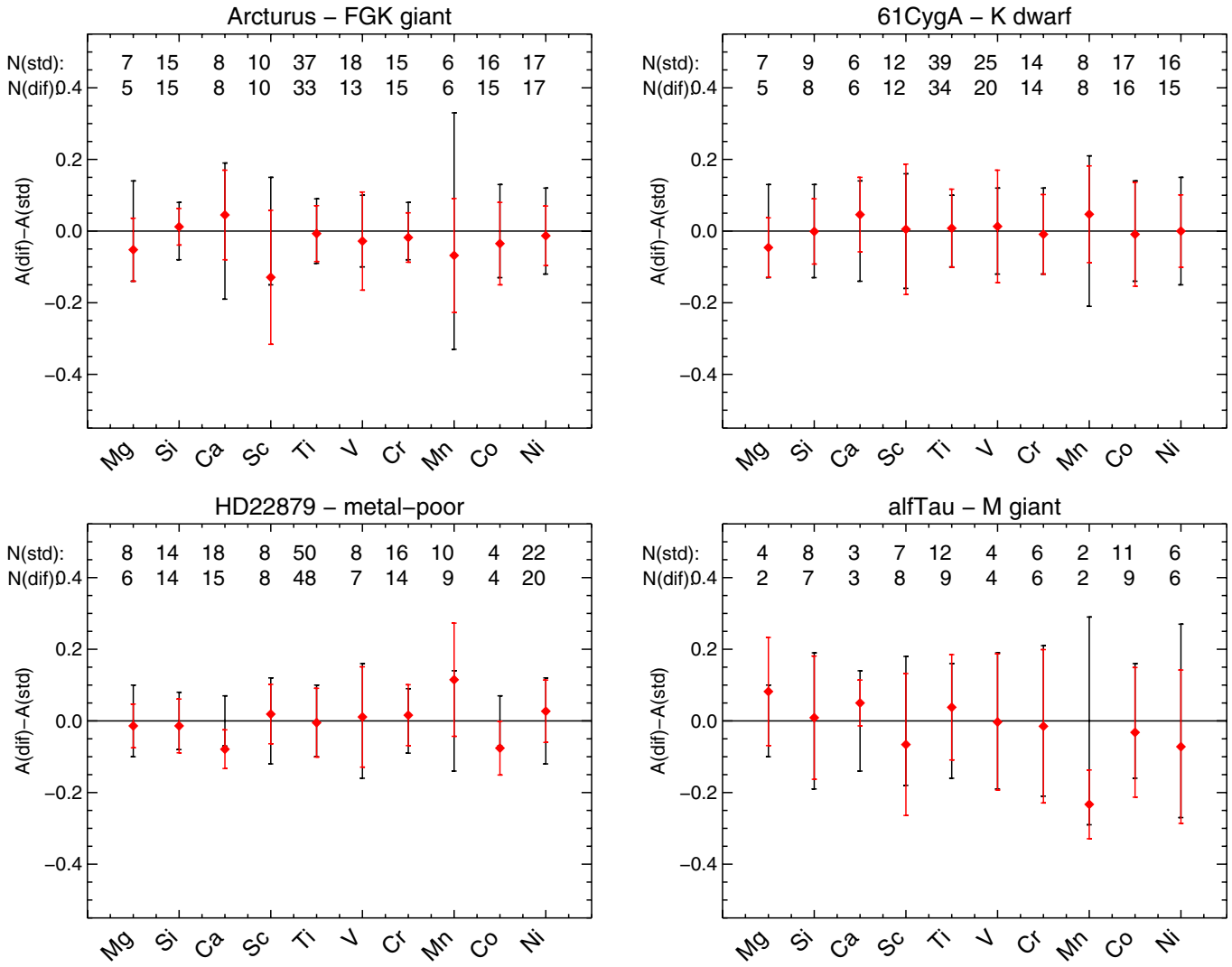

Fig. 4. Line-to-line abundance scatter of the reference stars determined directly from the absolute values obtained from all methods, indicated with black error bars (std). Red diamonds represent the difference of these abundances with respect to the final abundances obtained by performing a differential analysis with respect to the Sun (dif), with the error bar representing the line-to-line scatter. At the top of each panel we report the number of lines used for the determination of the abundances with both approaches.

The two-step differential approach for M-giants is less obvious because strong lines for the Sun might be saturated or blended for α Tau due to the difference in effective temperature of about 2000 K and gravity of 3.5 dex. The lines used to determine abundances were carefully inspected for blends and normalisation problems. These few overlapping lines between the Sun and α Tau are able to provide more accurate abundances without affecting the final absolute abundance significantly. There is one exceptional case where no overlapping lines were found: V. For V, four clean lines could be used that are not detectable in the Sun, yielding relatively consistent results between different methods. The Mn line at λ5004 Å lacks a good continuum in its vicinity. Thus, the absolute abundance obtained for this line gave very different results for each method, which can be noted from the large error bar; it should be treated with care.

It is important to discuss here that the reference star of the metal-poor group was chosen to be the most metal-rich star because it provided a better link between the Sun and the rest of the metal-poor stars. We performed similar differential tests with the star HD 140283 ([Fe/H] ~ −2.5) and the Sun and found that most of the lines were lost, either because they were too weak in the metal-poor star or saturated in the Sun. Furthermore, no V and Co lines were visible in our spectral range for HD 140283. This implies that when using HD 140283 as reference, no V and Co abundances could be provided for any star in the metal-poor group. The few lines left for the rest of the elements (varying normally from 1 to 3) were so weak that only synthesis methods could provide abundances, which were very uncertain, mostly due to different normalisation placements.

To conclude, the absolute abundances of the Sun provide the zero point for all abundances of the reference benchmark stars of all groups, where a reference star was used to differentiate with respect to the Sun, except for the FG-dwarfs, for which the reference star was directly the Sun. The abundance of V for M-giants needs a special treatment as no common good lines of V in the reference star and the Sun could be found. In this case, the zero point for V was the abundance of α Tau (see below).

4.1.4. Vanadium for α Tau

The lines λ5592, λ5632, λ6002, and λ6565 Å are clean lines (not blended by molecules) in this cool giant, which can be used to

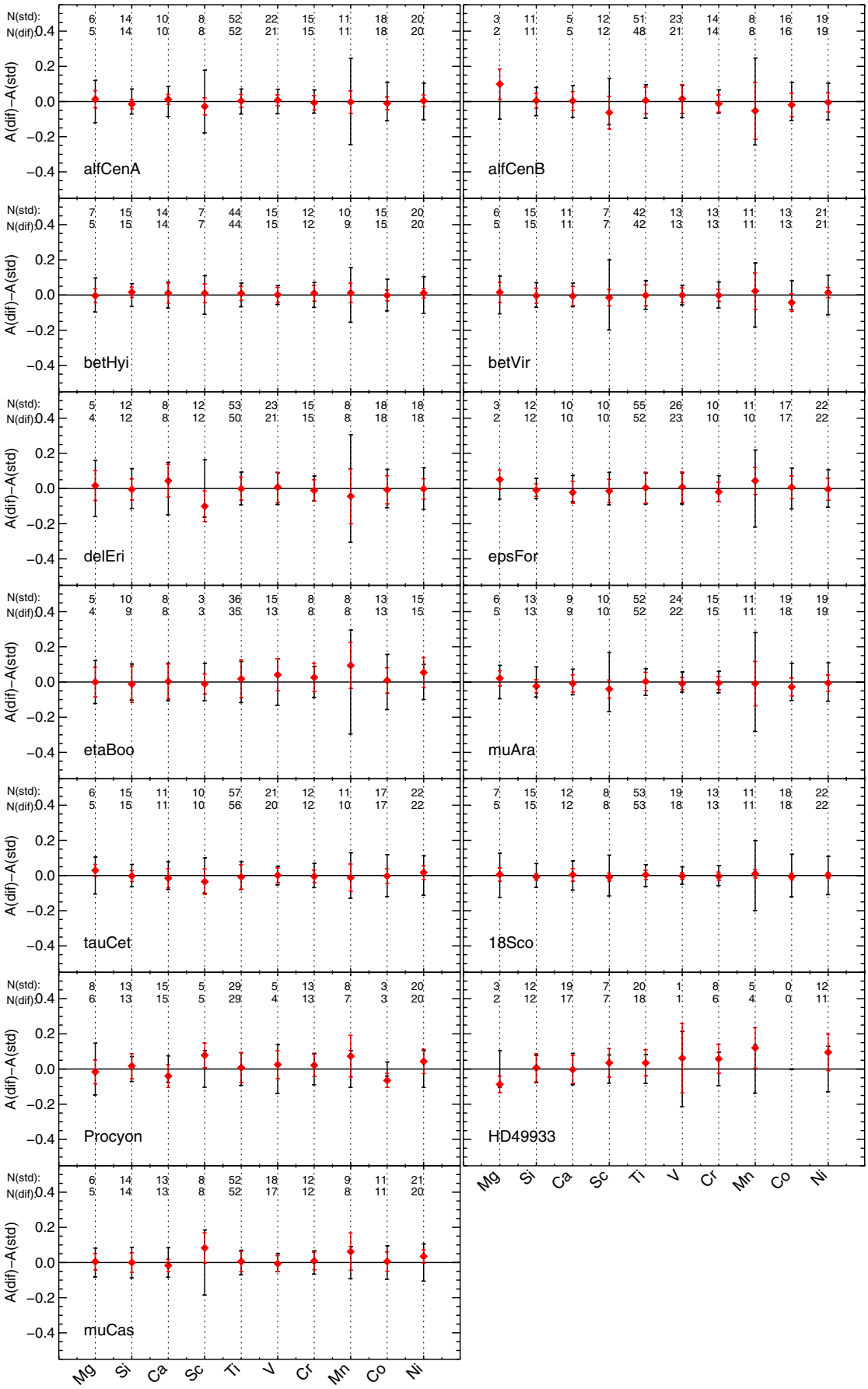

Fig. 5. Comparison of the abundances of FG-dwarfs determined using the standard approach and by performing a differential analysis with respect to the Sun. Same as Fig. 4.

measure V abundances. The continuum normalisation is difficult for this star, which probably is the reason for large discrepancies among the different methods seen in some extreme cases, which can even exceed 0.5 dex (see line λ5592 Å in Table C.7). It is impressive to realise that even when using the same atomic data and atmospheric models and the same very high S/N and resolution spectra, different methods can obtain very different abundances for a given line. This particular case is a strong argument that it is better to employ differential approaches because this cancels some of the systematic errors of a given method. In this way, one is able to not only achieve a higher precision for a measured line, but it also allows a better comparison of the results with another independent method.

4.2. Differential vs. absolute approach of group stars

It is instructive to visualise the global effect of the abundances obtained in the standard and the differential way for the stars of the same groups. Figures 5, 7–10 show the comparison of differential versus standard approach for the groups of FG-dwarfs, FGK-giants, K-dwarfs, metal-poor and M-giants, respectively. As for the reference stars, we plot the scatter of the line-to-line and method-to-method for the standard approach with black error bars, while the same scatter, but for the differential approach, is plotted with red error bars. The red diamond shows the difference in the final value obtained with both approaches. The numbers at the top indicate the number of lines used in the standard and the differential approach. Each panel shows one star, which is indicated in the bottom left part of the figure.

The FG-dwarfs in general have many lines, which remains the same when differentiating with the Sun in most of the cases (see Fig. 5). It is expected that this group uses many lines because these lines were selected from the analysis of the *Gaia*-ESO Survey, which mostly contains solar-type stars (e.g. Smiljanic et al. 2014). The lines are clean and numerous, making the standard deviation in general very small, even in the standard approach. The scatter of the differential approach is, however, still considerably lower at values of about 0.01 dex. Recent works on main-sequence stars performed differential analyses of chemical abundances with respect to the Sun (e.g. Meléndez et al. 2012; Bensby et al. 2014; Liu et al. 2015; Battistini & Bensby 2015), which allows a very precise analysis of relative differences in Galactic stellar populations. We note that the dispersion of Mn is systematically higher than that of the other elements. As mentioned in Sect. 4.1.1, the lines are affected by hfs, adding a source of error in the EW measurement and line modelling. Several Mn lines are very strong, partly due to effects of hfs, therefore we allowed for stronger lines than in the reference stars ($\log(EW/\lambda) < -4.6$) to have more lines to analyse. Like for the reference stars, the effects of hfs in the line-to-line scatter is significantly cancelled when differential abundances are determined. This is discussed in more detail in Sect. 4.3.

The case of Sc is worth commenting on because it also has a systematically high scatter in the standard approach. The differential analysis, however, yields a scatter that is similar to that of the other elements. The Sc lines are clean for these types of stars, and abundances for a given line agree quite well between methods. Two examples are shown in Fig. 6, which is similar to Fig. 1. We show abundances of Sc for a line-by-line and method-by-method approach of the stars α Cen A and β Vir, which presented significantly larger scatter in the standard analysis than the other elements in Fig. 5. The left panels of Fig. 6 show that the methods obtain more or less consistent results for the same

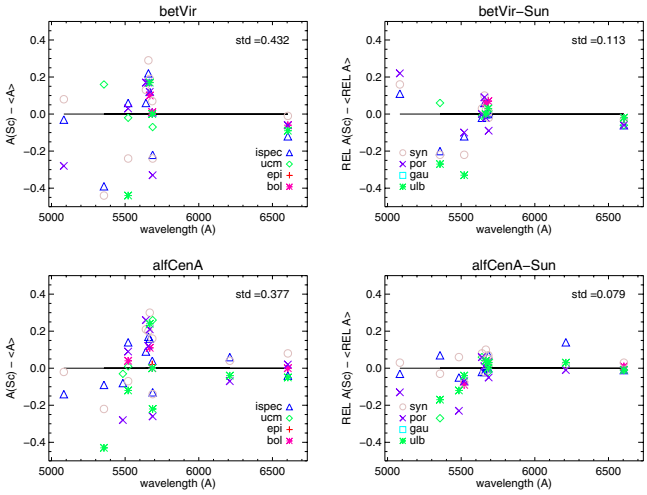

Fig. 6. Line-by-line abundances in the standard approach (*left*) and differential approach (*right*) of scandium for two FG-dwarfs. The different symbols represent different methods.

lines around λ5400 Å, but they are very different for the different lines. The Sc abundances derived from the neutral line λ5356 Å, for example, are systematically lower for all methods, suggesting either that the atomic data of this line could be revisited, or that the NLTE effects of this line are rather strong. NLTE corrections enhance the abundances of Sc of neutral lines in the Sun (Zhang et al. 2008). We recall that we showed in Fig. 3 that we obtained a large line-by-line dispersion for the Sun. If the dispersion were caused by NLTE effects, then a differential analysis would remove part of this effect, at least for the stars that are being differentiated with respect to the Sun.

It is instructive to discuss the case of 18 Sco, a classical solar twin. The same lines were used for the differential and standard approach, except for Mg and V. The Mg line at λ6319 Å and the V line at λ6296 Å had a gap in the solar atlas that was due to a blend from a telluric feature. The line-to-line scatter is greatly decreased in the differential approach, which is expected because the spectra of these twins are almost identical. For this reason, chemical analyses of solar twins are commonly performed differentially (e.g. Meléndez et al. 2014, 2012; Nissen 2015, and references therein). This allows detecting slight differences in their chemical pattern with great accuracy; they would otherwise be undetectable.

The FGK-giants (Fig. 7) also have a relatively large number of lines analysed, although slightly fewer than the FG-dwarfs. In our reduced EW cut, several lines are rejected because they saturate in giants. The final value using the two approaches remains unchanged within the errors, and the scatter systematically decreases. Only Mn for μ Leo has a different final abundance in the standard and the differential approach. We inspected the two lines used (λ5004 and λ5117 Å) that had a continuum that was difficult to identify in their vicinity for two stars, μ Leo and Arcturus. The abundances of Mn for μ Leo that rely only on these two lines should be treated with care. The number of lines for FG-dwarfs remains very similar between the standard and the differential approach, meaning that Arcturus is a good reference star for the FGK-giants.

In the K-dwarfs (see Fig. 8), many lines were used to determine elemental abundances of δ Eri, but for 61 Cyg B, fewer lines were used. This star is very cold, meaning that most of the lines are blended with molecules and cannot be used. Of these fewer selected lines, almost all overlap with 61 Cyg A, allowing

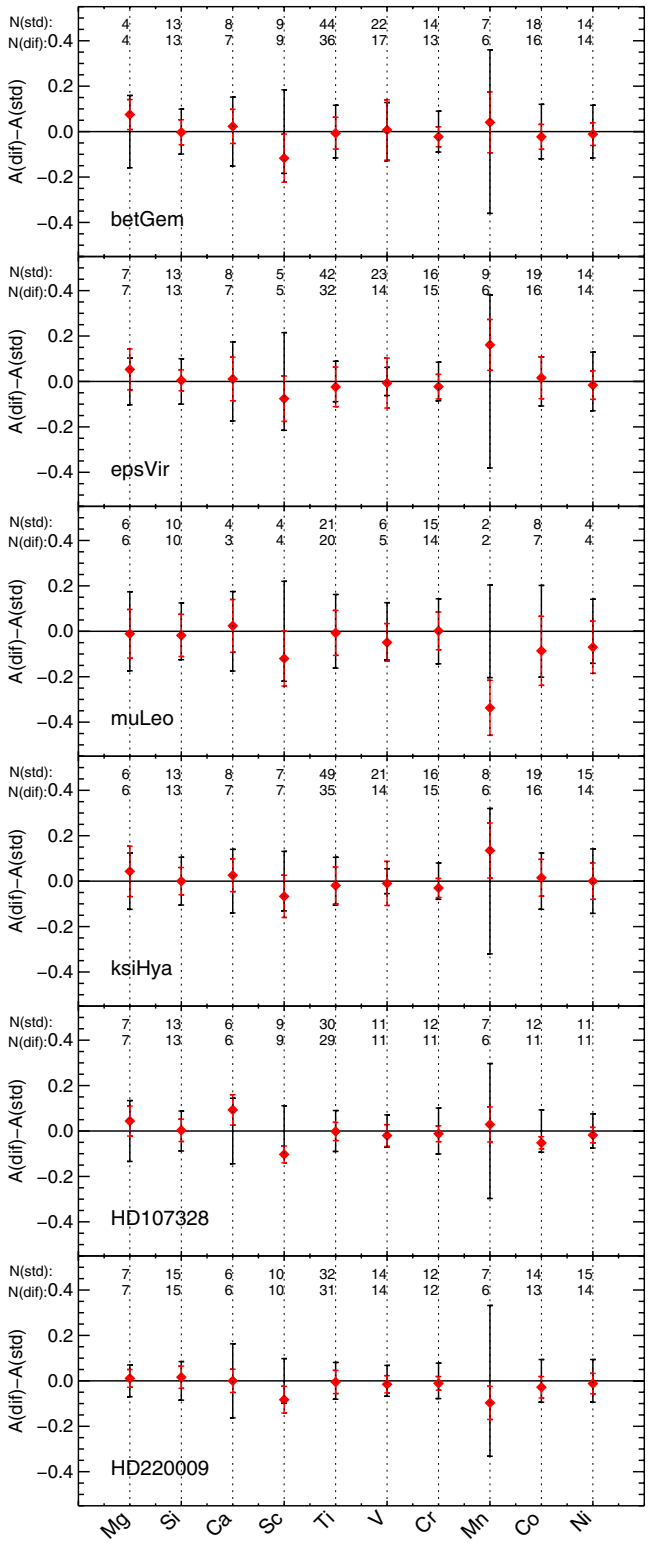

Fig. 7. Comparison of the abundances of FGK-giants determined using the standard approach and by performing a differential analysis with respect to Arcturus. Same as Fig. 4.

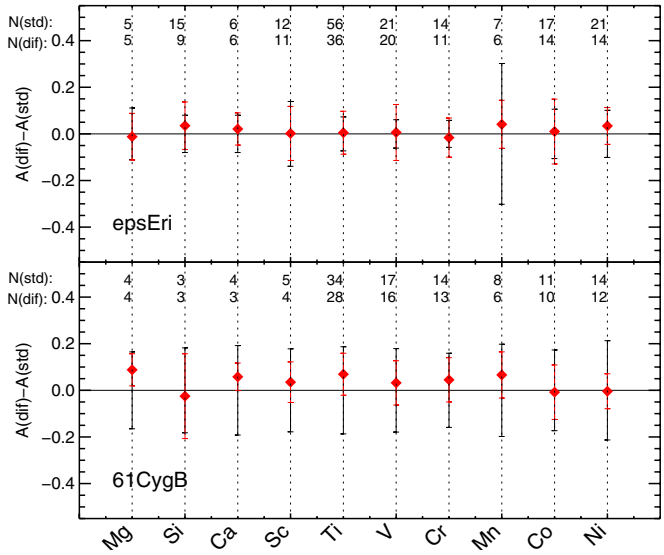

Fig. 8. Comparison of the abundances of K-dwarfs determined using the standard approach and by performing a differential analysis with respect to 61 Cyg A. Same as Fig. 4.

us to perform a differential analysis that in this case improves the precision of our measurements in every case while keeping the final abundance unchanged within the errors. We point out here that the Si line at λ6371 Å was removed from the analysis of 61 Cyg B because it was contaminated with a telluric line.

Metal-poor stars are more difficult to analyse in a differential approach because they are all very different from each other, spanning a metallicity range of 1.5 dex or more. Moreover, $T_{\rm eff}$ and $\log g$ of the metal-poor group also cover a wide range. Fig. 9 shows that the number of lines decreases in every case with respect to the FG-dwarfs, which is expected because of the low metallicities. Gmb 1830 still preserves most of the lines after performing differential analysis, with the finally abundances practically unchanged. Interestingly, HD 122563 also preserves most of the lines after differentiating, with results notably better in every case. This is an example of the degeneracies of stellar parameters: a very metal-poor giant has most of its lines of the same size as a more metal-rich dwarf. We are able to measure V for HD 122563 from one line, whose final value differs by ~0.2 dex when using standard or differential approach. This line, however, should be treated with care because it is located on the wing of Hβ, making the continuum more difficult to set.

Very few lines (Mg, Si, Mn) or none at all (V and Co) are detected in HD 140283, as previously discussed. It is unfortunate that two initially selected silicon lines (λ5701 and λ5948 Å) had to be removed because they were blended by telluric features in every spectrum of our library. The right wing of the λ5948 Å line can still be used for synthesis methods, yielding an abundance that is consistent with the only weak but clean line at λ5708 Å we have left. The abundance of Mn is less precise when the differential approach is employed. Although the final value agrees within the errors, it is worth commenting that the only line used (λ4823 Å) is slightly blended in the left wing in the spectrum of HD 22879, the reference star. The Mn abundance obtained from this line for the reference star varies between EW and synthesis method by 0.1 dex, probably because of hfs (see Sect. 4.3). Finally, HD 84937 has few lines in general, but they are not lost after performing differential analysis. Some elements cannot be measured in the standard approach (V, Mn, Co), and thus cannot be measured in the differential approach either.

The last group of M-giants is the most difficult. These cool giants have few clean and unsaturated lines in general, especially from our initial selection of lines, which was made based on the *Gaia*-ESO data, which contain very few of such cool giants. Furthermore, detecting the continuum is very challenging, as is

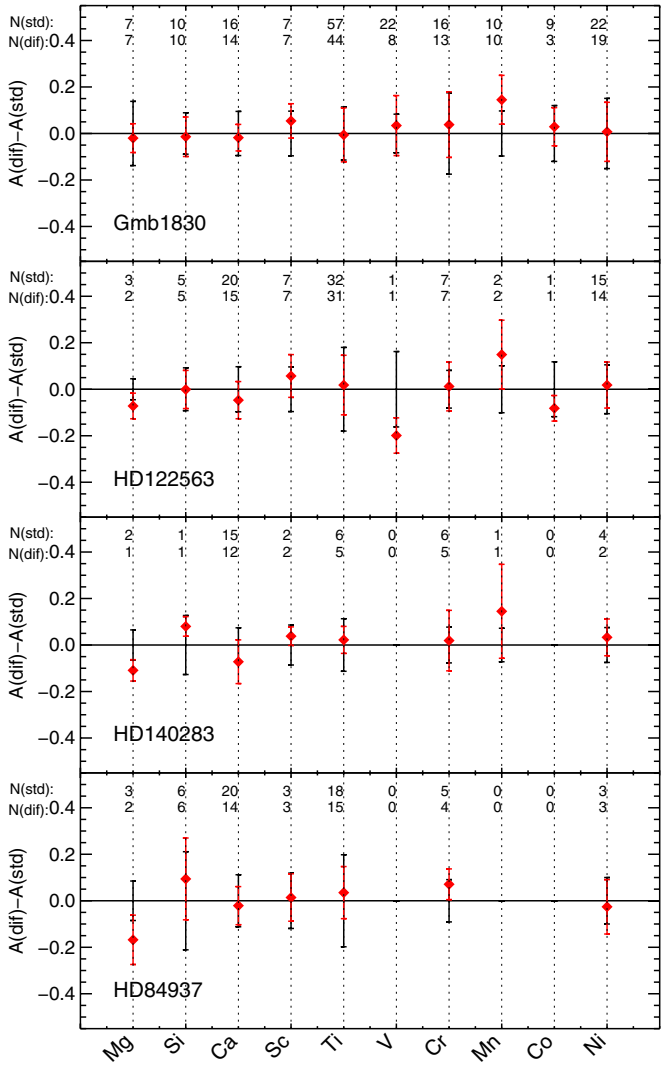

Fig. 9. Comparison of the abundances of metal-poor stars determined using the standard approach and by performing a differential analysis with respect to HD 22879. Same as Fig. 4.

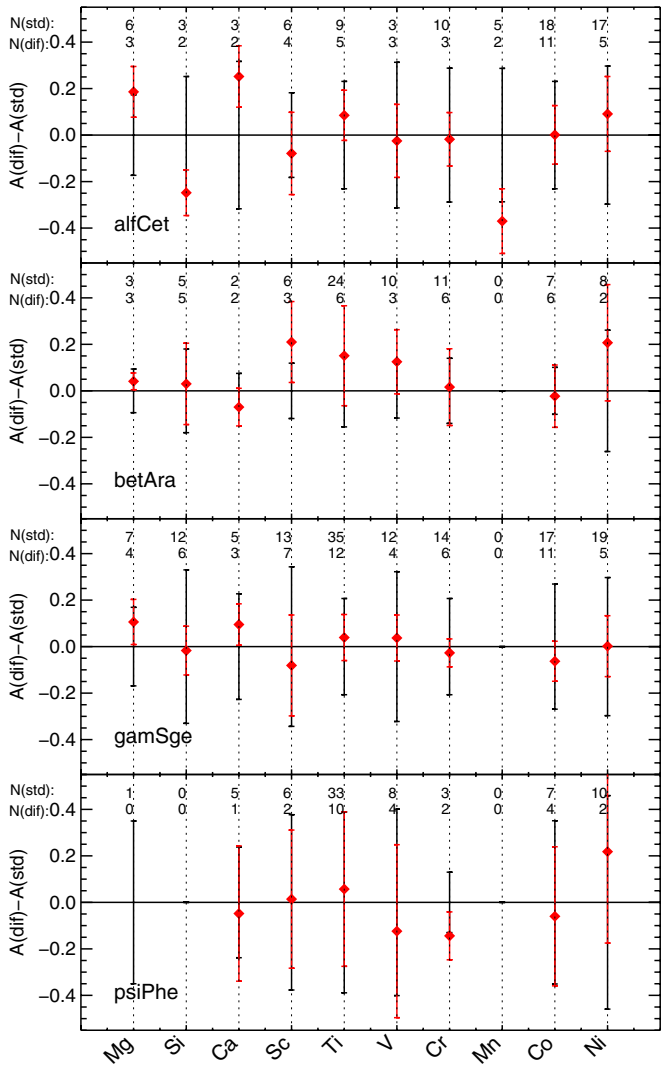

Fig. 10. Comparison of the abundances of M-giants determined using the standard approach and by performing a differential analysis with respect to α Tau. Same as Fig. 4.

fitting the correct profile to the lines. This causes a large dispersion of measured abundances line-to-line and method-to-method in general, especially for the extremely cool star ψ Phe. Figure 10 shows that the error bars are significantly larger than those of the other groups. However, the differential analysis yields better results in terms of precision in most of the cases, in particular for α Cet and γ Sge. There are several cases where lines did not provide reliable abundances because the spectrum in that region was too crowded with molecules. In these cases, the lines were rejected by hand, which meant that we do not have abundances for some of the elements. These cases have zeroes at the top sequences of Fig. 10.

4.3. Hyperfine structure splitting

The odd-Z elements Sc, V, Mn, and Co analysed in this work are affected by hyperfine structure splitting. Since we used methods that considered hfs and some that did not, we performed an analysis to quantify the effect of hfs in the measured abundances. In Fig. 11 we plot in each panel the absolute abundances of the Sun for the four odd-Z elements for each line and method, as a function of wavelength. The open black triangles correspond to the abundances derived from the EW and iSpec methods (i.e. no hfs), while the filled red circles represent the abundances obtained by the methods considering hfs. The dotted black line represents the standard deviation of all measurements, while the red dashed line represents the standard deviation of the methods that only consider hfs.

The figure shows that V, Sc, and Co, although affected by hfs, the systematic effect in the final abundance is not significant, where the averaged absolute value and the scatter on a line-by-line and method-by-method basis essentially remains the same. This is expected because the line profiles in the Sun for these elements are symmetric and can be well represented with a Gaussian profile. Some individual line abundances of V and Co might be affected - those where the non-hfs abundances are systematically higher than the hfs abundances: for V only one line at λ4875 Å, for Co the four lines around λ5500 Å: λ5483, λ5530, and λ5590 Å. Mn, however, shows a strong effect due to hfs, explaining the large scatter seen in Fig. 3. In contrast to V, Sc, and Co, several strong Mn lines present a pronounced boxy shape, in particular, λ5407, λ5420, and λ5516 Å. The line profile at λ5420 Å is shown in Fig. 1 of Scott et al. (2015). This analysis suggests that only Mn hfs should be taken into account,

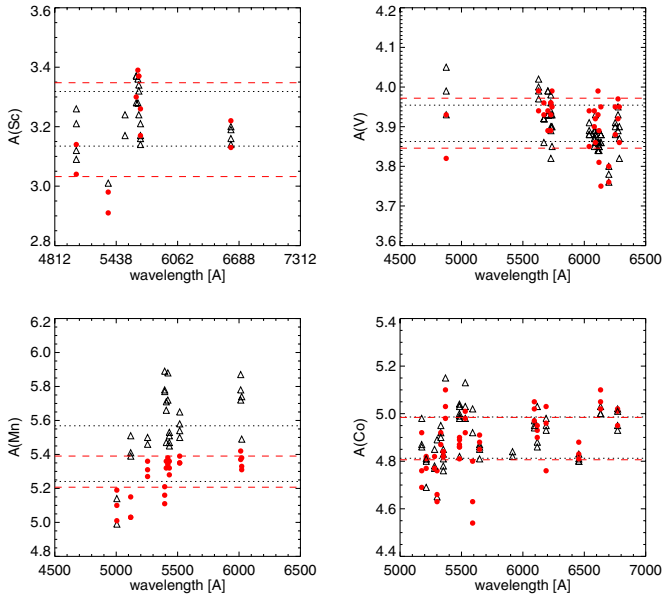

Fig. 11. Abundances of the Sun for the odd-Z elements determined by the different methods as a function of wavelength. We plot the methods that consider hfs in the abundance determination as red filled circles. As black open triangles we plot the methods that neglect hfs.

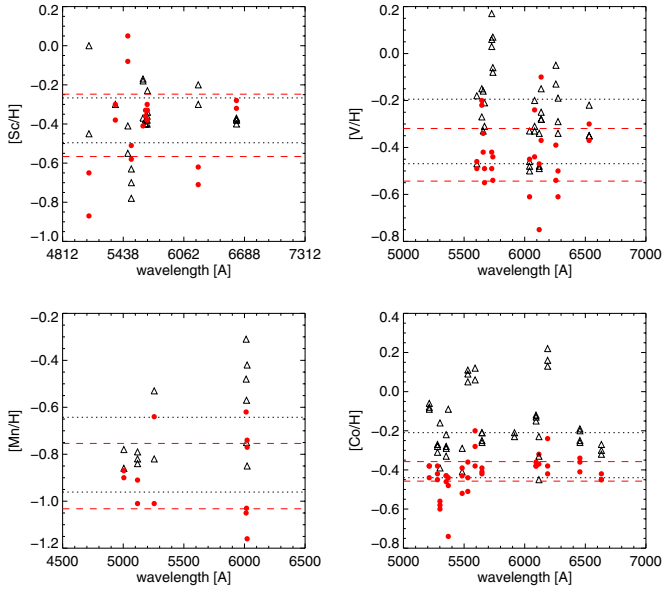

Fig. 12. Similar as Fig. 11, but for Arcturus with respect to the Sun.

which in our analysis means that only the abundances of Mn obtained from ULB, GAUGUIN, and Synspec should be taken for the Sun. For the remaining odd-Z elements, all methods can be used without affecting the line-to-line precision and absolute value of the solar abundance.

Next, we investigated whether the differential approach cancels the effect of hfs, such that all measurements can be employed, regardless of the consideration of hfs. For this we performed a similar analysis to that shown in Fig. 11, but compared the differential abundances obtained by the methods. We started with the reference benchmarks, which are very different from each other. In Fig. 12 we show the case of Arcturus with respect to the Sun. In contrast to the Sun, we can see that the effects of hfs are strong for this giant for V and Co. The lines are stronger than in the Sun, making the effect of hfs more pronounced. Since we see that hfs affects differently the different kind of stars, the effect of hfs cannot be cancelled when performing a differential analysis with respect to stars that are different from each other. Similarly, hfs significantly affects the abundances of Co and V. For Mn, this is more difficult to determine because only few lines were used. The metal-poor reference star HD 22879 presents a slight offset in the abundances with and without hfs for Sc and V, but for Mn and Co the offset is unclear, again due to the few lines used. The cool dwarf 61 Cyg A only shows a significant offset for vanadium. This analysis suggests that although hfs is not prominent for the determination of Sc, V, and Co for the Sun, it strongly affects stars different from the Sun. Thus, we confirm that to achieve more reliable results in a homogeneous manner, only methods employing hfs should be considered for all the reference stars, including the Sun.

Finally, we investigated the effect of hfs in the differential analysis when stars are similar to each other, that is, for stars within their group. Examples are shown in Fig. 13 for μ Ara, a star from the FG-dwarf group and for HD 107328, a star from the FGK-giant group. We chose these examples as one case presenting systematic differences when considering hfs (μ Ara) and one case not presenting significant differences (HD 107283). In the first case, the dwarf star has a similar temperature and surface gravity as the Sun, but it is considerably more metal-rich than the Sun, therefore its lines are much stronger than those in the Sun. Even in the differential approach, the effects of hfs in this case are not totally cancelled, where V, Mn, and Co show notable overabundances for methods that neglect hfs. On the other hand, HD 107283 has a more similar metallicity than Arcturus, but a slightly higher surface gravity and higher temperature. There is no evidence of any odd-Z element having particularly different abundances when methods consider hfs or not. We know from Fig. 12 that V and Co are strongly affected by hfs. This suggests that for HD 107283, which was analysed differentially with respect to Arcturus, the differential procedure cancels the effects of hfs.

To conclude, since the GBS are slightly different from each other, the effects of hfs cannot be cancelled by using a differential approach for all stars in a group in the same way. Furthermore, since our aim is to achieve the most reliable abundances in a homogeneous way for all GBS, we restrict the abundance determination of Sc, V, Mn, and Co to only the methods that consider hfs. That is, we neglect the results obtained by iSpec, Bologna, Porto, UCM, and Epinarbo for these elements.

4.4. Final abundances

As a final step, we visually inspected the profiles of all selected lines individually and removed unreliable abundances of lines with blends or potentially compromised profiles. The final selected lines for each star can be found at the CDS. These are 34 tables (C.1–C.34, one for each star) containing the individual abundances for each line for the ten elements analysed in this article. The first column indicates the atomic number of the element; the second column the wavelength of the line in Å; the third column the final abundance for that line obtained with the process described above (the differential abundances for that line were averaged between the methods analysing that line and then the absolute abundance determined for the reference benchmark star was added to the averaged differential abundance); the fourth column lists the NLTE correction obtained for that line

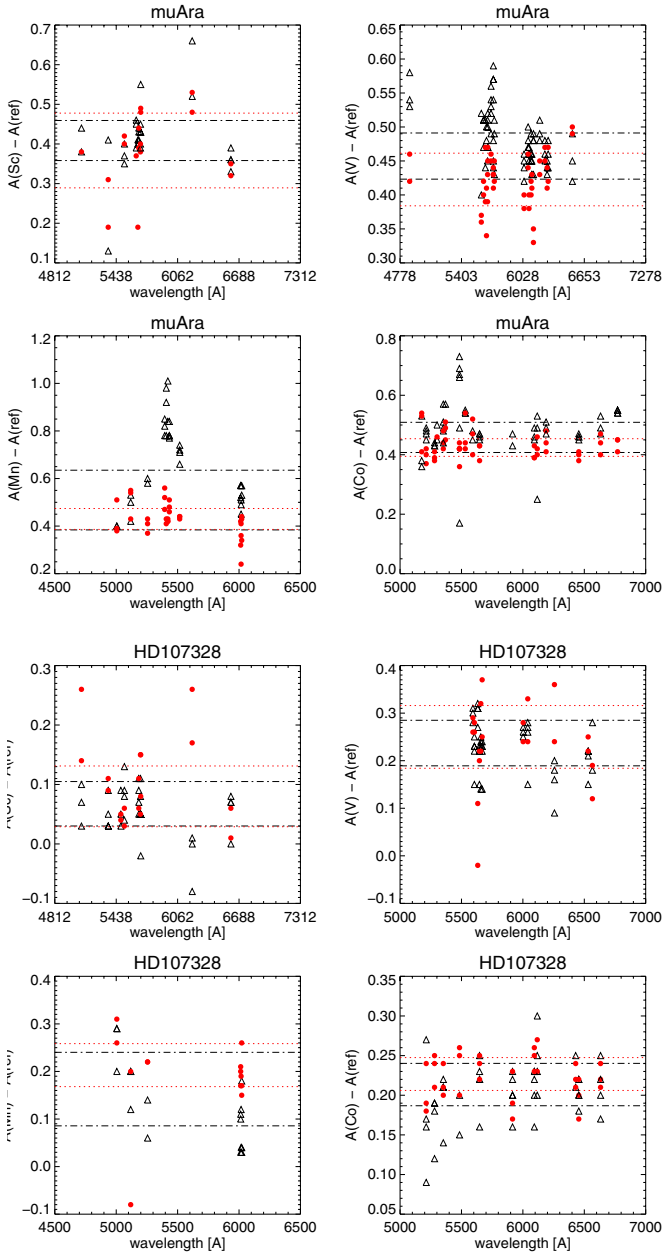

Fig. 13. Similar as Fig. 11, but for an FG-dwarfs star (μ Ara) with respect to the Sun and for an FGK-giants (HD 107328) with respect to Arcturus. The name of the star is indicated in the title of each panel.

(see Sect. 5.4); and Cols. 5–10 show the different measurements of EWs of the Porto, Epinarbo, Bologna, UCM, and ULB methods, respectively. The final eight columns correspond to the starting point of this work, namely the direct abundance measurement for this line by each method.

After selecting the good lines (those that were unsaturated and unblended, in common between the reference star and the star under investigation), the final value was determined by averaging all selected lines of all methods. The final value for each star and element is listed in Tables A.1–A.4 for Mg, Si, Ca, and Ti, respectively, and in Tables A.5–A.10, for Sc, V, Cr, Mn, Co, and Ni, respectively. The first column in the tables indicates the final abundance in [X/H] notation, and the remaining columns represent different sources of uncertainties, which are explained in detail in Sect. 5.

More specifically, the final abundance was calculated in the following way:

$$[\mathrm{X/H}] = \langle \mathrm{A(X)} - \mathrm{A(X)_{ref}} \rangle + \langle \mathrm{A(X)_{ref}} - \mathrm{A(X)_{\odot}} \rangle , \quad (1)$$

where $\langle \mathrm{A(X)} - \mathrm{A(X)_{ref}} \rangle$ is the final averaged differential abundance of the star with respect to the reference star; $\langle \mathrm{A(X)_{ref}} - \mathrm{A(X)_{\odot}} \rangle$ corresponds to the final averaged differential abundance of the reference star with respect to the Sun.

The final abundances are derived assuming LTE. The reason is that NLTE corrections for these ten elements for the variety of spectral classes, gravities, and metallicities of the GBS are not available. We calculated dedicated NLTE difference coefficients for some of the elements for all the stars, but these calculations are not possible to do for every atom configuration (see Sect. 5.4). Since our work aims at homogeneity, we provide LTE abundances for all elements and stars as our default abundance and provide the average departure from NLTE of all the lines when available. The final values for the odd-Z are listed in Tables A.5, A.6, A.8 and A.9 and only contain the abundances obtained by the ULB, GAUGUIN, and Synspec methods. However, we decided to keep the unused EWs and abundances in our final tables for each star, to enable further investigations of hfs effects in the future.

4.5. Golden lines

The atomic data of all the lines employed in this work can be found in Table C.35, where we list the wavelength, $\log gf$, low-excitation potential, the quality flags from the GES line list (see Sect. 2.2), and flags that indicate whether the line is a "golden line" (see also Paper III) or not. There are five columns with flags for a golden classification, one for each of the groups mentioned above. In the columns two flags are indicated (Y and N). We defined a line to be golden line when it was analysed in at least 50% of the stars in the group; in this case, the flag corresponds to the letter "Y" (yes, it is a golden line). When the line was analysed for less than 50% of the stars in the group, then the line is not a golden line and the flag has the letter "N" (no, it is not a golden line). Finally, when the line was not analysed for any of the stars in that group, then there is no flag.

To derive the final abundances, we used all the lines, not only the golden lines. Nonetheless, it is useful to have a global view of which lines are used most. For magnesium all lines except one are classified as golden for the FGK-giants. However, there is no Mg golden line for all groups. For the case of silicon, the group of FG-dwarfs all the lines are classified as golden and one line (λ5684 Å) is a golden line for all groups. Of the numerous lines analysed for Ca, there are several that are golden lines in different groups, which means that the Ca lines change significantly in different spectra. Interestingly, cool stars (giants and K-dwarfs) use fewer lines (3–7 lines) than metal-poor and FG-dwarfs (18–19 lines). The most numerous lines are those of titanium, with the FG-dwarfs having many golden lines. Metal-poor stars also use several Ti lines, although very few were classified as golden. Giants and K-dwarfs generally do not use lines bluer than 5300 Å, they probably saturate or blend with other lines because they are cooler than the solar-type stars. All scandium lines are found in FG-dwarfs, and about half of the lines were classified as golden. The line λ5686 Å is a golden line for the dwarfs and FGK-giants, but was not used by the other two groups. Almost all of the used Sc lines except one (λ5641 Å) were classified as golden for the FGK-giants.

Vanadium is another element with numerous lines employed. For dwarfs and FGK-giants most of them were used, with several being classified as golden. Metal-poor stars employ very few (eight lines), none of them golden. M-giants, on the other hand, employ even fewer lines (four lines), but all of them are golden. Chromium behaves line Ca in the sense that golden lines are distributed between the different groups, and very few lines are golden lines. The line λ5628 Å is a golden line for all groups except in the metal-poor stars, for which we did not use that line. No line redder than 5600 Å was employed by the metal-poor stars. Most of the Mn lines were used by the FG-dwarfs and were classified as golden. On the other hand, most of the lines were used by the metal-poor, but only one line (λ4823 Å) was classified as golden. For M-giants, only two lines were used, none of them golden. All lines used for FGK-giants (only six lines) are golden.

Most of the cobalt lines were analysed for the dwarfs, and most of them were golden for the FG-dwarfs and only those redder than 5500 Å for the K-dwarfs. Metal-poor stars only employ three Co lines, none of them golden. Two lines are golden lines for all groups except the metal-poor stars (λ5647, λ5915 Å). Finally, Ni has many golden lines for several groups. For FG-dwarfs, all of them were golden except one; for FGK-giants, all of them were golden, although fewer were used than for the FG-dwarfs. Metal-poor stars employ numerous lines, but very few are golden. The cool stars use fewer lines than the previous groups, but several of these lines are golden. More details for each element and nature of lines can be found in Sect. 6.

5. Sources of uncertainties in the derived abundances

In this section we discuss the effect of different sources of uncertainties on the final abundances. Most uncertainties have a systematic origin, such as the consideration of stellar parameters. We also discuss the effects of NLTE corrections for some of the elements.

5.1. Line-by-line scatter

In general, we have a fair amount of lines and methods providing abundances for each element/star, which allows us to determine a standard deviation around the mean of all these measurements. These values for each element/star are indicated as column $\sigma(\epsilon)$ of Tables A.1–A.10.

5.2. Systematic errors due to the consideration of [Fe/H] in LTE

We defined in Paper III our metallicity as the value obtained for the iron abundance after NLTE correction. This raises the question of how reliable our determination of more elements is when they are determined using material and methods that consider LTE. To assess this question, we made an extra run (see Sect. 3.2) in determining abundances, but considering [Fe/H] as the value obtained in LTE, that is, before the NLTE correction (i.e. [Fe/H] = [Fe/H] – $\Delta_{\rm LTE}$ as explained in Paper III). In this section we aim to determine the effect of NLTE corrections for iron in the resulting elemental abundances. The resulting abundances were determined as explained in Sect. 4, and the error due to LTE is considered as the difference between the two results. These differences are listed as ΔLTE in the final Tables A.1–A.4 for Mg, Si, Ca, and Ti, respectively, and in Tables A.5–A.10, for Sc, V, Cr, Mn, Co, and Ni, respectively.

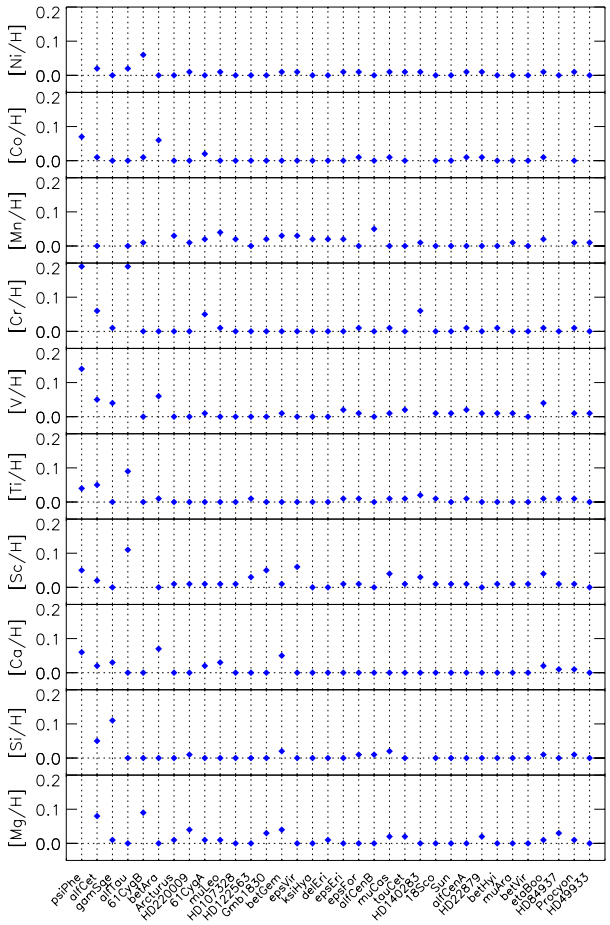

Fig. 14. Differences of abundances obtained using the final [Fe/H] value from Paper III compared to the [Fe/H] value before the NLTE corrections of iron. Stars are sorted according to temperature.

The difference in the abundances obtained considering the metallicity after and before NLTE corrections is displayed for all elements and stars in Fig. 14. The error due to the NLTE corrections in the iron abundances for the determination of these α and iron-peak elements is negligible in most of the cases. This is expected given the normally small corrections of NLTE for metallicity, which are in most of the cases smaller than 0.1 dex (see Paper III). The effect of this difference causes different results in individual abundances, which are usually below 0.02 dex, although some cases such as [Si/H] for the cool giant γ Sge have a difference of 0.1 dex in the resulting abundance. We note that even for this extreme case, this difference is smaller than the differences in the value for Si abundance because of errors in the stellar parameters of the line-by-line scatter.

Chromium abundances of the cool giants α Tau and ψ Phe have the largest differences of 0.19 dex when considering the iron abundances under LTE or after NLTE corrections. This difference is, however, similar to the line-by-line scatter of the abundances determined from the six selected Cr lines for α Tau. The line-to-line scatter of [Cr/H] of ψ Phe is slightly lower, but only two lines were employed in that case.

5.3. Errors due to uncertainties in stellar parameters

We quantified the errors that are due to uncertainties in stellar parameters in the same way as in Paper III: we determined abundances using the procedure explained above, but changed the value of the stellar parameters considering their error (see Sect. 3.2). This process was repeated eight times, twice for each parameter ($T_{\rm eff}$, $\log g$, [Fe/H] and $v_{\rm mic}$), by adding and subtracting the error from the respective parameter. Then, the error was considered to be the difference between the values obtained from the two runs of each parameter. These values are represented as Δ[Fe/H], $\Delta T_{\rm eff}$, $\Delta \log g$, and $\Delta v_{\rm mic}$ for the error in metallicity, temperature, surface gravity, and microturbulence velocity, respectively. They are listed in Tables A.1–A.10.

The differences are displayed for all elements and stars in Fig. 15. For this illustration we considered the total error of the stellar parameters, defined by

$$\Delta = \sqrt{(\Delta_{\rm [Fe/H]})^2 + (\Delta_{T_{\rm eff}})^2 + (\Delta_{\log g})^2 + (\Delta_{v\rm mic})^2}. \quad (2)$$

This difference is plotted in Fig. 15, but it should not be treated as a total error because it would be overestimated. This way of treating the total error assumes that the different parameters are not correlated to each other, which is not the case. If a covariance between parameters would be taken into account, the error would be smaller. In the final tables we give each error independently, here for the discussion we consider the total error as defined above. The total differences are usually comparable with the line-to-line scatter, although in some cases they can be significant. This reflects on the one hand the sometimes rather large error in the stellar parameters (see Table 3 and Papers I and III for details) and on the other hand the dependency of the different elements on stellar parameters. For example, the cool stars have relatively large differences in most of the determined abundances, but the uncertainties of the stellar parameters are also relatively large. Furthermore, for the cool stars the differences are in general large for most of the elements, which might be due to the fewer lines employed for the abundance determination. Solar-like stars, on the other hand, have in most of the cases differences below ~0.05 dex, except for a few cases such as Mn for α Cen B, Mg for δ Eri, and Ti, V, and Mn for ϵ For. The 0.31 km s^{-1} error in $v_{\rm mic}$ of α Cen B causes a difference of 0.08 dex in Mn, which is expected since α Cen B is a metal-rich star and its lines are strong, meaning that they depend more strongly on microturbulence (see e.g. Gray 1992). The remaining parameter uncertainties produce negligible differences in the abundance of Mn (see Table A.8). The line-to-line scatter is larger than this uncertainty. This is probably because of the same reason, given that this star is metal-rich, the Mn abundances are more uncertain for strong lines that have large hfs. For the Mg abundance of δ Eri the situation is very similar to Mn for α Cen B, the large error in $v_{\rm mic}$ causes a larger difference in [Mg/H]. This star is also slightly metal-rich, making the abundance determination of strong lines more sensitive to this parameter. A similar behaviour is seen for some elements for the metal-rich giant μ Leo. Finally, the error of ~80 K in the temperature of ϵ For produces a difference in [X/H] of 0.08, 0.08, and 0.09 dex for Ti, V, and Mn, respectively. This agrees with what has been discussed for example in Thorén et al. (2004) for this star.

The metal-poor stars for most of the elements show a difference below 0.1 dex in the determined abundances. Uncertainties of that order are found for Ti, Cr, and Ni, suggesting that these elements are particularly sensitive to the stellar parameters in this type of star. In the chemical analysis of 14 metal-poor stars of Hollek et al. (2011) an extensive discussion can be found on how the different elements are affected by stellar parameters. Their Table 7 describes in detail how the abundances can change with errors in stellar parameters. If an error of 150 K is considered in the temperature (the temperature uncertainties of our metal-poor sample are ~100 K), then the abundances of Ti, Cr, and Ni can result in a difference of up to ~0.2 dex. The remaining elements have differences of ~0.15 dex for this temperature error. Similarly, if $v_{\rm mic}$ has a difference of 0.3 dex, then abundances of Ni, Cr, and Mn can be affected by ~0.15 dex as well. Like Hollek et al. (2011), we find that the uncertainty in surface gravity is less significant for most of the species (see Tables A.1 to A.10).

As commented before, the error due to $\log g$ uncertainties for Arcturus was calculated considering a value that is half as high as what we reported in Paper I. We expect the errors in the abundances to be approximately twice as large. We obtained uncertainties due to $\log g$ error for Arcturus of about 0.01–0.02 dex (see Tables A.1–A.10), with the error obtained in Paper I, the uncertainties would be 0.03–0.04 dex, which is still smaller than other uncertainties listed in the tables.

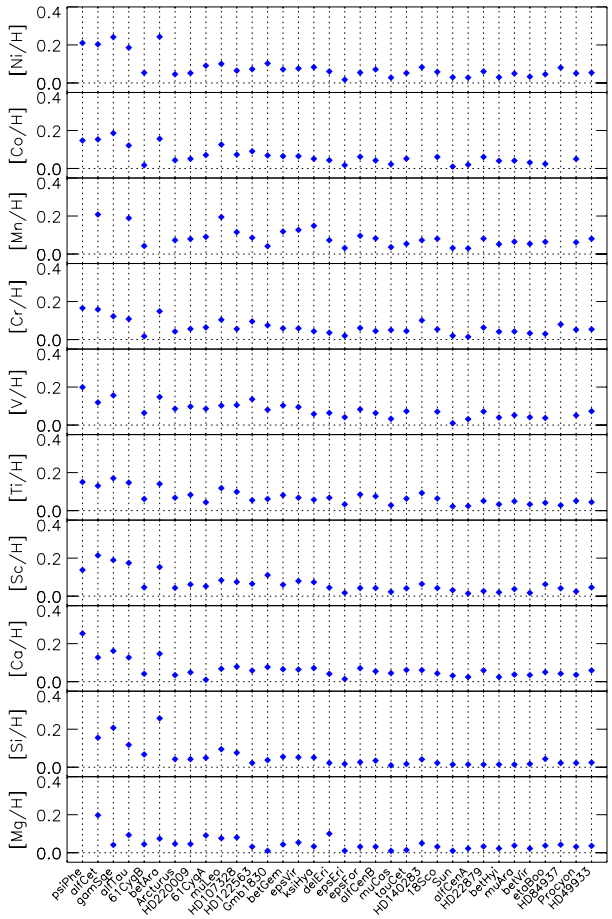

Fig. 15. Differences of abundances obtained using the uncertainties of stellar parameters. The individual values shown from Tables A.1 to A.10 were summed quadratically.

5.4. Departures from NLTE

NLTE corrections were computed for selected lines of magnesium (Osorio et al. 2015), silicon (Bergemann et al. 2013),

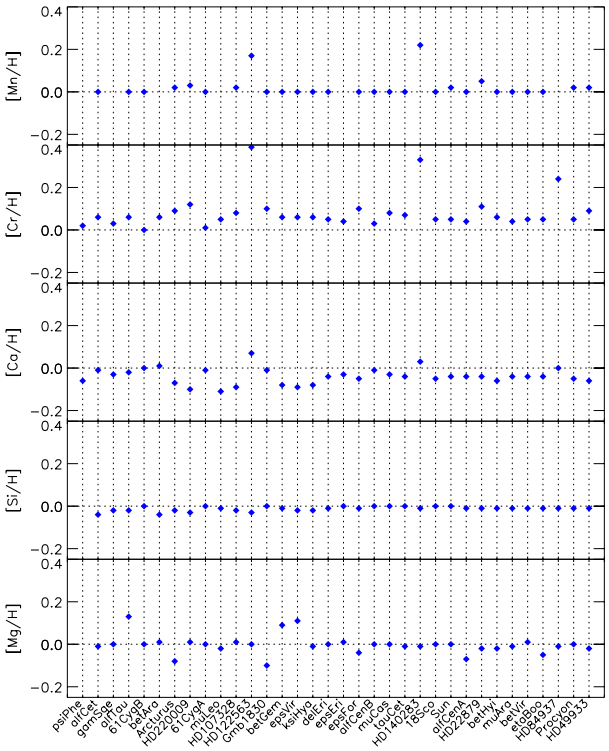

Fig. 16. Departures from NLTE of Mn, Cr, Ti, Ca, Si, and Mg for all stars, sorted according to temperature.

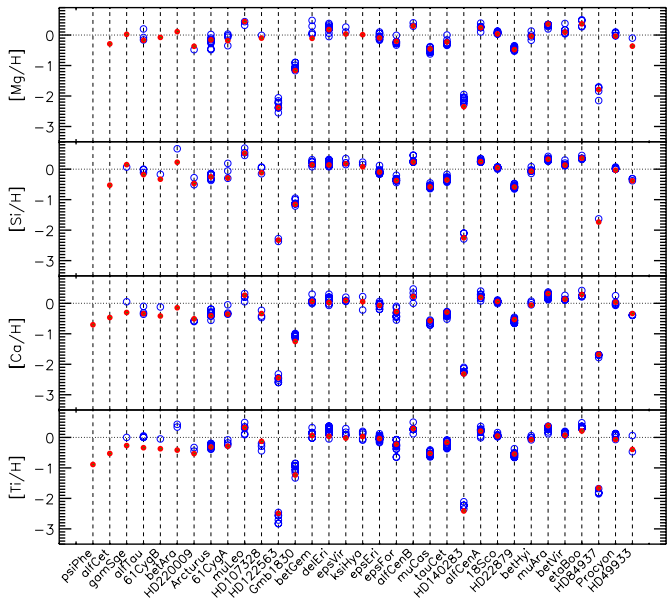

Fig. 17. Abundances of α-elements for the GBS sample sorted according to effective temperature. Filled red circles represent our final values, while open blue circles represent different results from the literature (see Appendix B).

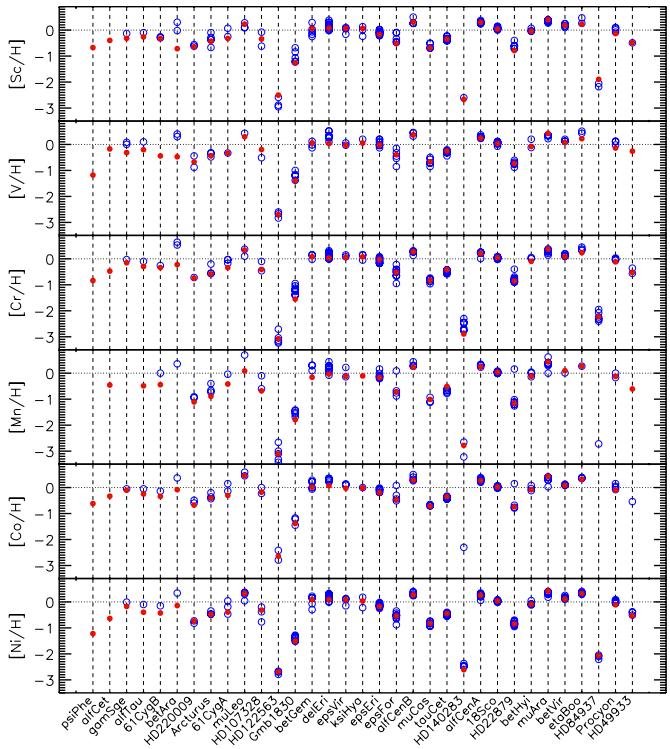

Fig. 18. Abundances of iron−peak elements. See caption of Fig. 17.

calcium (Lind et al. 2013), chromium (Bergemann & Cescutti 2010), and manganese (Bergemann & Gehren 2008). The main uncertainty in these calculations is typically related to the inelastic hydrogen collision rates. For magnesium, these rates have been accurately computed from quantum mechanical methods, while the other studies relied on the classical formula of Drawin (1968), rescaled by a factor $S_{\rm H}$ that is calibrated empirically. Full details are given in the respective papers. Another source of uncertainty is related to the equivalent widths. The corrections were performed considering an average EW of all methods.

The mean corrections for the elements where we calculated the departures from NLTE are displayed in Fig. 16 for all stars, sorted according to temperature. In general, the NLTE corrections are lower than 0.1 dex, which is comparable with the uncertainties discussed above. Metal-poor stars, however, show a large departure from NLTE of Cr of up to 0.3 dex, which is consistent with Bergemann & Cescutti (2010). Silicon abundances show small departure from NLTE for all stars. Mn differs more strongly for the metal-poor stars, but for the remaining stars, the departures are also normally very small, consistent with Bergemann & Gehren (2008).

6. Discussion of individual abundances

In Figs. 17 and 18 we show our final results, which are displayed with red filled circles. These values are listed in the second column of Tables A.1–A.4 for Mg, Si, Ca, and Ti, respectively, and of Tables A.5–A.10, for Sc, V, Cr, Mn, Co, and Ni, respectively. The blue open circles are different values taken from an extensive search from the literature, which were then transformed into [X/H] scale using the solar abundances employed by the different literature works. For a description of our literature search and a general discussion of our results in the context of previous studies, see Appendix B. In this section we focus on a detailed discussion of each element individually. We point out here that this discussion is intended for consultation on the results of the elements for the benchmark stars, focusing on the main aspects and results in a general way. Thus, this section does not contain important fundamental information needed to conclude this work.

6.1. Magnesium

Although we analysed fewer spectral lines of magnesium than lines of other elements (see Table 2), the abundance of this element is very important in spectroscopic studies partly because of the MgI b triplet around 5180 Å. These lines are commonly used to derive the surface gravity of a star, especially for spectra with low resolution or low S/N (see e.g. Lee et al. 2008; Jofré et al. 2010; Li et al. 2014, for stellar parameter determination of SDSS or LAMOST spectra) because many of the weaker lines vanish. Since Mg is an α-element, [Mg/Fe] can have different values depending on the chemical enrichment history of the environment where the star formed. Furthermore, Mg and O are the α-elements that separate the best in the [α/Fe] vs. [Fe/H] diagrams used to distinguish Galactic components using chemical tagging (Hawkins et al. 2015). Because of the strength of the MgIb triplet, the abundance of this element is known for a vast amount of stars, especially distant metal-poor stars that are observed with low-resolution spectra (e.g. Lee et al. 2011; Fernández-Alvar et al. 2015). For these reasons, a well-defined scale of Mg abundances is very important for stellar spectroscopy as well as Galactic science.

Eight of the twelve initially selected lines were used to determine Mg, with the triplet being excluded because its reduced equivalent width was larger than −4.8 for the reference stars. The atomic data of these lines can be found in the electronic Table C.35. Each line was classified as a golden line for at least one stellar group, meaning that they were used at least by 50% of the stars in their group. The lines at λ6318 and λ6319 Å were golden lines for all groups except for the metal-poor stars. The line λ8712 Å has no quality flag from the GES linelist, which means that its synthesis and atomic data quality have not yet been analysed. We still included this line because some few lines are in the range of Giraffe HR21 (and *Gaia*-RVS).

For magnesium we calculated the differences from LTE for each of the lines and stars; they are very small in most of the cases. The largest averaged departure from NLTE of −0.1 dex is for Gmb1830 (see Table A.1). As discussed in Appendix B, the abundances of this star were determined using an effective temperature that is very different from the typical spectroscopic temperature, which might cause the calculations for departures from LTE in Paper III to be incorrect. The remaining stars present a small NLTE correction, usually below 0.05 dex, except for the giants α Tau, β Gem, ϵ Vir, and Arcturus, which have an averaged difference of about 0.1 dex. Large departures from NLTE are found for most of the lines that were used to determine Mg for these stars. The lines we used to determine Mg in giants all show an excitation potential higher than 5 eV (see Table C.35). As discussed in Gratton et al. (1999), NLTE corrections for warm giants can become large for high-excitation Mg lines. Osorio et al. (2015) recently presented a detailed 3D-NLTE analysis of Mg of some of the GBS, in particular the Sun, Arcturus, Procyon, and the metal-poor stars. Although they found that NLTE departures do not significantly affect the solar abundances, for Arcturus differences of up to 0.3 dex can be reached. We found an average difference of 0.08 dex for Arcturus, with extreme cases of around 0.15 dex for the lines at λ8712 and λ8717 Å. Osorio et al. (2015) also discussed that 3D effects become strong as well, making it more difficult to make a one-to-one comparison with our case.

In general, our results agree well with the literature. The solar abundance of Mg is quite different from the scale of Grevesse et al. (2007) for the ten elements we analysed. Nevertheless, when uncertainties are taken into account, the values agree. In our extensive literature search, we did not find Mg abundances for the cool GBS, except for α Tau, which was analysed by Alves-Brito et al. (2010) and by Thevenin (1998). From Alves-Brito et al. (2010) we derived two values for [Mg/H] because they provided two values for [Fe/H] using two atmosphere models. In Table B.1 the value of [Mg/H] = −0.16 corresponds to the abundances obtained with MARCS models. Thevenin (1998), on the other hand, obtained a value of 0.2. We obtain a value of −0.32, which is lower than that of Alves-Brito et al. (2010), but when considering the uncertainties in our measurement (up to 0.17 dex), the two results agree.

We obtain a value of [Mg/H] = 0.012 for ξ Hya. The standard deviation of the line-to-line scatter is relatively large (0.1 dex), but the errors due to stellar parameters or NLTE corrections are very small. This star is a relatively metal-rich giant ([Fe/H] = +0.16 ± 0.2), therefore its spectrum is more difficult to analyse, which explains why the scatter in the [Mg/H] abundance is quite high. We did not find a value of [Mg/H] reported in the literature for this star. This star has a ratio of [Mg/Fe] = −0.15, which is consistent with [Mg/Fe] ratios of metal-rich stars observed in the Galactic disk (see e.g. Bensby et al. 2014; Mikolaitis et al. 2014; Bergemann et al. 2014; Holtzman et al. 2015, for recent studies)

Based on our literature search, we provide new values of [Mg/H] for α Cet, γ Sge, 61 Cyg B, and β Ara. These are all cool stars for which we analysed between three and four lines, among them the line at λ6319 Å. The line-to-line scatter can be large for these measurements (about 0.1 dex). The uncertainty due to stellar parameters can also produce large errors, up to 0.2 dex when the error in $T_{\rm eff}$ is taken into account for α Cet. Given the difficulty of analysing such cool spectra, we find it encouraging to be able to measure Mg with our combined method. The final lines were carefully inspected to ensure reliability of this new measurement. The [Mg/Fe] ratios of α Cet, γ Sge, and β Ara are slightly higher than solar (0.16, 0.19, and 0.16, respectively), which is within the typical values found for disk giants for solar and slightly lower metallicities (Holtzman et al. 2015). The [Mg/Fe] ratio of 61 Cyg B is higher (+0.3 dex) than that of its binary companion 61 Cyg A (+0.15 dex). When considering the errors, especially the metallicity of 61 Cyg B, which is 0.38 dex (see Table 3), the two ratios agree better.

6.2. Silicon

Silicon has several clean lines in the optical part of the spectrum, making it an important α-capture element because it plays an important role in testing supernovae and chemical evolution models. It is believed that silicon is created during the later evolution of massive stars (Woosley & Weaver 1995) and by Type Ia supernovae (Tsujimoto et al. 1995). Some works studying Galactic chemical evolution models that use spectroscopic analyses of stars and measure silicon are Edvardsson et al. (1993), Timmes et al. (1995), Valenti & Fischer (2005), Bensby et al. (2003) and Mikolaitis et al. (2014).

We have a total of 13 neutral and 2 ionised Si lines, all of them with rather high excitation (>4.9 eV). The 15 lines were classified as golden lines for the group of FG-dwarfs, 13 of them as golden for the FGK-giants. For extremely metal-poor stars such as HD 140283, lines usually below λ4100 Å are preferred to determine Si abundances (see e.g. Gratton et al. 2003, who have determined Si for many metal-poor GBS), which lie bluewards from our spectral region. We were still able to determine the abundance of Si for this extreme case based on only one very weak line (λ5708 Å), which has an EW of 2.2 mÅ

as measured by the ULB method. Only the ULB and iSpec (which are based on synthesis) methods provided an abundance for this line, which was checked with the synthesis performed to a rather stronger line, but blended with telluric features. Our result for [Si/H] of −2.2 agrees well with previously reported works of −2.3 (Gratton et al. 2003) or of −2.1 (Thevenin 1998; Francois 1986).

We found that the line λ8899 Å, which is a golden line for the FG-dwarf and FGK-giant groups, yields an absolute abundance that agrees between the methods, but the absolute abundance is systematically lower (about 0.4 dex) than when looking at the value obtained for that line with the differential approach. This suggests that the atomic data of this line need to be revised.

We performed NLTE corrections for this element, showing that in most of the cases the corrections are zero or below 0.03 dex. These corrections are negligible compared to the line-by-line scatter found for Si for all cases. The analysis of Si abundances in LTE and NLTE of Shi et al. (2012) agrees with ours in the sense that the abundance differences are very small in the optical region. We note, however, that Shi et al. (2012) derived significantly larger departures from NLTE for strong lines in the infrared (between 10 200 and 10 900 Å).

For the cool stars α Cet, 61 Cyg B, and β Ara we only used 2–5 lines because most of the lines were blended with molecules or the continuum could not be properly placed. The line-to-line scatter for these cases is rather large (>0.1 dex), but for the remaining stars the scatter in general is below 0.1 dex. The cool stars α Tau, ϵ Eri, and 61 Cyg A also show a rather large line-to-line scatter, but given the difficulty in analysing cool spectra, we find the values acceptable. The uncertainties in Si abundances due to errors in stellar parameters is smaller than the line-to-line scatter for most of the stars. β Ara is an exception in presenting large differences in [Si/H] of up to 0.17 dex when considering the errors of [Fe/H] and $v_{\rm mic}$, but this star has uncertain parameters and it is very cool, which makes the analysis of spectra in general more difficult.

The abundance of Si we obtain for the Sun agrees very well with Grevesse et al. (2007) within the errors. When comparing our results of silicon abundances with the literature (see Fig. 17), we conclude that our values for most of the stars agree very well with those reported in previous works, with the exception of β Ara (+0.67, Luck 1979), which considers a value for $T_{\rm eff}$ 500 K and for $v_{\rm mic}$ 3 km s^{-1} higher than our own. For 61 Cyg A our value agrees very well with that of Affer et al. (2005), but it disagrees with the result of Mishenina et al. (2008).

Finally, we are the first, to our knowledge, who give a value of [Si/H] for the cool giant α Cet that is based on the analysis of the two lines λ5684 Å and λ5701 Å. The line-to-line scatter is 0.1 dex, but we show in Table C.6, few methods (those performing synthesis) were able to analyse these lines, thus the scatter is overestimated due to the small statistic of this measurement. We visually inspected these lines to ensure the reliability of this new measurement. The [Si/Fe] value of α Cet is rather low (−0.07) which is lower than [Mg/Fe]. This star is very cool and the errors in the measurement of Si abundances are significant in all our sources of uncertainties. When considering the errors, [Si/Fe] and [Mg/Fe] are consistent. It is worth to comment the trend in temperature found for Si abundances by Holtzman et al. (2015) in the large sample of APOGEE giants. The coolest stars (those around 3500 K such as α Cet) have systematically lower (even negative) [Si/Fe] ratios with respect to the warmer giants.

6.3. Calcium

Similar to the case of the Mg Ib lines, the Ca II triplet around 8500 Å is a very important feature for which to derive surface gravities. Furthermore, the *Gaia*-RVS spectra are centred on this feature, and so are the spectra of RAVE and the HR21-Giraffe setup of the *Gaia*-ESO survey. Examples of works determining parameters using this feature are Kordopatis et al. (2011) and Bailer-Jones et al. (2013). Furthermore, calcium is an α-capture element, and like Si and Mg, a star can have different values of [Ca/Fe] depending on the age and star formation history of the gas that formed the star (e.g. Venn et al. 2004; Nissen & Schuster 2010).

All the initially selected 22 lines were considered for the final abundance determination. Eighteen of them are neutral and four are ionised lines. For the M-giant group, three lines were used, for the FGK-giant group, seven lines (all golden), for K-dwarfs six lines (three golden), for FG-dwarfs 19 lines and for metal-poor stars 18 lines. The line at λ5867 Å is classified as golden for all groups except for the metal-poor stars. Five lines are golden lines in both the FG-dwarfs and the metal-poor groups. The overlap between metal-poor and giants or the K-dwarfs is much smaller because these lines become too strong ($\log(EW/\lambda) > -4.8$) for cooler stars. The lowest excitation potential of Ca lines is about 1.9 eV, while the highest is 8.4 eV.

We performed NLTE corrections for this element as described in Sect. 5.4, with large negative corrections for FGK-giants. This averaged NLTE correction is not representative for the majority of the individual corrections in this case. The red ionised lines at λ8912 and λ8927 Å have corrections of up to −0.25 dex, while the other lines have corrections below 0.05 dex. Solar-like stars usually have smaller NLTE corrections than the line-to-line or the errors due to stellar parameters. The aforementioned two lines are also considered in the final Ca abundance and also have large corrections, although slightly smaller than for giants (of 0.1 dex). Because more lines were used for the final abundance, these two NLTE-sensitive lines have less weight in the final value.

Uncertainties in final Ca abundances are normally below 0.1 dex when considering errors in stellar parameters or the line-to-line scatter. The uncertainties in $\log g$ produce a negligible difference or zero difference in the measured Ca abundance in most cases. The uncertainty in $v_{\rm mic}$, in contrast, produces differences in [Ca/H] that more significant, but still small except for the cool stars. Uncertainties in temperature produce slightly smaller differences in the final Ca abundance than $v_{\rm mic}$ with the warm giants showing a larger difference than warm dwarfs. Metallicity errors do not significantly affect the final Ca abundance, in a similar way as $\log g$.

We were able to determine Ca abundances for all GBS, which is important because this makes Ca a good element for calibration of homogeneous α-abundances using all benchmark stars. The abundance of Ca we obtain for the Sun agrees very well with Grevesse et al. (2007) (see Fig. 3). Our results for the remaining stars also agree well with those found in the literature. One exception is the cool giant γ Sge, for which Boyarchuk et al. (1995) obtained a value of [Ca/H] = 0.05, which is 0.4 dex higher than our result. They used a temperature higher by 100 K, a surface gravity lower by 0.3 dex, and a metallicity higher by 0.2 dex. For the same line we used here (λ6156 Å), they determined a value of $\log \epsilon = 6.4$, while we determine 6.0. The $\log gf$ value they employed agrees with ours within 0.1 dex. We

attribute the difference to the stellar parameters and probably different methodologies and continuum placement.

We did not find works reporting abundances of Ca for the cool giants ψ Phe, α Cet, and β Ara. Our abundances were determined from one and two lines. In these stars a difference in $v_{\rm mic}$ causes a difference in [Ca/H] of about ~0.1 dex or more, while the rest of the uncertainties do not cause a significant change in the final abundance. We visually inspected these lines to ensure the reliability of our results. The [Ca/Fe] ratio for these cool giants are consistent with the expectation of chemical evolution models. The [Ca/Fe] ratio of ψ Phe of 0.5 agrees with α-enhanced stars at low metallicities (−1.25, see Table 3). For the remaining giants, [Ca/Fe] ratios between 0 and −0.15 were obatined, which agrees with the systematic lower [Ca/Fe] ratios found by Bodaghee et al. (2003) and Holtzman et al. (2015) with respect to other α-elements in their samples of stars.

Although we provide a measurement for [Ca/H] for ψ Phe, this was derived using the [Fe/H] value determined by us in Paper III. We recall that in Paper I we were unable to use a reliable stellar evolutionary track to measure $\log g$ when using the metallicity determined in Paper III, thus solar metallicity was employed. The stellar parameters of this star have recently been determined by Schönrich & Bergemann (2014), who obtained a rather metal-rich star of metallicity $+0.1 \pm 0.4$, with temperature and surface gravity consistent with Paper I. This shows how difficult the abundance determination of this cool giant is. Therefore, we recommend to take this value of Ca with caution, and we suggest that this line should be reanalysed using a revisited value of metallicity.

6.4. Titanium

Titanium is sometimes referred to as an iron-peak element (Timmes et al. 1995), but its overabundance at low metallicities follows the α-element behaviour. Optical spectra for FGK stars show numerous Ti lines, which makes this element a common one in chemical analyses of stars because this abundance can be determined from spectra at almost every wavelength range. As a result of its α nature, Ti abundances are widely used to study the structure and evolution of our Galaxy (e.g. Nissen & Schuster 2010; Mikolaitis et al. 2014; Boeche et al. 2014). Titanium lines are in addition sometimes employed in metal-poor stars to determine parameters when there are not enough iron lines to evaluate the excitation and ionisation balance (e.g., Preston & Sneden 2000).

Titanium is the element for which we have the most lines, and thus the mean and standard deviation for the derivation of the final abundances allowed us to sigma-clip the bad lines quite straightforwardly. We worked with a final selection of 55 neutral lines and 12 ionised ones, all of them with a very low excitation (<3.1 eV). For the stars belonging to the group of M-giants we used 12 lines, 7 of which were classified as golden. Of these 7 lines, one Ti II (λ5005 Å) and three Ti I (λ5689, λ5702 and λ6091 Å were classified as golden for remaining groups except for the metal-poor one. For Mg, we included a line (λ7819 Å) that has no quality flag from the line list. This line shows good results, and its synthesis and atomic data should be analysed in more detail for future versions of the GES line list.

NLTE corrections for Ti were not computed as for the previous cases, therefore the respective column in Table A.4 is empty. The corrections are probably small for FGK stars (Takeda 2007; Bensby et al. 2003), however. As extensively discussed by Bodaghee et al. (2003), neutral Ti lines are more sensitive to NLTE effects, especially for metal-poor stars. Our abundances are mostly based on Ti I lines, meaning that uncertainties due to NLTE need to be investigated in detail in the future. The large parameter coverage of the GBS, together with the many Ti lines makes this task challenging. The line-to-line scatter of Ti abundances, in particular for metal-poor stars, is very large, which can be attributed to NLTE effects, in which abundances obtained from ionised and neutral lines are different. Since we do not have ionised and neutral lines for all the elements in this study, we preferred to take a final averaged value instead of two separate values, but we list abundances for each line (tables at the CDS) to enable choosing only ionised Ti lines, which are probably less sensitive to NLTE effects (Brown et al. 1983; Bodaghee et al. 2003).

Uncertainties that are due to NLTE corrections of iron from Paper III yield very small or zero differences in Ti abundances. Even smaller are the differences in Ti abundances when uncertainties of $\log g$ are considered, where most of these stars, especially the warm stars, have a zero difference. One exception is the cool giant γ Sge, for which an error of 0.35 dex in $\log g$ causes a difference of 0.07 dex in [Ti/H]. Uncertainties in effective temperature do not significantly affect the final values of Ti abundances. Metallicity uncertainties have in general a small impact on the final Ti abundances of less than 0.05 dex. Finally, errors in $v_{\rm mic}$ produce greater differences when the spectral lines are strongest (cool or metal-rich stars), as expected. The line-to-line scatter is below 0.1 dex, except for metal-poor and cool stars. These stars have a slightly larger line-to-line scatter that is mostly due to the few lines used to measure the Ti abundance and stronger NLTE effects.

Our abundance of Ti for the Sun perfectly agrees with the solar abundance of Grevesse et al. (2007). Our values agree very well in general with the literature, as shown in Fig. 17. In the same way as for Ca, we are able to determine abundances of Ti for all GBS in a homogeneous fashion. For the cool stars γ Sge, α Tau, and 61 Cyg B, however, we obtain [Ti/H] values that are systematically lower than in the literature. As above, the abundance of Ti was determined for γ Sge by Boyarchuk et al. (1995), who used a hotter and more metal-rich set of atmospheric parameters than we did. The star α Tau was analysed by Alves-Brito et al. (2010) and by Thevenin (1998) reporting Ti and Mg abundances (see above). These two works agree with a value of [Ti/H] zero or slightly above, which is 0.4 dex above our result. We note that Alves-Brito et al. (2010) used a solar metallicity for α Tau, while our [Fe/H] is −0.4. For 61 Cyg B, a value of [Ti/H] of −0.05 was reported by Luck & Heiter (2005), which is 0.3 dex below our result. In Paper III we discussed that our measurement of metallicity had a difference of 0.3 dex with respect to this work and also assessed the reasons for this.

The case of Gmb1830 is worth commenting on. We found ten measurements of the Ti abundance in the literature for this star, for which the results varied from −1.33 (Gratton et al. 2003) to −0.85 (Thevenin 1998). Our result of [Ti/H] = −1.64 is 0.3 dex lower than the literature range of values. We discussed in Paper III the effect on abundances of having a significant difference of effective temperature between the fundamental value determined in Paper I and the spectroscopic value. The metallicity is too low, and as a consequence, the abundances are likewise too low.

The final case worth mentioning is the star HD 49933, for which Takeda (2007) provided two values for the abundance of titanium that come from the analysis of neutral and ionised Ti lines and have a difference of 0.5 dex. Their Fig. 11 shows

the difference between [TiI/H] and [TiII/H] as a function of temperature. For hot stars this difference increases, explaining the difference of 0.5 dex they obtained for HD 49933. Our value is computed from averaging all lines and lies in between, as expected. We note that the line-to-line scatter of this star, as well as of Procyon, which are the hottest stars of our sample, is rather large (above 0.07 dex). For these stars, like for the metal-poor stars, the abundance differences from ionised and neutral lines might be an NLTE effect. One might consider lines of ionisation stages separately to decrease this scatter. In this case, we aim for a homogeneous analysis of 33 different stars and ten different chemical elements, therefore we prefer to have a larger line-to-line scatter in the Ti abundance of hot stars insted of two separate [Ti/H] values. Since we provide the individual abundances for all lines in Tables C.1–C.34, the separate Ti abundances can easily be calculated if needed.

For β Ara our Ti abundance is much lower than the only reported one by Luck (1979) by 0.8 dex. The atmospheric parameters considered by us and by Luck (1979) are very different, causing this difference, which goes in the same direction as [Si/H]. The errors of this star, in particular the line-to-line scatter, are very large. We provide a measurement of Ti for the rest of the cool giants (ψ Phe and α Cet) for which we could not find a value of [Ti/H] in the literature. The [Ti/Fe] ratios obtained for these stars are +0.36 for ψ Phe, which is consistent with the enhancement of this element seen for metal-poor stars. As discussed for Ca, this abundance should be taken with care and a revision for the metallicity is needed. The cool giants α Cet and α Tau have solar [Ti/Fe], which is consistent with the ratios obtained for Ca. However, β Ara has a very low [Ti/Fe] abundance (−0.4), but the errors of this value are very large when considering the errors of Ti and Fe together. Determination of Ti abundances in giants is difficult, which can also be seen in the large dispersion of cool giants in the [Ti/Fe] vs. [Fe/H] diagram of Holtzman et al. (2015).

6.5. Scandium

This element is important for studying the structure and chemical evolution of the Milky Way because [Sc/Fe] v/s [Fe/H] seem to be related differently for the different Galactic components (Adibekyan et al. 2012). This suggests that although both elements are synthesised through the same process – core-collapse and thermonuclear supernovae (Pagel 1997) – the physical environment (in particular the IMF) in which these supernovae occurred are different in different parts of the Galaxy. For example, the Sc yields show very strong variations as a function of the mass of the progenitor in the computations of Chieffi & Limongi (2002), producing scatter in [Sc/Fe] vs. [Fe/H].

For scandium, we have six neutral and seven ionised lines, all of which with low excitation (<1.9 eV). All the lines were used for FG-dwarfs, all except two for the K-dwarfs. All ionised lines (three of which are golden) and no neutral line were used for the stars of the metal-poor group, and FGK-giants considered four ionised and all the neutral lines. The group of M-giants used four ionised and three neutral lines. Three ionised lines (λ5667, λ5684, and λ6604 Å) were used in common for all the groups, but are only golden for some of the groups. The metal-poor stars are those that need stronger lines to be visible at low metallicities, which saturate for cooler more metal-rich stars.

We did not calculate NLTE corrections for Sc, but an extensive discussion on NLTE corrections of Sc for the Sun can be found in Zhang et al. (2008). They found large NLTE differences to abundances from neutral Sc lines (about 0.15 dex) in the Sun. Battistini & Bensby (2015) recently studied the differences in [Sc/Fe] with and without NLTE corrections for Sc, finding that at low metallicities these differences are larger. No particular trend was found in temperature or surface gravity. Unfortunately, there is still little information on NLTE corrections for Sc for stars that are very different than the Sun, which is true for most of the stars studied in this work.

Scandium is an odd-Z element that can be affected by hfs. As extensively discussed in Sect. 4.3, the total effect of hfs in determining odd-Z element abundances is different for each GBS. Although we did not see a clear systematic difference on the effects of hfs in Sc, we restricted our determination of Sc to only the methods considering hfs to be consistent with the analysis of the other odd-Z elements analysed in this work.

We provide abundances of Sc for all GBS. The line-to-line scatter can be quite large in many cases, probably due to the imbalance between abundances obtained between Sc I and Sc II (see Table A.5). This scatter is normally below 0.1 dex except for the Sun, which is also shown Fig. 3. We note that the abundance of the Sun is not determined with a differential analysis, therefore it is expected that the scatter on a line-by-line basis can increase with respect to the rest of the stars. Table A.5 also shows that the difference in [Sc/H] is normally much smaller than the line-to-line scatter.

Our result of scandium for the Sun agrees very well with the solar abundance of Grevesse et al. (2007). For the remaining stars our results also agree very well with the literature, except for β Ara and Gmb1830. As discussed above for titanium, β Ara has only been analysed by Luck (1979), who systematically found higher abundances than we did for the reasons mentioned above. We found five works in the literature that reported abundances of Sc for Gmb1830, which vary from −1.23 to −0.68 (both values determined by Takeda 2007, and the other works lie in between). As mentioned before, Takeda (2007) made a separate analysis of ionised and neutral lines, providing two different values. Our value agrees with the low value of Takeda (2007).

We were able to determine [Sc/H] for ψ Phe and α Cet. For this we used two lines in common (λ5667 and λ5684 Å). The abundances are uncertain, with a large line-by-line scatter, as shown in Table A.5 for these stars. We checked the line profiles and decided to keep the abundances, even if the different methods gave different results, because we could not find an obvious reason to reject these lines. These lines are used for all group of stars. The [Sc/Fe] ratios of the cool giants have expected values (see trends of Battistini & Bensby 2015, for dwarfs) when considering the uncertainties, with +0.16, −0.05, and +0.16 for ψ Phe, α Cet, and α Tau. The [Sc/Fe] ratio of β Ara has a similar behaviour as [Ti/Fe], that is, it is rather low (−0.3). This abundance is very uncertain, but a revision of the stellar parameters or a 3D-NLTE investigation of its line profiles might bring this star back to normal chemical evolution level expectations.

6.6. Vanadium

The nucleosynthesis channel of vanadium is not properly understood, and the supernovae yields lead to largely underestimated values compared to observed abundances (see Nomoto et al. 2013, for a recent review). Regarding its Galactic distribution and enrichment history, [V/Fe] shows a very large dispersion,

suggesting different trends for different data (Bodaghee et al. 2003; Battistini & Bensby 2015; Holtzman et al. 2015). The formation channels of this element and the usage of V to track the chemical enrichment history of the Milky Way can be better controlled when better and more consistent observed abundances are derived.

Vanadium is another odd-Z element sensitive to hfs. Although this effect is hidden in the line-to-line and node-to-node scatter, it can produce significant systematic differences in the determination of V for some of the stars. In our aim to have a homogeneous analysis for all GBS, we restricted the determination of V to methods that took hfs into account.

We determined homogeneous abundances of vanadium for all the GBS. In total, 30 neutral V lines were selected, all of them at a wavelength below λ6600 Å, except for λ8933 Å. The lines have a very low excitation potential, with the highest excitation of 1.2 eV. All the four lines used for the M-giants were classified as golden, while all the eight lines used for the metal-poor group were not classified as golden. Many lines were used for the dwarfs and the FGK-giants.

As discussed in Scott et al. (2015) and Battistini & Bensby (2015), departures from NLTE for V lines in the Sun have not been reported. We here determined abundances from the neutral line alone, and as known from other iron-peak elements, neutral lines suffer more from NLTE effects than ionised ones. We agree with the claim of Scott et al. (2015) that a study of NLTE of V is urgently needed. We did not analyse ionised lines to see whether a systematic difference would indicate possible NLTE effects.

For our internal uncertainties, the final V abundances when changing the overall [Fe/H] – either considering its uncertainty or the value determined from LTE – do not change significantly, being usually less than 0.05 dex. The cool dwarf 61 Cyg A presents a slightly larger difference of 0.08, which is still very small and can be neglected for the line-by-line scatter obtained for V abundance of that star. The dependency of V on $\log g$ errors is almost zero in all cases, while the dependency on $T_{\rm eff}$ or $v_{\rm mic}$ can be significant, although it is always lower than 0.1 dex. This behaviour is expected because all lines employed here are neutral lines, therefore we see a similar behaviour to what would happen when iron were determined from Fe I lines alone, which is a strong dependency on $T_{\rm eff}$ and $v_{\rm mic}$. The larger uncertainty in the V abundances is thus the line-to-line scatter, which can be slightly above 0.1 dex for some cases, such as the very hot or very cool stars, which is probably due to the fewer lines employed for these stars. For solar-like stars, the scatter is very small, usually below 0.05 dex.

The abundance of vanadium obtained by us for the Sun agrees within the errors with the solar abundance of Grevesse et al. (2007), with our abundance being slightly lower. As previously discussed, our value agrees well with Battistini & Bensby (2015). For the remaining stars, the agreement with the literature is in general very good, as Fig. 18 shows. We note that there are only a few measurements of the V abundance in the metal-poor stars HD 122563 (Fulbright 2000; Westin et al. 2000), Gmb1830 (Thevenin 1998; Fulbright 2000; Gratton et al. 2003; Kotoneva et al. 2006; Takeda 2007) and HD 22879 (Reddy et al. 2006; Neves et al. 2009; Gratton et al. 2003; Fulbright 2000; Zhang & Zhao 2006). Fulbright (2000), for example, who reported an abundance of V for the three stars mentioned here, analysed five V lines, only two of which overlap with our selection of lines. Our values agree well for HD 122563 and HD 22879. For Gmb 1830, our value follows the same direction as the remaining elements, that is, it is underabundant with respect to the literature. The reason is the different $T_{\rm eff}$ employed in this work, which needs urgent revision. We also note that for the hot metal-poor dwarf HD 84937 and for the very metal-poor star HD 140283, we did not find a measurement of [V/H] in the literature.

We recall that we did not find lines in common between α Tau and the Sun, therefore the V abundances were determined with respect to the absolute value for α Tau. Our result for that star agrees within the errors with Thevenin (1998) and our results for γ Sge agree well within the errors with Boyarchuk et al. (1995). For β Ara again our only comparison is the work of Luck (1979), which is higher than our values. For the other two cool giants ψ Phe and α Cet we did not find a measurement of V in the literature. The abundances are determined from three to four lines, obtaining a high line-to-line scatter, especially for ψ Phe. Both stars have a rather high [V/Fe] (about +0.2), but given the high dispersion of [V/Fe] measured on disk stars, especially on giants (Holtzman et al. 2015), it is difficult to ensure that these values are expected.

The cool dwarf 61 Cyg B is another case where we did not find a reported value in the literature. For this star we used 16 lines, with five methods providing abundances for them. The line-to-line scatter is below 0.1 dex, which is encouraging for this cool dwarf that has so many molecular bands blending the atomic lines. The errors due to stellar parameters are negligible except for the error due to $v_{\rm mic}$, which is expected since the V lines of 61 Cyg B are rather strong. The [V/Fe] ratio for this cool dwarf is around solar, consistent with the trends found by Battistini & Bensby (2015) or Bodaghee et al. (2003), although their study involved warmer stars. Finally, the hottest GBS, HD 49933, has no [V/H] reported in the literature. Our value has a large line-to-line scatter (or better said in this case, a method-to-method scatter) lower than 0.1 dex. Only one line was used to determine V (λ5627 Å), which is very weak; its EW is only measured with the Porto method of 8.2 mÅ. The abundance obtained by the Porto method is significantly higher than the abundances obtained by the other three synthesis methods that were used to analyse this line, suggesting a strong hfs effect. These EW values do not contribute to the final result of V abundances, but these detailed results can be found in Table C.21. The [V/Fe] ratio for HD 49933 is high, of +0.3, which would still follow the trend of Battistini & Bensby (2015) for metallicities of −0.4.

6.7. Chromium

The scatter of Cr is very small since there is not very much variety in the SN II yields, and [Cr/Fe] is almost zero for all metallicities (Timmes et al. 1995; Kobayashi & Nakasato 2011). However, several works in the literature reported that while for Cr II this is the case, for Cr I the [Cr/Fe] ratio increases with metallicity (Gratton & Sneden 1991; Bai et al. 2004; Cayrel et al. 2004; Lai et al. 2008; Adibekyan et al. 2012). Bergemann & Cescutti (2010) explained this discrepancy by finding that neutral Cr lines are strongly sensitive to NLTE for metal-poor stars.

We have a final selection of 23 Cr I lines, which have a rather low excitation (<3.8 eV). Only two lines were simultaneously analysed for the five groups of stars (λ5272 and λ5287 Å), mainly because lines that are strong enough to be visible in metal-poor stars are usually saturated in more metal-rich stars. The lines classified as golden in four groups – all except the metal-poor one – are the Cr line at λ5272, λ5827, and λ5628 Å.

For the group of M-giants, only these three lines out of six are classified as golden.

Chromium is the only iron-peak element for which we calculated the departures from NLTE for each star and line used in this analysis (see Sect. 5.4). In consistency with Bergemann & Cescutti (2010), the differences for solar-type stars are about 0.05 dex, while for metal-poor stars they are very large (0.24 dex for HD 84937, −0.39 dex for HD 122563).

The systematic uncertainty due to strong NLTE effects for Cr I lines is much larger than the uncertainties in Cr abundances, which is due to errors in stellar parameters or the line-to-line scatter. As in the case of vanadium, the main change in Cr abundance occurs when the error of temperature and at a certain level the microturbulence velocity are taken into account. The reason is the same: in this analysis we only studied neutral lines, which means that the measured abundances of Cr or Fe have the same impact from the different parameters. Our line-to-line abundance determination is in most of the cases very accurate, with a line-to-line scatter of about 0.05 dex or in several cases even lower. A few exceptions, mostly stars for which only a few lines were analysed, present a line-to-line scatter slightly above 0.1 dex. These are only a few cases, and in general are cool and metal-poor stars.

Our solar abundance is slightly lower than the value of Grevesse et al. (2007), but it agrees well within the errors. The abundance corrected for a departure from NLTE of 0.05 dex (see Table A.7 for the Sun) would produce a better agreement with Grevesse et al. (2007), but we restricted our analysis to LTE for homogeneity. The remaining stars agree well with the literature, as shown in Fig. 18. We were able to homogeneously determine the abundances of Cr for all GBS. The star Arcturus merits a comment: our value of [Cr/H] = −0.58 is 0.38 dex lower than the result obtained by Thevenin (1998). Our result agrees very well with the other two values of Ramírez & Allende Prieto (2011) and Luck & Heiter (2005), however.

Figure 18 shows that there is a scatter in Cr for ϵ For spanning from [Cr/H] = −0.22 (Thorén et al. 2004) to [Cr/H] = −0.95 (Gratton et al. 2003). The main reason for the discrepancy in the literature values is the different consideration of the stellar parameters in each of these works. In the particular example mentioned above, there is a difference in $T_{\rm eff}$ of about 400 K, in $\log g$ of ∼0.8 dex, and [Fe/H] of about 0.4 dex. Thorén et al. (2004) showed that a difference of 150 K can produce a difference of up to 0.09 dex in the abundance of Cr for ϵ For. Furthermore, Cr is sensitive to NLTE for metal-poor stars (see Sect. 5.4), which might cause a scatter in the literature. As explained in Paper III, the literature is highly inhomogeneous, which is the reason why we re-determined the abundances of all GBS in an homogeneous way.

The cool giant β Ara again has a value of the abundance of Cr from Luck (1979) that is much higher than our value. We provide [Cr/H] for the two very cool giants ψ Phe and α Cet, and no comparison is available in the literature. The abundances were determined from a few lines (λ5272, λ5287, and λ5628 Å) that have large errors, especially when considering the errors of the measured [Fe/H]. NLTE corrections for these lines are in both cases about 0.05 to 0.08 dex. The line-to-line scatter is small (0.16 dex) given the difficulty of analysing such cool giants. The [Cr/Fe] ratio would become +0.4 and solar for ψ Phe and α Cet, respectively. Chromium is an iron-peak element, and thus it is expected to follow a rather flat trend in metallicity (Bensby et al. 2014), although studies of lower resolution that also target giant stars have found some higher abundances of Cr, like the one of ψ Phe (Mikolaitis et al. 2014). The abundances of this star, especially the ratios as a function of iron, need to be treated with care until the iron abundance is revised.

6.8. Manganese

Manganese is produced more by SNe Ia than by Fe. Thus, from [Fe/H] ∼ −1, [Mn/Fe] begins to show an increasing trend toward higher metallicity, which is caused by the delayed enrichment of SNe Ia (Kobayashi & Nakasato 2011). Furthermore, this trend varies within the different Galactic components (Adibekyan et al. 2012; Barbuy et al. 2013), from cluster to field stars (Gratton 1989), and it is different for the Milky Way and dwarf galaxies (Prochaska & McWilliam 2000; North et al. 2012). Measuring accurate abundances of Mn is thus also important for studying the structure of our Galaxy because, for example, there is observational evidence of the existence of low [α/Fe] stars (e.g. Nissen & Schuster 2010; Jackson-Jones et al. 2014), which are important for discussions of the formation history of the Galactic halo (e.g. Hawkins et al. 2014). The majority of low [α/Fe] stars probably also have high [Mn/Fe] because of the SN Ia contribution, as explained in Kobayashi & Nakasato (2011). Hawkins et al. (2015) recently showed Mn to be one of the best candidates to distinguish Galactic components. While thin-disk stars have enhanced [Mn/Fe] ratios, thick disk stars have solar [Mn/Fe]. The authors explain this difference with the fact that Mn is produced at a higher fraction than Fe during SNIa, meaning that at a given metallicity, α-poor stars (which have been polluted by more SNIa) will have higher [Mn/Fe] ratios than their α-rich counterparts.

The abundance determination of Mn is complicated, however. It has significant hyperfine structure splitting, which broadens the spectral lines. As discussed in Sect. 4.3, reliable abundances should preferentially not be obtained by only using the EW and one total oscillator strength of a given line. North et al. (2012) showed that a difference of up to 1.7 dex can be obtained depending on whether hfs is or is not taken into account for Mn. The large scatter found for this element on a method-by-method and line-by-line basis when the absolute abundances are taken into account might be attributed to the fact that EW methods did not consider hfs, while the synthesis methods (except iSpec) synthesise the line profiles including hfs. We showed the systematic difference of Mn abundances for the EW and iSpec method in Fig. 11 compared to the other synthesis methods that considered hfs, the latter being 0.13 dex lower in the Sun. Differentially, systematic differences of Mn abundances for methods with or without hfs were considerable for several stars. For this reason, Mn was determined only considering the synthesis methods that took hfs into account. Furthermore, many Mn lines lie in spectral regions that are crowded, making the continuum identification nontrivial, which contributes to a large line-to-line scatter with respect to other elements.

Our Mn abundance determination was based in the analysis of 10 Mn I lines, all of them with an excitation potential of between 0 and ∼3 eV. All these lines were used for the FG-dwarfs group, except for the bluest one, λ4823 Å. For the M-giants stars we used only two lines (λ5004 and λ6021 Å), none of them classified as golden. The latter line was used for all groups. Almost all lines were used to determine Mn in the metal-poor stars, none of them golden, except for λ4823 Å. For the FGK-giants, only six lines were used, but all of them were classified as golden.

The NLTE effects in Mn I have been studied for the Sun and for metal-poor stars by Bergemann & Gehren (2008), who

found that NLTE effects on the formation of Mn lines can be very strong, in fact the abundances of Mn deviated from a given line by up to 0.4 dex depending on the stellar parameters of the star. We note that they did not consider hfs of Mn in their study. In the recent study of Battistini & Bensby (2015), the Mn NLTE corrections of Bergemann & Gehren (2008) have been applied for a large sample of stars, finding that indeed differences of 0.4 dex are possible, especially for metal-poor stars. In this study, hfs was taken into account. We applied the NLTE corrections of Bergemann & Gehren (2008) for Mn for most of the GBS, finding that in most cases the corrections are negligible. Metal-poor stars have large corrections, however, but of 0.2 dex rather than 0.4 dex. We stress that these corrections are subject to the uncertainties that are due to the EW measured in lines where hfs is very pronounced and need to be taken with care.

In general, Mn abundances only weakly depend on stellar parameters, which behave as the other iron-peak elements discussed above. That is, its uncertainty due to different $\log g$ or [Fe/H] (errors or the consideration of [Fe/H] before NLTE corrections of iron abundances) is negligible compared to the uncertainty due to $T_{\rm eff}$ or $\upsilon_{\rm mic}$. The line-to-line scatter can be up to 0.15 dex, especially for giants. We attribute this high scatter to the different ways of dealing with hfs in our different methods.

For the Sun the comparison between our value and that of Grevesse et al. (2007) shows a systematic offset, with our result being lower than those of Grevesse et al. (2007). This presents a similar behaviour as V, which we attribute to the LTE analysis used here and NLTE analysis performed by Grevesse et al. (2007). As for V, our results for Mn for the Sun agree well with Battistini & Bensby (2015). The comparison for the remaining stars with the literature (Fig. 18) shows very good agreement for warm stars, but for the cool stars HD 107328, μ Leo, and 61 Cyg A we see systematic higher literature abundances. Manganese in HD 107328 has been studied by Luck & Heiter (2007) and by Thevenin (1998), obtaining a value of [Mn/H] of −0.6 and −0.1, respectively. Our value of −0.68 agrees very well with Luck & Heiter (2007). The case of μ Leo has been investigated by Luck & Heiter (2007), obtaining a value of [Mn/H] of 0.7, which is 0.4 dex higher than our value of 0.33. Finally, the star 61 Cyg A has been studied by Luck & Heiter (2005), who obtained a value of [Mn/H] = −0.04. As previously discussed, we determined a value of [Fe/H] for this star that was about 0.4 dex lower than this value in Paper III, which translates into an abundance lower by 0.4 dex, which is what we see here. Furthermore, for 61 Cyg B a measurement of [Mn/H] has been reported by Luck & Heiter (2005) that is higher than our value. This is because the metallicity is higher by the same amount.

There are several values of [Mn/H] reported for the metal-poor stars in the literature. One example analysing many of them is Gratton et al. (2003), who used lines lying blueward of our spectral range. We did not detect any Mn line for the main-sequence metal-poor HD 84937. For β Ara, we did not find reliable lines to provide a value of [Mn/H], therefore Luck (1979) is still the only reference to our knowledge reporting a [Mn/H] value for this star. For the stars ψ Phe and γ Sge we were unable to find reliable lines for Mn abundances, and no work in the literature has reported a value for Mn either.

We were able to provide a new measurement of Mn for α Cet, α Tau, ξ Hya, and HD 49933, however. For the M-giants we used the two lines mentioned above. For λ5004 Å no NLTE corrections were provided, while for λ6021 Å, the corrections were negligible. The [Mn/Fe] value for both stars is very similar (−0.49 and −0.47 for α Tau and α Cet, respectively), which is also observed for the APOGEE giants in Holtzman et al. (2015). The Mn abundances of ξ Hya were determined based on six lines, among them the two ones used for the M-giants. No NLTE corrections could bed calculate for this metal-rich giant, which is also true for δ Eri and μ Leo, which are two other very metal-rich stars. The line-to-line scatter of the Mn abundances of ξ Hya is relatively large (0.1 dex), which is expected for metal-rich giants, whose lines are very strong and have large hfs. The [Mn/Fe] ratio of ξ Hya is −0.1, which is slightly lower than what is observed in Galactic disk populations, where [Mn/Fe] tends to increase with metallicity. Although Battistini & Bensby (2015) observed some metal-rich dwarfs with [Mn/Fe] values of −0.2, Holtzman et al. (2015) reported the bulk of giants at higher [Mn/Fe] values. Although we cannot directly compare the two datasets and our results because each of them is calibrated differently, the [Mn/Fe] value obtained for ξ Hya, α Cet, and α Tau are normal for disk stars.

The hot dwarf HD 49933 is the last star of our sample for which we provide new Mn abundances. They are based on four rather weak lines with a typical EW of 10 mÅ. We were able to perform NLTE corrections, which for all lines are of about 0.03 dex or lower. The line-to-line scatter of this abundance determination is relatively high (0.07 dex), reflecting the uncertainties of the different methods in measuring the abundance from these weak lines. The line λ5407 Å is particularly uncertain in the different methods, and it is also particularly weak (13 mÅ). The [Mn/Fe] value for HD 49933 is −0.3, consistent with the negative trend towards lower metallicities seen when LTE abundances are used in dwarfs (Battistini & Bensby 2015).

6.9. Cobalt

Cobalt has a very similar behaviour as Cr in terms of supernova yields (Kobayashi & Nakasato 2011). It is another odd-Z iron-peak element that is principally synthesised in explosive silicon burning in SNII (Woosley & Weaver 1995; Nomoto et al. 2013), but also in SNIa (Bravo & Martínez-Pinedo 2012). The chemical evolution of Co is thought to follow the same trend with metallicity as Cr, which is that Co evolves with Fe and [Co/Fe] remains constant. Observations show, however, that Co behaves like an α-element in the sense that it is enhanced at low metallicities by more or less the same amount as the α-elements, decreasing towards solar values at higher metallicities (Cayrel et al. 2004; Nomoto et al. 2013; Ishigaki et al. 2013; Battistini & Bensby 2015).

We employed 21 lines of Co I for our analysis; they have excitation potentials from ∼1 to ∼4 eV. Only three lines were useful for measuring [Co/H] of the metal-poor stars, but none of them was classified as golden. Lines used for all the groups are λ5280 and λ5352 Å, but they are not golden for all groups. The lines λ5647 and λ5915 Å are golden lines used for all groups except for the metal-poor groups. For the FG-dwarfs we used 19 lines, of which only two were not classified as golden. For the K-dwarfs 8 out of the 16 lines were classified as golden. FGK-giants have a total of 16 analysed lines (13 golden); M-giants a total of 11 (7 golden).

An NLTE analysis for cobalt has been carried out by Bergemann et al. (2010), obtaining corrections of up to 0.6 dex for neutral Co lines depending on temperature and surface gravity and low metallicities. They claimed that the main stellar parameter that controls the magnitude of NLTE effects in Co is in fact metallicity. Although their analysis includes some GBS such

as HD 84937, the corrections were made for lines lying blueward of our wavelength coverage. We provide Co abundances for more metal-rich stars compared to the sample of Bergemann et al. (2010), making it difficult to estimate a value of NLTE effects in our case. Since we only have neutral Co lines, a possible ionisation imbalance due to NLTE cannot be the source of the line-by-line scatter in our abundances. It might systematically affect the absolute value of Co, however.

Since Co is an odd-Z element, it is affected by hfs. As discussed in Sect. 4.3, the splitting affects the net abundances by different amounts for each GBS, even in the differential approach. For this reason, we restricted the abundance determination of Co to only methods considering hfs. The uncertainties of Co determination behave like the rest of the iron peak elements, namely small uncertainties for surface gravity and metallicity variations, and slightly larger uncertainties for temperature and $v_{\rm mic}$ variations. These uncertainties are usually smaller than the line-to-line scatter. The latter is normally lower than 0.1 dex, except for some giants, in particular the cool ones. Since we base our abundances on neutral lines for this iron-peak element, it is expected that the errors in $T_{\rm eff}$ and $v_{\rm mic}$ contribute the most to the uncertainties in the Co abundances.

The abundances of Co for the Sun agree very well with the solar abundances of Grevesse et al. (2007). The agreement for the remaining stars with the literature is also very good, except for β Ara, which we again compare with the abundances of Luck (1979), having the same behavior as the remaining elements, that is, our abundances are lower than those of Luck (1979) because of a systematic difference in the stellar parameters. We were able to provide abundances for the cool giants ψ Phe and α Cet, which have no Co abundance reported in the literature to our knowledge. The measurements come from 4 lines for ψ Phe and from 11 lines for α Cet, obtaining a line-to-line scatter lower than for other elements on these stars. The uncertainties of this measurement due to errors in [Fe/H] and $v_{\rm mic}$ are higher than 0.1 dex, which is expected because the error in [Fe/H] (see Table 3) is very large as well. When considering the metallicities of these stars, the [Co/Fe] abundance obtained is +0.34 for ψ Phe and −0.07 for α Cet, both being consistent with trends observed for stellar populations of these metallicities (Ishigaki et al. 2013; Battistini & Bensby 2015).

On the other hand, we did not detect Co lines for the metal-poor stars HD 140283 and HD 84937 or for the hot (and very metal-poor) HD 49933. A value for [Co/H] exists in the literature for HD 140283 as determined by Thevenin (1998) of −2.3, while a value for HD 49933 has been provided by Takeda (2007). For HD 84937, the abundance of Co still remains to be determined.

6.10. Nickel

Nickel is the last iron-peak element analysed in this work. Its production mechanism is similar to iron; it is principally produced in SNIa (Nomoto et al. 2013). Abundances of Ni scale linearly with Fe (Edvardsson et al. 1993; Reddy et al. 2006; Nomoto et al. 2013; Holtzman et al. 2015), with a remarkably low dispersion. The behaviour of Ni abundances at low metallicities is more uncertain, making the chemical enrichment history of this element difficult to model. It has been shown that low-α stars in the halo, which are believed to have formed in a smaller gas cloud than typical Milky Way stars, have Ni abundances that are much lower than what models predict (Nissen & Schuster 2010; Kobayashi & Nakasato 2011; Hawkins et al. 2015).

The fact that the dispersion in the [Ni/Fe] is so small is partly due to the many clean Ni lines available in optical spectra for several spectral type of stars. We selected 24 Ni I lines, with excitation potentials between 1.6 and 4.3 eV, approximately. There are three Ni lines (λ5846, λ6176 and λ6327 Å) that overlap for all five star groups, but none of them are golden lines for all groups. The two first ones are not golden only for the metal-poor stars. Almost all lines used for the dwarfs and FGK-giants were classified as golden (only the line λ5137 Å was not golden, and was not used by any other group). The metal-poor stars used mostly non-golden lines, while the M-giant group had three golden and three non-golden lines.

There is little known on the departure from NLTE of Ni in stellar atmospheres. A recent summary of results on NLTE differences of nickel has been presented by Vieytes & Fontenla (2013). Unfortunately, they studied lines at the near-UV, finding that the effects can be quite significant in some cases. We did not calculate NLTE corrections for Ni in our stars, but as discussed in Scott et al. (2015), they are probably small for neutral Ni lines in the optical range.

The uncertainties in the Ni determination are very similar to the remaining iron-peak elements for which we analysed only neutral lines. Errors due to metallicity (LTE or uncertainty) and errors in surface gravity give negligible changes in Ni abundances. Uncertainties in $T_{\rm eff}$ and $v_{\rm mic}$ give somewhat larger differences in the final Ni abundance, although they are still small and usually of about 0.05 dex or lower. The line-to-line scatter is the larger source of uncertainty for most of the cases, although our measurements for each line are quite accurate and the scatter is usually just higher than 0.05 dex.

For the Sun our result for nickel agrees well with Grevesse et al. (2007), our value is slightly lower than theirs. For the remaining stars our results also agree very well with the literature. The dispersion in the literature is particularly low for this element. For β Ara we again obtain a lower abundance than Luck (1979), as expected. For α Tau and 61 Cyg B our results are slightly different from those of Thevenin (1998) and Luck & Heiter (2005), respectively. Differences for 61 Cyg B are seen in the remaining iron-peak elements, and the reason is the difference in the value employed for [Fe/H] by us and by Luck & Heiter (2005).

We were able to determine Ni abundances for all GBS, providing new values for the coolest stars ψ Phe and α Cet. The abundance of Ni for ψ Phe was determined using two clean lines at λ5587 and λ5846 Å. Synthesis and EW methods were able to provide abundances for these lines, but with large differences that caused a very large scatter (0.34 dex). For α Cet [Ni/H] was determined using five lines, including those used for ψ Phe. Because these lines are clean, synthesis and EW methods were able to derive abundances. We had several measurements from which to calculate a line-to-line scatter with significance. The value of 0.16 is indeed very low for such a cool and complicated star. The scatter is similar to the error propagated from the $v_{\rm mic}$ uncertainty. The [Ni/Fe] ratio of these cool giants are very close to solar, with ψ Phe having a value of 0.03, but α Cet slightly lower (−0.15 dex). As shown in Holtzman et al. (2015), the systematic offset of [Ni/Fe] ratios for very cool giants becomes larger for higher metallicities.

Although a direct comparison of our results with those of Holtzman et al. (2015) cannot be taken to be too significant because of the different spectral ranges and calibrations employed, it is interesting that our systematic offsets for very cool giants show the same trend as the APOGEE data. The absolute

values cannot be directly compared, but there is a bias in homogeneous abundance determination towards very cool giants that goes in the same direction in our analysis and in that of APOGEE.

7. Summary and conclusions

The GBS are 34 stars spanning a wide region in the HR diagram. Their atmospheric parameters ($T_{\rm eff}$, $\log g$, and [Fe/H]) and spectra are excellent material to evaluate methods for analysing stellar spectra and for cross-calibrating different stellar spectroscopic surveys. Since the on-going and future surveys collect high-resolution data, methods analysing these spectra do not only aim at determining the main stellar parameters, but also abundances of individual elements. In this article, which is the fourth of the series of papers on the GBS, we determined abundances of four α and six iron-peak elements.

The abundances were determined using eight different methods, combining different strategies of measuring equivalent widths and computing synthetic spectra. The methods were applied on a spectral library especially created for this project with the tools described in Blanco-Cuaresma et al. (2014b); the project covers the wavelength ranges of ~480–680 nm and ~848–875 nm, the latter overlapping with the *Gaia*-RVS spectral range.

The analysis was made using the MARCS atmosphere models and the common line list of the *Gaia*-ESO Survey (Heiter et al. 2015b). The abundances were determined by fixing the stellar parameters as defined in Heiter et al. (2015a) for $T_{\rm eff}$ and $\log g$ and as defined in Jofré et al. (2014b) for [Fe/H] and $v_{\rm mic}$. Three runs were performed by all methods: the first one using the above parameters; the second one considering a slightly different [Fe/H] aiming at quantifying the effect of NLTE in the iron abundances; the third one considering the above parameters and their uncertainties, aiming at quantifying the the effect of the uncertainties in stellar parameters on the derived abundances.

To reduce the sources of scatter among different lines and methods, our analysis was made in a differential mode, by considering common lines between two stars. For this, we separated the GBS into five groups: metal-poor, FG-dwarfs, FGK-giants, M-giants, and K-dwarfs. For each group we chose one reference star: HD 22879, the Sun, Arcturus, α Tau, and 61 Cyg A, respectively. The differential analysis was made between the reference star and the remaining stars in that group. Finally, the reference stars were analysed differentially with respect to the Sun, which was set to be our zero point. Each final line used in our analysis was carefully inspected to ensure reliable abundances. This subject was discussed extensively.

We performed NLTE corrections on a line-by-line basis of the elements Mn, Cr, Ca, Si, and Mg. For most of the cases these corrections were below 0.1 dex, although Cr for metal-poor stars had a more significant departure of up to 0.3 dex for HD 122563, for instance. Furthermore, we compared our results with those of the literature and showed that our results agree very well in general, except for Gmb1830. We explained this difference by the possibly too low temperature we employed for this star. In the last part of this article we discussed in more detail the results for each individual element, described the general behaviour, and explained special cases.

We provided homogeneous abundances of ten elements for the GBS and quantified several sources of uncertainties, such as the line-to-line scatter and the differences obtained in the abundances when the stellar parameter uncertainties are taken into account. Furthermore, we quantified the effects of NLTE departures for iron, which translate into a different [Fe/H] value. We also performed direct NLTE calculations in four elements on a line-by-line basis. These values for each star and element can be found in Tables A.1–A.4 for Mg, Si, Ca, and Ti, respectively, and in Tables A.5–A.10, for Sc, V, Cr, Mn, Co, and Ni, respectively.

In addition to final abundances and their uncertainties, we presented all the material we used to derive the final values of Tables A.1 to A.10. That is, we provided the atomic data of each line, the final abundance we obtained for each line, the abundances derived by each method and each line, the equivalent widths determined by our methods, and the NLTE correction of each line. We believe this material is crucial for calibrating and developing new methods and for better understanding FGK stars in general.

The GBS are bright stars, many of them are visible to the naked eye on a clear night. They are so well known that some of them even belong to ancient star catalogues compiled by our ancestors several millennia ago[4]. Bright stars have always been necessary pillars to guide us in the sky. Now the *Gaia* satellite is orbiting in space, collecting data for the largest and most accurate 3D stellar map in our history. The spectra of millions of as yet unknown stars as observed by *Gaia*, *Gaia*-ESO, GALAH, RAVE, APOGEE, 4MOST, or any other future survey, will be analysed and parametrised according to calibration samples. With our dedicated documentary work on their atmospheric properties and spectral line information, the GBS provide fundamental material to connect these surveys and and contribute to a better understanding of our home galaxy.

Acknowledgements. P.J. is pleased to thank A. Casey for fruitful discussions and suggestions on the subject, and K. Hawkins and T. Mädler for their support. We thank S. Hubrig for providing us with the as yet unpublished reduced spectrum of α Cen A. We also acknowledge the constructive report from the referee. This work was partly supported by the European Union FP7 programme through ERC grant number 320360 and also by the Leverhulme Trust through grant RPG-2012-541. U.H. acknowledges support from the Swedish National Space Board (Rymdstyrelsen). This research has made use of the SIMBAD database, operated at CDS, Strasbourg, France.

Appendix A: Final abundances

In this Appendix we report the results obtained for the abundances of four α elements and six iron-peak elements, which are listed in independent tables. The first column indicates the star, which is listed in increasing order of temperature. The second column indicates the final value of [X/H] determined as discussed above. The third column corresponds to the standard deviation on a line-by-line basis for each measurement. The next four columns indicate the difference obtained in the abundances when considering the errors of the metallicity, effective temperature, surface gravity, and microturbulence velocity, respectively (see text). The column labelled ΔLTE corresponds to the difference obtained in the abundance when the metallicity used was the one before NLTE corrections (see Paper III and Sect. 3.2). The column labelled NLTE lists the averaged NLTE correction, when available. The last column indicates the number of lines used to derive the final abundance.

[4] MUL.APIN is one of the first stellar catalogues compiled by the Babylonians three thousand years ago. The GBS Arcturus, Aldebaran, Pollux, and Procyon are part of it.

Table A.1. Final abundances for magnesium.

Star	[Mg/H]	$\sigma(\log\epsilon)$	Δ[Fe/H]	$\Delta T_{\rm eff}$	$\Delta\log g$	$\Delta v_{\rm mic}$	ΔLTE	NLTE	NLIN
psiPhe	–	–	–	–	–	–	–	–	–
alfCet	–0.271	0.109	0.062	0.165	0.080	0.039	0.277	–0.010	03
gamSge	0.042	0.097	0.005	0.005	0.017	0.047	0.021	0.000	04
alfTau	–0.172	0.151	0.034	0.017	0.084	0.053	0.000	0.130	04
61CygB	–0.061	0.069	0.002	0.036	0.021	0.001	0.000	0.002	04
betAra	0.131	0.036	0.016	0.018	0.014	0.093	0.000	0.013	03
Arcturus	–0.158	0.088	0.050	0.010	0.014	0.025	0.010	–0.080	07
HD 220009	–0.347	0.039	0.041	0.000	0.017	0.024	0.070	0.009	07
61CygA	–0.184	0.083	0.091	0.007	0.013	0.000	0.048	0.000	07
muLeo	0.466	0.107	0.013	0.030	0.017	0.067	0.012	–0.015	06
HD 107328	–0.079	0.066	0.054	0.006	0.024	0.058	0.007	0.009	07
HD 122563	–2.354	0.055	0.003	0.034	0.005	0.080	0.005	–0.005	02
Gmb1830	–1.141	0.062	0.002	0.013	0.005	0.004	0.095	–0.103	07
betGem	–0.086	0.066	0.035	0.015	0.003	0.034	0.044	0.095	04
epsVir	0.057	0.090	0.050	0.021	0.005	0.032	0.001	0.107	07
ksiHya	0.034	0.111	0.018	0.014	0.007	0.032	0.006	–0.012	06
delEri	0.179	0.085	0.077	0.005	0.002	0.082	0.025	0.000	04
epsEri	–0.078	0.100	0.017	0.007	0.002	0.007	0.004	0.006	05
epsFor	–0.206	0.054	0.002	0.030	0.002	0.008	0.007	–0.040	02
alfCenB	0.296	0.086	0.042	0.005	0.006	0.014	0.027	0.000	02
muCas	–0.454	0.047	0.012	0.007	0.002	0.004	0.057	0.002	05
tauCet	–0.224	0.034	0.036	0.001	0.011	0.018	0.059	–0.006	05
HD140283	–2.326	0.046	0.005	0.050	0.005	0.000	0.000	–0.010	01
18Sco	0.038	0.038	0.009	0.027	0.005	0.007	0.001	–0.004	05
Sun	0.000	0.080	0.025	0.002	0.000	0.005	0.001	0.002	05
alfCenA	0.241	0.049	0.035	0.013	0.003	0.005	0.010	–0.072	05
HD 22879	–0.476	0.061	0.018	0.029	0.001	0.010	0.049	–0.022	08
betHyi	–0.038	0.039	0.027	0.015	0.004	0.005	0.004	–0.022	05
muAra	0.360	0.043	0.039	0.022	0.005	0.009	0.002	–0.012	05
betVir	0.093	0.058	0.033	0.015	0.005	0.005	0.001	0.006	05
etaBoo	0.367	0.085	0.043	0.014	0.016	0.017	0.044	–0.055	04
HD 84937	–1.764	0.106	0.043	0.037	0.005	0.005	0.032	–0.010	02
Procyon	–0.037	0.068	0.001	0.027	0.010	0.010	0.018	0.002	06
HD 49933	–0.364	0.047	0.009	0.031	0.005	0.020	0.008	–0.020	02

Table A.2. Final abundances for silicon.

Star	[Si/H]	$\sigma(\log\epsilon)$	Δ[Fe/H]	$\Delta T_{\rm eff}$	$\Delta\log g$	$\Delta v_{\rm mic}$	ΔLTE	NLTE	NLIN
psiPhe	–	–	–	–	–	–	–	–	–
alfCet	–0.524	0.098	0.022	0.141	0.039	0.063	0.062	–0.040	02
gamSge	0.150	0.105	0.124	0.080	0.151	0.050	0.110	–0.025	06
alfTau	–0.179	0.172	0.033	0.045	0.084	0.073	0.001	–0.024	08
61CygB	–0.328	0.182	0.027	0.043	0.041	0.029	0.000	0.000	03
betAra	0.228	0.175	0.164	0.056	0.085	0.180	0.005	–0.036	05
Arcturus	–0.252	0.051	0.014	0.026	0.023	0.022	0.012	–0.021	15
HD 220009	–0.472	0.049	0.006	0.025	0.038	0.025	0.042	–0.025	15
61CygA	–0.289	0.091	0.044	0.019	0.017	0.005	0.003	0.000	09
muLeo	0.522	0.093	0.011	0.040	0.033	0.078	0.000	–0.015	10
HD 107328	–0.119	0.049	0.009	0.036	0.046	0.041	0.009	–0.017	13
HD 122563	–2.325	0.082	0.001	0.024	0.006	0.040	0.005	–0.030	05
Gmb1830	–1.151	0.085	0.037	0.019	0.011	0.001	0.013	0.000	10
betGem	0.139	0.055	0.006	0.027	0.016	0.037	0.031	–0.013	13
epsVir	0.178	0.046	0.012	0.016	0.006	0.046	0.007	–0.016	13
ksiHya	0.077	0.060	0.002	0.009	0.005	0.051	0.007	–0.016	13
delEri	0.139	0.060	0.005	0.013	0.006	0.025	0.017	–0.007	12

Table A.2. continued.

Star	[Si/H]	$\sigma(\log\epsilon)$	Δ[Fe/H]	$\Delta T_{\rm eff}$	$\Delta\log g$	$\Delta v_{\rm mic}$	ΔLTE	NLTE	NLIN
epsEri	–0.095	0.102	0.006	0.010	0.008	0.006	0.001	0.000	09
epsFor	–0.375	0.036	0.016	0.019	0.016	0.010	0.013	–0.010	12
alfCenB	0.234	0.043	0.008	0.008	0.009	0.026	0.032	–0.001	11
muCas	–0.579	0.056	0.004	0.007	0.004	0.008	0.051	–0.001	14
tauCet	–0.354	0.031	0.007	0.013	0.013	0.015	0.005	0.000	15
HD 140283	–2.246	0.042	0.005	0.040	0.015	0.005	0.000	–0.010	01
18Sco	0.048	0.018	0.010	0.003	0.006	0.017	0.002	–0.005	15
Sun	0.000	0.080	0.010	0.007	0.000	0.014	0.002	–0.005	15
alfCenA	0.250	0.027	0.012	0.001	0.005	0.009	0.009	–0.007	14
HD 22879	–0.586	0.075	0.010	0.009	0.007	0.009	0.020	–0.008	14
betHyi	–0.067	0.030	0.019	0.005	0.005	0.007	0.004	–0.009	15
muAra	0.327	0.038	0.017	0.001	0.008	0.014	0.004	–0.008	13
betVir	0.132	0.043	0.019	0.007	0.005	0.011	0.001	–0.009	15
etaBoo	0.362	0.103	0.030	0.007	0.008	0.026	0.027	–0.010	09
HD 84937	–1.731	0.176	0.002	0.021	0.008	0.002	0.000	–0.008	06
Procyon	–0.033	0.071	0.005	0.023	0.006	0.010	0.018	–0.011	13
HD 49933	–0.383	0.080	0.011	0.014	0.008	0.021	0.001	–0.009	12

Table A.3. Final abundances for calcium.

Star	[Ca/H]	$\sigma(\log\epsilon)$	Δ[Fe/H]	$\Delta T_{\rm eff}$	$\Delta\log g$	$\Delta v_{\rm mic}$	ΔLTE	NLTE	NLIN
psiPhe	–0.694	0.291	0.241	0.016	0.002	0.084	0.147	–0.060	01
alfCet	–0.456	0.132	0.025	0.029	0.015	0.117	0.055	–0.015	02
gamSge	–0.292	0.089	0.071	0.045	0.013	0.136	0.065	–0.033	03
alfTau	–0.340	0.064	0.015	0.043	0.009	0.125	0.009	–0.020	03
61CygB	–0.403	0.059	0.010	0.007	0.008	0.043	0.000	–0.003	03
betAra	–0.136	0.081	0.064	0.063	0.003	0.117	0.110	0.010	02
Arcturus	–0.405	0.125	0.017	0.012	0.014	0.035	0.009	–0.072	08
HD 220009	–0.493	0.051	0.004	0.020	0.027	0.039	0.014	–0.095	06
61CygA	–0.356	0.104	0.013	0.005	0.000	0.007	0.058	–0.015	06
muLeo	0.280	0.116	0.018	0.036	0.023	0.060	0.032	–0.113	03
HD 107328	–0.321	0.067	0.043	0.014	0.062	0.058	0.006	–0.085	06
HD 122563	–2.434	0.080	0.003	0.051	0.006	0.040	0.005	0.068	15
Gmb1830	–1.243	0.057	0.056	0.049	0.004	0.038	0.025	–0.009	14
betGem	0.076	0.075	0.050	0.010	0.016	0.050	0.127	–0.076	07
epsVir	0.106	0.096	0.020	0.014	0.009	0.056	0.000	–0.090	07
ksiHya	0.068	0.072	0.016	0.007	0.007	0.068	0.004	–0.084	07
delEri	0.025	0.093	0.022	0.004	0.007	0.039	0.021	–0.041	08
epsEri	–0.055	0.069	0.003	0.014	0.002	0.009	0.003	–0.027	06
epsFor	–0.272	0.062	0.028	0.057	0.008	0.032	0.003	–0.051	10
alfCenB	0.225	0.054	0.025	0.012	0.002	0.048	0.018	–0.014	05
muCas	–0.573	0.035	0.007	0.018	0.004	0.037	0.002	–0.035	13
tauCet	–0.291	0.055	0.008	0.011	0.004	0.064	0.011	–0.037	11
HD 140283	–2.311	0.094	0.004	0.060	0.003	0.015	0.002	0.031	12
18Sco	0.058	0.036	0.010	0.028	0.001	0.034	0.001	–0.047	12
Sun	0.000	0.090	0.015	0.008	0.000	0.029	0.002	–0.044	13
alfCenA	0.194	0.028	0.025	0.006	0.001	0.015	0.010	–0.044	10
HD 22879	–0.531	0.054	0.016	0.051	0.005	0.028	0.012	–0.038	18
betHyi	–0.061	0.057	0.020	0.018	0.002	0.012	0.004	–0.061	14
muAra	0.320	0.049	0.038	0.017	0.001	0.024	0.007	–0.037	09
betVir	0.135	0.055	0.021	0.016	0.000	0.018	0.003	–0.039	11
etaBoo	0.290	0.100	0.046	0.002	0.003	0.035	0.037	–0.035	08
HD 84937	–1.665	0.082	0.017	0.039	0.006	0.010	0.022	0.003	14
Procyon	0.036	0.065	0.007	0.035	0.000	0.023	0.014	–0.049	15
HD 49933	–0.336	0.080	0.010	0.027	0.000	0.048	0.002	–0.062	17

Table A.4. Final abundances for titanium.

Star	[Ti/H]	$\sigma(\log\epsilon)$	Δ[Fe/H]	$\Delta T_{\rm eff}$	$\Delta\log g$	$\Delta v_{\rm mic}$	ΔLTE	NLTE	NLIN
psiPhe	–0.886	0.332	0.026	0.075	0.018	0.165	0.135	–	10
alfCet	–0.525	0.108	0.061	0.027	0.068	0.104	0.064	–	05
gamSge	–0.266	0.099	0.008	0.038	0.068	0.158	0.002	–	12
alfTau	–0.338	0.147	0.006	0.037	0.031	0.138	0.091	–	12
61CygB	–0.369	0.090	0.002	0.016	0.009	0.069	0.026	–	28
betAra	–0.414	0.215	0.052	0.082	0.028	0.102	0.033	–	06
Arcturus	–0.313	0.078	0.017	0.046	0.013	0.051	0.015	–	37
HD 220009	–0.534	0.051	0.006	0.068	0.021	0.040	0.017	–	31
61CygA	–0.288	0.109	0.026	0.027	0.002	0.010	0.000	–	39
muLeo	0.322	0.099	0.002	0.060	0.018	0.105	0.010	–	20
HD 107328	–0.131	0.040	0.032	0.077	0.020	0.065	0.011	–	29
HD 122563	–2.496	0.128	0.001	0.057	0.009	0.041	0.007	–	31
Gmb1830	–1.238	0.116	0.035	0.058	0.005	0.019	0.006	–	44
betGem	0.060	0.070	0.021	0.063	0.012	0.053	0.013	–	36
epsVir	–0.025	0.087	0.012	0.065	0.011	0.032	0.009	–	32
ksiHya	0.028	0.081	0.010	0.040	0.006	0.042	0.010	–	35
delEri	0.038	0.066	0.010	0.029	0.003	0.058	0.007	–	50
epsEri	–0.036	0.092	0.011	0.032	0.000	0.008	0.016	–	36
epsFor	–0.224	0.088	0.023	0.078	0.009	0.026	0.023	–	52
alfCenB	0.293	0.076	0.020	0.020	0.001	0.067	0.008	–	48
muCas	–0.524	0.057	0.008	0.026	0.002	0.024	0.032	–	52
tauCet	–0.165	0.070	0.008	0.024	0.009	0.065	0.019	–	56
HD 140283	–2.418	0.058	0.010	0.090	0.005	0.041	0.027	–	05
18Sco	0.046	0.026	0.011	0.062	0.008	0.027	0.017	–	53
Sun	0.000	0.070	0.014	0.010	0.000	0.025	0.013	–	54
alfCenA	0.206	0.037	0.017	0.021	0.004	0.014	0.018	–	52
HD 22879	–0.545	0.096	0.002	0.053	0.007	0.017	0.005	–	50
betHyi	–0.074	0.040	0.014	0.033	0.004	0.009	0.008	–	44
muAra	0.388	0.052	0.025	0.051	0.010	0.020	0.013	–	52
betVir	0.068	0.060	0.011	0.030	0.005	0.013	0.003	–	42
etaBoo	0.212	0.108	0.034	0.022	0.007	0.023	0.010	–	35
HD 84937	–1.664	0.112	0.005	0.024	0.030	0.004	0.033	–	15
Procyon	–0.069	0.085	0.001	0.048	0.006	0.011	0.015	–	29
HD 49933	–0.394	0.074	0.010	0.032	0.011	0.030	0.004	–	18

Table A.5. Final abundances for scandium.

Star	[Sc/H]	$\sigma(\log\epsilon)$	Δ[Fe/H]	$\Delta T_{\rm eff}$	$\Delta\log g$	$\Delta v_{\rm mic}$	ΔLTE	NLTE	NLIN
psiPhe	–0.674	0.507	0.077	0.025	0.060	0.094	0.045	–	02
alfCet	–0.397	0.199	0.158	0.015	0.111	0.110	0.068	–	04
gamSge	–0.319	0.290	0.025	0.029	0.108	0.154	0.005	–	07
alfTau	–0.264	0.198	0.025	0.035	0.068	0.158	0.114	–	08
61CygB	–0.324	0.075	0.005	0.010	0.020	0.040	0.000	–	04
betAra	–0.716	0.213	0.111	0.098	0.023	0.043	0.000	–	03
Arcturus	–0.428	0.140	0.003	0.033	0.018	0.033	0.024	–	10
HD 220009	–0.643	0.046	0.005	0.047	0.029	0.034	0.012	–	10
61CygA	–0.324	0.169	0.056	0.007	0.018	0.007	0.012	–	12
muLeo	0.230	0.062	0.022	0.044	0.018	0.068	0.018	–	04
HD 107328	–0.342	0.048	0.001	0.056	0.031	0.043	0.012	–	09
HD 122563	–2.500	0.077	0.051	0.016	0.026	0.039	0.030	–	07
Gmb1830	–1.264	0.075	0.114	0.002	0.014	0.008	0.052	–	07
betGem	0.062	0.122	0.013	0.053	0.020	0.035	0.018	–	09
epsVir	0.065	0.084	0.025	0.037	0.009	0.072	0.062	–	05
ksiHya	0.062	0.114	0.007	0.039	0.016	0.062	0.008	–	07

Table A.5. continued.

Star	[Sc/H]	$\sigma(\log\epsilon)$	Δ[Fe/H]	$\Delta T_{\rm eff}$	$\Delta\log g$	$\Delta v_{\rm mic}$	ΔLTE	NLTE	NLIN
delEri	0.077	0.104	0.000	0.029	0.006	0.040	0.006	–	12
epsEri	–0.164	0.097	0.009	0.023	0.011	0.008	0.010	–	11
epsFor	–0.508	0.067	0.014	0.038	0.023	0.025	0.022	–	10
alfCenB	0.304	0.085	0.009	0.020	0.006	0.039	0.009	–	12
muCas	–0.686	0.069	0.009	0.012	0.005	0.021	0.092	–	08
tauCet	–0.343	0.062	0.003	0.010	0.013	0.039	0.014	–	10
HD 140283	–2.668	NaN	0.005	0.047	0.044	0.002	0.027	–	02
18Sco	0.043	0.016	0.006	0.019	0.010	0.041	0.013	–	08
Sun	0.000	0.140	0.009	0.018	0.000	0.031	0.016	–	08
alfCenA	0.297	0.052	0.001	0.010	0.004	0.015	0.023	–	08
HD 22879	–0.788	0.075	0.013	0.015	0.009	0.019	0.010	–	08
betHyi	–0.043	0.039	0.007	0.021	0.008	0.010	0.015	–	07
muAra	0.401	0.057	0.003	0.044	0.013	0.022	0.012	–	10
betVir	0.183	0.039	0.004	0.013	0.007	0.018	0.010	–	07
etaBoo	0.227	0.087	0.011	0.006	0.008	0.056	0.039	–	03
HD 84937	–1.895	0.150	0.005	0.032	0.019	0.026	0.017	–	03
Procyon	–0.134	0.061	0.004	0.019	0.007	0.015	0.021	–	05
HD 49933	–0.488	0.050	0.000	0.021	0.011	0.040	0.004	–	07

Table A.6. Final abundances for vanadium.

Star	[V/H]	$\sigma(\log\epsilon)$	Δ[Fe/H]	$\Delta T_{\rm eff}$	$\Delta\log g$	$\Delta v_{\rm mic}$	ΔLTE	NLTE	NLIN
psiPhe	–1.178	0.353	0.035	0.136	0.043	0.146	0.138	–	04
alfCet	–0.172	0.274	0.011	0.055	0.060	0.106	0.213	–	03
gamSge	–0.314	0.156	0.003	0.058	0.079	0.125	0.157	–	04
alfTau	–0.204	0.240	0.005	0.047	0.040	0.101	0.225	–	04
61CygB	–0.442	0.097	0.005	0.023	0.011	0.074	0.030	–	16
betAra	–0.474	0.087	0.047	0.128	0.041	0.029	0.375	–	03
Arcturus	–0.441	0.103	0.009	0.064	0.009	0.057	0.012	–	18
HD 220009	–0.674	0.051	0.015	0.087	0.017	0.038	0.019	–	14
61CygA	–0.331	0.115	0.086	0.026	0.004	0.010	0.006	–	25
muLeo	0.296	0.080	0.008	0.080	0.015	0.061	0.025	–	05
HD 107328	–0.197	0.062	0.018	0.094	0.013	0.052	0.012	–	11
HD 122563	–2.696	0.007	0.038	0.128	0.008	0.000	0.005	–	01
Gmb1830	–1.395	0.103	0.001	0.076	0.002	0.012	0.000	–	08
betGem	0.059	0.157	0.000	0.091	0.003	0.054	0.019	–	17
epsVir	–0.031	0.071	0.005	0.087	0.007	0.028	0.014	–	14
ksiHya	0.053	0.072	0.004	0.051	0.005	0.031	0.011	–	14
delEri	0.037	0.046	0.001	0.036	0.002	0.055	0.023	–	21
epsEri	–0.017	0.118	0.001	0.038	0.003	0.008	0.025	–	20
epsFor	–0.395	0.030	0.033	0.075	0.000	0.015	0.030	–	23
alfCenB	0.363	0.054	0.001	0.024	0.004	0.064	0.023	–	21
muCas	–0.663	0.027	0.012	0.031	0.003	0.010	0.032	–	17
tauCet	–0.248	0.028	0.005	0.024	0.022	0.089	0.045	–	20
HD 140283	–	–	–	–	–	–	–	–	–
18Sco	0.035	0.013	0.005	0.070	0.006	0.010	0.016	–	18
Sun	0.000	0.040	0.002	0.012	0.000	0.010	0.014	–	17
alfCenA	0.241	0.031	0.010	0.027	0.002	0.009	0.050	–	21
HD 22879	–0.731	0.050	0.010	0.068	0.110	0.012	0.013	–	08
betHyi	–0.079	0.037	0.003	0.045	0.000	0.005	0.014	–	15
muAra	0.427	0.028	0.007	0.059	0.002	0.012	0.024	–	22
betVir	0.074	0.032	0.009	0.037	0.001	0.005	0.005	–	13
etaBoo	0.223	0.071	0.029	0.031	0.002	0.009	0.063	–	13
HD 84937	–	–	–	–	–	–	–	–	–
Procyon	–0.140	0.088	0.010	0.050	0.005	0.002	0.021	–	04
HD 49933	–0.260	0.085	0.038	0.060	0.010	0.007	0.020	–	01

Table A.7. Final abundances for chromium.

Star	[Cr/H]	$\sigma(\log\epsilon)$	Δ[Fe/H]	$\Delta T_{\rm eff}$	$\Delta\log g$	$\Delta v_{\rm mic}$	ΔLTE	NLTE	NLIN
psiPhe	–0.835	0.103	0.138	0.070	0.023	0.070	0.195	0.025	02
alfCet	–0.472	0.115	0.133	0.068	0.030	0.075	0.191	0.060	03
gamSge	–0.152	0.060	0.035	0.043	0.056	0.104	0.017	0.025	06
alfTau	–0.295	0.214	0.019	0.033	0.020	0.097	0.190	0.060	06
61CygB	–0.339	0.095	0.000	0.008	0.015	0.019	0.075	0.005	13
betAra	–0.223	0.165	0.119	0.080	0.009	0.066	0.000	0.063	06
Arcturus	–0.582	0.069	0.008	0.035	0.010	0.014	0.013	0.091	15
HD 220009	–0.742	0.030	0.017	0.052	0.010	0.019	0.011	0.115	12
61CygA	–0.341	0.111	0.058	0.020	0.006	0.008	0.048	0.015	14
muLeo	0.335	0.083	0.009	0.049	0.008	0.092	0.014	0.050	14
HD 107328	–0.410	0.035	0.012	0.054	0.013	0.019	0.005	0.079	11
HD 122563	–3.080	0.105	0.015	0.087	0.005	0.054	0.002	0.386	07
Gmb1830	–1.551	0.141	0.023	0.061	0.006	0.047	0.010	0.098	13
betGem	0.077	0.044	0.020	0.054	0.006	0.028	0.008	0.057	13
epsVir	0.057	0.054	0.008	0.051	0.003	0.028	0.004	0.059	15
ksiHya	0.077	0.042	0.012	0.029	0.008	0.032	0.001	0.059	15
delEri	0.031	0.061	0.004	0.021	0.001	0.035	0.007	0.054	15
epsEri	–0.028	0.084	0.003	0.024	0.002	0.009	0.009	0.044	11
epsFor	–0.518	0.055	0.003	0.056	0.006	0.015	0.024	0.097	10
alfCenB	0.274	0.049	0.002	0.016	0.000	0.039	0.014	0.034	14
muCas	–0.825	0.050	0.002	0.026	0.003	0.046	0.014	0.082	12
tauCet	–0.417	0.036	0.000	0.019	0.004	0.051	0.009	0.067	12
HD 140283	–2.892	0.130	0.013	0.098	0.005	0.032	0.060	0.334	05
18Sco	0.049	0.023	0.006	0.051	0.004	0.017	0.013	0.049	13
Sun	0.000	0.060	0.003	0.011	0.000	0.023	0.013	0.051	15
alfCenA	0.205	0.041	0.005	0.015	0.007	0.011	0.016	0.045	15
HD 22879	–0.856	0.085	0.002	0.060	0.005	0.021	0.002	0.111	16
betHyi	–0.098	0.045	0.002	0.042	0.001	0.014	0.028	0.059	12
muAra	0.370	0.038	0.006	0.040	0.004	0.016	0.009	0.041	15
betVir	0.081	0.034	0.008	0.026	0.006	0.012	0.003	0.047	13
etaBoo	0.236	0.081	0.017	0.020	0.004	0.022	0.018	0.047	08
HD 84937	–2.228	0.066	0.002	0.076	0.005	0.001	0.010	0.237	04
Procyon	–0.118	0.064	0.011	0.050	0.009	0.015	0.020	0.052	13
HD 49933	–0.529	0.082	0.004	0.054	0.008	0.024	0.002	0.088	06

Table A.8. Final abundances for manganese.

Star	[Mn/H]	$\sigma(\log\epsilon)$	Δ[Fe/H]	$\Delta T_{\rm eff}$	$\Delta\log g$	$\Delta v_{\rm mic}$	ΔLTE	NLTE	NLIN
psiPhe	–	–	–	–	–	–	–	–	–
alfCet	–0.457	0.048	0.013	0.037	0.045	0.204	0.030	–0.000	02
gamSge	–	–	–	–	–	–	–	–	–
alfTau	–0.487	0.096	0.005	0.058	0.033	0.176	0.000	–0.000	02
61CygB	–0.443	0.096	0.005	0.012	0.015	0.042	0.030	–0.000	06
betAra	–	–	–	–	–	–	–	–	–
Arcturus	–0.893	0.139	0.018	0.033	0.018	0.059	0.051	0.017	06
HD 220009	–1.107	0.088	0.026	0.051	0.032	0.053	0.028	0.027	06
61CygA	–0.417	0.112	0.094	0.005	0.007	0.008	0.062	–0.000	08
muLeo	0.087	0.201	0.087	0.061	0.094	0.147	0.070	–	02
HD 107328	–0.680	0.045	0.011	0.044	0.037	0.101	0.042	0.015	06

Table A.8. continued.

Star	[Mn/H]	$\sigma(\log\epsilon)$	Δ[Fe/H]	$\Delta T_{\rm eff}$	$\Delta\log g$	$\Delta v_{\rm mic}$	ΔLTE	NLTE	NLIN
HD 122563	–3.104	0.135	0.039	0.071	0.006	0.050	0.007	0.170	02
Gmb1830	–1.788	0.186	0.019	0.032	0.004	0.021	0.060	–0.000	10
betGem	–0.159	0.122	0.017	0.055	0.007	0.096	0.054	–0.000	06
epsVir	–0.125	0.103	0.020	0.062	0.004	0.111	0.042	–0.000	06
ksiHya	–0.105	0.105	0.036	0.039	0.002	0.136	0.034	–0.000	06
delEri	–0.032	0.089	0.002	0.023	0.001	0.069	0.087	–0.000	08
epsEri	–0.161	0.061	0.002	0.026	0.001	0.014	0.039	–	06
epsFor	–0.720	0.079	0.021	0.094	0.014	0.037	0.009	–0.000	10
alfCenB	0.232	0.094	0.006	0.018	0.005	0.076	0.083	–0.000	08
muCas	–1.010	0.026	0.007	0.029	0.005	0.023	0.006	–0.000	08
tauCet	–0.511	0.039	0.007	0.022	0.010	0.054	0.001	–0.000	10
HD 140283	–2.777	NaN	0.005	0.072	0.005	0.035	0.010	0.220	01
18Sco	0.040	0.018	0.004	0.075	0.003	0.048	0.010	–0.000	11
Sun	0.000	0.090	0.017	0.012	0.000	0.042	0.001	0.017	10
alfCenA	0.245	0.030	0.016	0.021	0.001	0.026	0.003	–0.000	11
HD 22879	–1.157	0.078	0.018	0.079	0.007	0.010	0.005	0.047	10
betHyi	–0.121	0.033	0.018	0.047	0.003	0.013	0.004	–0.000	09
muAra	0.430	0.044	0.014	0.059	0.005	0.043	0.017	–0.000	11
betVir	0.096	0.056	0.039	0.038	0.001	0.020	0.003	–0.000	11
etaBoo	0.271	0.065	0.041	0.034	0.001	0.040	0.035	–0.000	08
HD 84937	–	–	–	–	–	–	–	–	–
Procyon	–0.125	0.067	0.019	0.060	0.005	0.012	0.013	0.019	07
HD 49933	–0.607	0.074	0.062	0.062	0.010	0.020	0.031	0.023	04

Table A.9. Final abundances for cobalt.

Star	[Co/H]	$\sigma(\log\epsilon)$	Δ[Fe/H]	$\Delta T_{\rm eff}$	$\Delta\log g$	$\Delta v_{\rm mic}$	ΔLTE	NLTE	NLIN
psiPhe	–0.617	0.361	0.099	0.002	0.072	0.090	0.156	–	04
alfCet	–0.332	0.128	0.088	0.012	0.079	0.106	0.045	–	11
gamSge	–0.101	0.088	0.067	0.014	0.104	0.146	0.013	–	11
alfTau	–0.248	0.181	0.026	0.016	0.045	0.108	0.045	–	11
61CygB	–0.338	0.153	0.003	0.005	0.016	0.015	0.029	–	10
betAra	–0.083	0.102	0.074	0.010	0.055	0.141	0.069	–	06
Arcturus	–0.407	0.050	0.010	0.012	0.015	0.043	0.015	–	16
HD 220009	–0.674	0.040	0.016	0.023	0.037	0.032	0.014	–	13
61CygA	–0.301	0.199	0.078	0.003	0.011	0.009	0.018	–	17
muLeo	0.452	0.094	0.028	0.008	0.031	0.125	0.006	–	07
HD 107328	–0.180	0.021	0.023	0.021	0.034	0.064	0.014	–	11
HD 122563	–2.642	–	0.013	0.087	0.005	0.000	0.005	–	01
Gmb1830	–1.384	0.119	0.056	0.032	0.007	0.013	0.005	–	03
betGem	0.015	0.050	0.019	0.030	0.016	0.058	0.007	–	16
epsVir	–0.027	0.075	0.007	0.045	0.005	0.039	0.006	–	16
ksiHya	–0.009	0.078	0.006	0.028	0.004	0.043	0.005	–	16
delEri	0.070	0.042	0.010	0.011	0.008	0.043	0.006	–	18
epsEri	–0.198	0.163	0.008	0.012	0.007	0.007	0.007	–	14
epsFor	–0.470	0.043	0.007	0.065	0.007	0.012	0.021	–	17
alfCenB	0.286	0.034	0.015	0.010	0.006	0.044	0.009	–	16
muCas	–0.718	0.040	0.001	0.020	0.013	0.010	0.022	–	11
tauCet	–0.350	0.030	0.000	0.013	0.028	0.062	0.009	–	17

Table A.9. continued.

Star	[Co/H]	$\sigma(\log\epsilon)$	Δ[Fe/H]	$\Delta T_{\rm eff}$	$\Delta\log g$	$\Delta v_{\rm mic}$	ΔLTE	NLTE	NLIN
HD 140283	–	–	–	–	–	–	–	–	–
18Sco	0.024	0.018	0.003	0.062	0.002	0.011	0.009	–	18
Sun	0.000	0.090	0.002	0.009	0.000	0.009	0.012	–	19
alfCenA	0.266	0.029	0.000	0.021	0.005	0.009	0.018	–	18
HD 22879	–0.742	0.025	0.004	0.057	0.018	0.009	0.032	–	04
betHyi	–0.077	0.025	0.000	0.037	0.003	0.007	0.009	–	15
muAra	0.424	0.030	0.001	0.050	0.003	0.012	0.010	–	18
betVir	0.082	0.041	0.010	0.034	0.003	0.006	0.001	–	13
etaBoo	0.321	0.065	0.019	0.023	0.000	0.018	0.016	–	13
HD 84937	–	–	–	–	–	–	–	–	–
Procyon	–0.099	0.019	0.002	0.053	0.005	0.002	0.015	–	03
HD 49933	–	–	–	–	–	–	–	–	–

Table A.10. Final abundances for nickel.

Star	[Ni/H]	$\sigma(\log\epsilon)$	Δ[Fe/H]	$\Delta T_{\rm eff}$	$\Delta\log g$	$\Delta v_{\rm mic}$	ΔLTE	NLTE	NLIN
psiPhe	–1.220	0.393	0.109	0.126	0.069	0.138	0.436	–	02
alfCet	–0.637	0.161	0.062	0.012	0.128	0.161	0.082	–	05
gamSge	–0.174	0.131	0.044	0.019	0.110	0.209	0.001	–	05
alfTau	–0.397	0.214	0.017	0.014	0.048	0.181	0.026	–	06
61CygB	–0.428	0.075	0.003	0.004	0.023	0.046	0.088	–	12
betAra	–0.142	0.250	0.086	0.036	0.030	0.218	0.018	–	02
Arcturus	–0.487	0.083	0.002	0.006	0.019	0.043	0.009	–	17
HD 220009	–0.737	0.045	0.009	0.008	0.036	0.043	0.017	–	14
61CygA	–0.390	0.101	0.092	0.003	0.010	0.008	0.004	–	16
muLeo	0.324	0.115	0.004	0.025	0.036	0.092	0.017	–	04
HD 107328	–0.315	0.034	0.005	0.007	0.038	0.053	0.016	–	11
HD 122563	–2.687	0.099	0.005	0.071	0.005	0.031	0.001	–	14
Gmb1830	–1.504	0.127	0.109	0.021	0.010	0.013	0.010	–	19
betGem	0.085	0.050	0.004	0.014	0.012	0.071	0.022	–	14
epsVir	0.087	0.063	0.005	0.029	0.005	0.072	0.018	–	14
ksiHya	0.035	0.080	0.004	0.022	0.013	0.083	0.000	–	14
delEri	0.092	0.058	0.008	0.006	0.005	0.063	0.003	–	18
epsEri	–0.177	0.079	0.013	0.010	0.006	0.012	0.015	–	14
epsFor	–0.541	0.063	0.005	0.049	0.008	0.028	0.034	–	22
alfCenB	0.271	0.054	0.017	0.010	0.005	0.072	0.013	–	19
muCas	–0.826	0.038	0.004	0.017	0.004	0.027	0.015	–	20
tauCet	–0.447	0.040	0.004	0.008	0.030	0.059	0.015	–	22
HD 140283	–2.609	0.079	0.006	0.076	0.006	0.020	0.007	–	02
18Sco	0.039	0.017	0.002	0.052	0.008	0.032	0.012	–	22
Sun	0.000	0.100	0.006	0.008	0.000	0.030	0.013	–	21
alfCenA	0.254	0.033	0.001	0.017	0.003	0.018	0.021	–	20
HD 22879	–0.847	0.087	0.003	0.058	0.004	0.016	0.033	–	22
betHyi	–0.085	0.027	0.003	0.032	0.015	0.005	0.013	–	20
muAra	0.416	0.046	0.006	0.042	0.001	0.030	0.002	–	19
betVir	0.106	0.029	0.010	0.030	0.002	0.014	0.008	–	21
etaBoo	0.325	0.085	0.014	0.018	0.001	0.037	0.027	–	15
HD 84937	–2.062	0.117	0.002	0.084	0.023	0.005	0.007	–	03
Procyon	–0.112	0.069	0.002	0.049	0.002	0.011	0.013	–	20
HD 49933	–0.528	0.104	0.002	0.049	0.005	0.020	0.008	–	11

Appendix B: Literature compilation of abundances

In this Appendix we list the individual abundances that we found in the literature for the benchmark stars. Each element is in a different table for all stars, with the abundance in [X/H] and the value obtained from the reference indicated in the table. In several cases the value [X/H] had to be calculated using the solar abundances, as indicated in the respective reference. An important part of our compilation comes from the Hypatia catalogue (Hinkel et al. 2014).

A general comparison of our results (see Appendix A) and the literature is shown in Figs. 17 and 18 in the text. An important feature to note from these two figures is that we did not find a value for all stars and elements in the literature. This is true in particular for the cool stars such as α Cet, ψ Phe, and γ Sge. In addition, we did not find reported abundances of V and Mn for our hottest GBS, HD 49933, and Mg for ξ Hya. However, there are cases where although there is a value from the literature, we were unable to provide an abundance, such as Co for HD 140283 and HD 49933, and Mn for HD 84937 and β Ara. Example works in the literature providing several of these abundances for our metal-poor GBS are Hollek et al. (2011) and Gratton et al. (2003). They analysed spectral lines lying below 4500 Å, which is outside the wavelength range of our spectra. We were still able to provide most of the abundances based on very few lines, but since we have several methods, we can be confident that our abundances are reliable. Our results, which are mostly determined from very few lines, agree well with the literature for metal-poor stars, which provide abundances of more lines located in the blue part of the spectrum.

As discussed in Sect. 4, for cool stars we could not trust any of the abundances determined from the selected lines after visual inspection for some cases, such as Mg, Si and Mn for ψ Phe, and Mn for γ Sge and β Ara. We preferred to be conservative and have fewer abundance determinations, but ensured that our values are accurate. It still remains a challenge to derive abundances for these elements and stars; we were unable find a value reported in the literature, either, except [Mn/H] for β Ara of 0.36 by Luck (1979).

In general, our newly determined abundances agree very well with the literature, especially for the solar-like stars. There are a few cases where our abundances do not agree as well, such as the Ti and Ca abundances for γ Sge, α Tau, and 61 Cyg B, where our abundances are slightly lower. These stars are, however, very uncertain because their low temperatures cause their spectra to have several molecular lines that might be blended atomic lines. It is interesting to note that the abundances we determine for Gmb1830 are systematically lower than several literature measurements. We recall that the effective temperature of Gmb1830 is about 400 K below the typically adopted spectroscopic temperature of this star. We showed in Paper III that this temperature gave us a metallicity with a strong ionisation and excitation imbalance, suggesting that the angular diameter of this star needs to be measured again. Therefore this star does not currently have a recommended benchmark $T_{\rm eff}$ (see discussion in Paper I). Here we showed that with the stellar parameters of Papers I and III, most of the abundances we obtained do not agree with previous works in the literature.

Table B.1. Literature compilation for magnesium.

Star	[Mg/H]	Reference
psiPhe	–	–
alfCet	–	–
gamSge	–	–
alfTau	–0.16	Alves-Brito et al. (2010)
	–0.08	Alves-Brito et al. (2010)
	0.2	Thevenin (1998)
61CygB	–	–
betAra	–	–
Arcturus	–0.15	Ramírez & Allende Prieto (2011)
	–0.27	Worley et al. (2009)
	–0.1	Fulbright et al. (2007)
	–0.21	Britavskiy et al. (2012)
	–0.48	Mishenina & Kovtyukh (2001)
	–0.21	Britavskiy et al. (2012)
	–0.45	Thevenin (1998)
	0.02	Luck & Heiter (2005)
HD 220009	–0.48	Smiljanic et al. (2007)
61CygA	0.03	Milone et al. (2011)
	–0.07	Mishenina et al. (2008)
	–0.35	Affer et al. (2005)
	–0.02	Luck & Heiter (2005)
muLeo	0.44	Luck & Heiter (2007)
	0.32	Smith & Ruck (2000)
HD 107328	–0.01	Luck & Heiter (2007)
HD 122563	–2.16	Fulbright (2000)
	–2.55	Hollek et al. (2011)
	–2.38	Hollek et al. (2011)
	–2.23	Westin et al. (2000)
	–2.06	Bergemann & Gehren (2008)
	–2.22	Mashonkina et al. (2008)
	–2.39	Mashonkina et al. (2008)
Gmb1830	–0.9	Takeda (2007)
	–0.99	Zhao & Gehren (2000)
	–1.06	Zhao & Gehren (2000)
	–1.17	Fulbright (2000)
	–1.09	Bergemann & Gehren (2008)
	–1.08	Kotoneva et al. (2006)
	–1.12	Gehren et al. (2006)
	–1.09	Gehren et al. (2006)
	–0.9	Gratton et al. (2003)
	–1.1	Thevenin (1998)
betGem	0.02	Allende Prieto et al. (2004)
	0.29	Luck & Heiter (2007)
	0.48	Luck & Heiter (2005)
	0.07	Thevenin (1998)
epsVir	0.26	Luck & Heiter (2007)
	0.1	Thevenin (1998)
ksiHya	–	–
delEri	0.06	Allende Prieto et al. (2004)
	0.19	Adibekyan et al. (2012)
	0.38	Luck & Heiter (2005)
	0.33	Bensby et al. (2014)
	–0.05	Affer et al. (2005)
	0.24	Bensby et al. (2003)
	0.2	Thevenin (1998)
	0.24	Bensby et al. (2005)
	0.27	Neves et al. (2009)
	0.19	Delgado Mena et al. (2010)
epsEri	–0.03	Allende Prieto et al. (2004)
	–0.067	Adibekyan et al. (2012)
	0.05	Takeda (2007)
	0.05	Luck & Heiter (2005)
	–0.12	Mishenina et al. (2004)
	–0.14	Zhao et al. (2002)
	0.1	Thevenin (1998)
	–0.07	Gonzalez & Laws (2007)

Table B.1. continued.

Star	[Mg/H]	Reference
	–0.06	Neves et al. (2009)
	–0.17	Delgado Mena et al. (2010)
epsFor	–0.28	Fulbright (2000)
	–0.01	Bensby et al. (2014)
	–0.26	Reddy et al. (2006)
	–0.22	Bensby et al. (2003)
	–0.33	Gratton et al. (2003)
	–0.22	Bensby et al. (2005)
alfCenB	0.4	Allende Prieto et al. (2004)
	0.29	Porto de Mello et al. (2008)
muCas	–0.55	Allende Prieto et al. (2004)
	–0.38	Takeda (2007)
	–0.62	Reddy et al. (2006)
	–0.47	Luck & Heiter (2005)
	–0.57	Mishenina et al. (2004)
	–0.48	Zhao & Gehren (2000)
	–0.41	Zhao & Gehren (2000)
	–0.51	Fulbright (2000)
	–0.54	Gratton et al. (2003)
tauCet	–0.25	Allende Prieto et al. (2004)
	–0.283	Adibekyan et al. (2012)
	–0.16	Takeda (2007)
	–0.34	Francois (1986)
	0	Thevenin (1998)
	–0.27	Neves et al. (2009)
	–0.31	Delgado Mena et al. (2010)
HD 140283	–2.05	Thevenin (1998)
	–2.21	Gratton et al. (2003)
	–2.04	Fulbright (2000)
	–2.16	Jonsell et al. (2005)
	–2.28	Francois (1986)
	–2.13	Carretta et al. (2000)
	–1.95	Bergemann & Cescutti (2010)
	–2.08	Bensby et al. (2014)
18Sco	0.07	Thevenin (1998)
	0.09	Neves et al. (2009)
	0.08	Allende Prieto et al. (2004)
	0.13	Luck & Heiter (2005)
	0.05	Galeev et al. (2004)
	0.05	da Silva et al. (2012)
	0.03	Delgado Mena et al. (2010)
	0.12	González Hernández et al. (2010)
Sun	–	–
alfCenA	0.28	Edvardsson et al. (1993)
	0.1	Bond et al. (2008)
	0.39	Allende Prieto et al. (2004)
	0.27	da Silva et al. (2012)
	0.24	Porto de Mello et al. (2008)
HD 22879	–0.38	Thevenin (1998)
	–0.44	Bensby et al. (2005)
	–0.4	Edvardsson et al. (1993)
	–0.43	Reddy et al. (2006)
	–0.5	Neves et al. (2009)
	–0.38	Gratton et al. (2003)
	–0.5	Fulbright (2000)
	–0.49	Nissen & Schuster (2010)
	–0.44	Zhang & Zhao (2006)
	–0.53	Nissen & Schuster (1997)
	–0.35	Bensby et al. (2014)
betHyi	0	Thevenin (1998)
	–0.17	Allende Prieto et al. (2004)
	–0.06	Francois (1986)
	0.13	Bensby et al. (2014)
muAra	0.34	Bensby et al. (2005)
	0.32	Neves et al. (2009)
	0.2	Bond et al. (2008)
	0.32	Francois (1986)
	0.34	da Silva et al. (2012)
	0.28	Delgado Mena et al. (2010)
	0.34	González Hernández et al. (2010)
	0.35	Bensby et al. (2014)
betVir	0.17	Thevenin (1998)
	0.17	Edvardsson et al. (1993)
	0.04	Allende Prieto et al. (2004)
	0.07	Takeda (2007)
	0.38	Luck & Heiter (2005)
etaBoo	0.5	Thevenin (1998)
	0.47	Edvardsson et al. (1993)
	0.29	Allende Prieto et al. (2004)
	0.27	Takeda (2007)
HD 84937	–2.15	Thevenin (1998)
	–1.7	Gratton et al. (2003)
	–1.73	Fulbright (2000)
	–1.84	Bergemann & Cescutti (2010)
Procyon	0.1	Thevenin (1998)
	0.07	Edvardsson et al. (1993)
	–0.01	Allende Prieto et al. (2004)
	–0.03	Takeda (2007)
	0.07	Luck & Heiter (2005)
HD 49933	–0.1	Takeda (2007)

Table B.2. Literature compilation for silicon.

Star	[Si/H]	Reference
psiPhe	–	–
alfCet	–	–
gamSge	0.07	Boyarchuk et al. (1995)
alfTau	–0.11	Alves-Brito et al. (2010)
	–0.02	Alves-Brito et al. (2010)
	0	Thevenin (1998)
61CygB	–0.17	Luck & Heiter (2005)
betAra	0.67	Luck (1979)
Arcturus	–0.19	Ramírez & Allende Prieto (2011)
	–0.37	Worley et al. (2009)
	–0.15	Fulbright et al. (2007)
	–0.17	Britavskiy et al. (2012)
	–0.33	Mishenina & Kovtyukh (2001)
	–0.3	Thevenin (1998)
	–0.14	Luck & Heiter (2005)
HD 220009	–0.51	Smiljanic et al. (2007)
	–0.28	McWilliam (1990)
61CygA	0.19	Mishenina et al. (2008)
	–0.3	Affer et al. (2005)
	–0.06	Luck & Heiter (2005)
muLeo	0.69	McWilliam (1990)
	0.54	Luck & Heiter (2007)
	0.45	Thevenin (1998)
HD 107328	0.07	McWilliam (1990)
	–0.15	Luck & Heiter (2007)
	0.05	Thevenin (1998)
HD 122563	–2.37	Fulbright (2000)
	–2.28	Westin et al. (2000)
Gmb1830	–1.13	Takeda (2007)
	–1.13	Fulbright (2000)
	–1.12	Kotoneva et al. (2006)
	–1.21	Valenti & Fischer (2005)
	–0.95	Luck & Heiter (2005)
	–1.14	Gratton et al. (2003)
	–1	Thevenin (1998)
betGem	0.31	Allende Prieto et al. (2004)
	0.15	McWilliam (1990)

Table B.2. continued.

Star	[Si/H]	Reference
	0.23	Luck & Heiter (2007)
	0.25	Luck & Heiter (2005)
	0.08	Thevenin (1998)
epsVir	0.35	McWilliam (1990)
	0.21	Luck & Heiter (2007)
	0.15	Thevenin (1998)
ksiHya	0.15	McWilliam (1990)
	0.23	Bruntt et al. (2010)
delEri	0.24	Allende Prieto et al. (2004)
	0.32	Bensby et al. (2014)
	0.151	Adibekyan et al. (2012)
	0.22	Bruntt et al. (2010)
	0.08	Valenti & Fischer (2005)
	0.22	Luck & Heiter (2005)
	0.16	Affer et al. (2005)
	0.29	Bensby et al. (2003)
	0.1	Thevenin (1998)
	0.18	Bodaghee et al. (2003)
	0.29	Bensby et al. (2005)
	0.1	Gilli et al. (2006)
	0.17	Neves et al. (2009)
	0.16	Delgado Mena et al. (2010)
epsEri	–0.01	Allende Prieto et al. (2004)
	–0.121	Adibekyan et al. (2012)
	–0.05	Takeda (2007)
	–0.12	Valenti & Fischer (2005)
	–0.08	Luck & Heiter (2005)
	–0.05	Mishenina et al. (2004)
	–0.16	Zhao et al. (2002)
	0.12	Thevenin (1998)
	–0.1	Bodaghee et al. (2003)
	–0.15	Gonzalez et al. (2001)
	–0.16	Gilli et al. (2006)
	–0.1	Gonzalez & Laws (2007)
	–0.12	Neves et al. (2009)
	–0.12	Delgado Mena et al. (2010)
epsFor	–0.33	Fulbright (2000)
	–0.2	Bensby et al. (2014)
	–0.31	Bond et al. (2006)
	–0.38	Reddy et al. (2006)
	–0.38	Valenti & Fischer (2005)
	–0.37	Bensby et al. (2003)
	–0.44	Gratton et al. (2003)
	–0.37	Bensby et al. (2005)
	–0.31	Bond et al. (2008)
alfCenB	0.23	Valenti & Fischer (2005)
	0.45	Thevenin (1998)
	0.46	Allende Prieto et al. (2004)
	0.23	Gilli et al. (2006)
	0.27	Neuforge-Verheecke & Magain (1997)
	0.25	Porto de Mello et al. (2008)
muCas	–0.52	Allende Prieto et al. (2004)
	–0.58	Takeda (2007)
	–0.58	Reddy et al. (2006)
	–0.64	Luck & Heiter (2005)
	–0.57	Fulbright (2000)
	–0.62	Mishenina et al. (2004)
	–0.45	Thevenin (1998)
	–0.53	Gratton et al. (2003)
tauCet	–0.3	Allende Prieto et al. (2004)
	–0.364	Adibekyan et al. (2012)
	–0.3	Bruntt et al. (2010)
	–0.29	Takeda (2007)
	–0.29	Bond et al. (2006)
	–0.31	Valenti & Fischer (2005)
	–0.39	Luck & Heiter (2005)

Table B.2. continued.

Star	[Si/H]	Reference
	–0.25	Francois (1986)
	–0.17	Thevenin (1998)
	–0.38	Bodaghee et al. (2003)
	–0.43	Gilli et al. (2006)
	–0.29	Bond et al. (2008)
	–0.36	Neves et al. (2009)
	–0.37	Delgado Mena et al. (2010)
HD 140283	–2.1	Thevenin (1998)
	–2.29	Gratton et al. (2003)
	–2.1	Francois (1986)
18Sco	0.03	Valenti & Fischer (2005)
	0.05	Thevenin (1998)
	0.05	Neves et al. (2009)
	0.05	Allende Prieto et al. (2004)
	0.06	Mishenina et al. (2004)
	0.045	Ramírez et al. (2009)
	0	Luck & Heiter (2005)
	0.06	Galeev et al. (2004)
	0.06	Gilli et al. (2006)
	0.08	da Silva et al. (2012)
	0.04	Delgado Mena et al. (2010)
	0.04	González Hernández et al. (2010)
Sun	–	–
alfCenA	0.23	Valenti & Fischer (2005)
	0.35	Thevenin (1998)
	0.25	Edvardsson et al. (1993)
	0.23	Bond et al. (2008)
	0.32	Allende Prieto et al. (2004)
	0.27	Gilli et al. (2006)
	0.24	da Silva et al. (2012)
	0.27	Neuforge-Verheecke & Magain (1997)
	0.24	Porto de Mello et al. (2008)
HD 22879	–0.59	Valenti & Fischer (2005)
	–0.58	Thevenin (1998)
	–0.57	Bensby et al. (2005)
	–0.65	Edvardsson et al. (1993)
	–0.63	Reddy et al. (2006)
	–0.57	Neves et al. (2009)
	–0.59	Gratton et al. (2003)
	–0.49	Mishenina et al. (2004)
	–0.56	Fulbright (2000)
	–0.53	Nissen & Schuster (2010)
	–0.62	Zhang & Zhao (2006)
	–0.62	Nissen & Schuster (1997)
	–0.47	Bensby et al. (2014)
betHyi	–0.06	Valenti & Fischer (2005)
	–0.02	Thevenin (1998)
	–0.07	Allende Prieto et al. (2004)
	–0.14	Francois (1986)
	0.08	Bensby et al. (2014)
muAra	0.28	Valenti & Fischer (2005)
	0.3	Thevenin (1998)
	0.36	Bensby et al. (2005)
	0.31	Neves et al. (2009)
	0.31	Bond et al. (2008)
	0.28	Gonzalez et al. (2001)
	0.33	Gonzalez & Laws (2007)
	0.26	Gilli et al. (2006)
	0.32	Francois (1986)
	0.32	Bodaghee et al. (2003)
	0.3	da Silva et al. (2012)
	0.32	Delgado Mena et al. (2010)
	0.31	González Hernández et al. (2010)
	0.42	Bensby et al. (2014)
betVir	0.14	Valenti & Fischer (2005)
	0.3	Thevenin (1998)

Table B.2. continued.

Star	[Si/H]	Reference
	0.14	Edvardsson et al. (1993)
	0.11	Allende Prieto et al. (2004)
	0.2	Mishenina et al. (2004)
	0.15	Takeda (2007)
	0.12	Luck & Heiter (2005)
etaBoo	0.45	Thevenin (1998)
	0.33	Edvardsson et al. (1993)
	0.36	Allende Prieto et al. (2004)
	0.34	Takeda (2007)
	0.32	Luck & Heiter (2005)
HD 84937	–1.63	Gratton et al. (2003)
Procyon	0.01	Valenti & Fischer (2005)
	0.05	Thevenin (1998)
	0.01	Edvardsson et al. (1993)
	0.07	Allende Prieto et al. (2004)
	0.01	Takeda (2007)
	0	Luck & Heiter (2005)
HD 49933	–0.38	Thevenin (1998)
	–0.31	Edvardsson et al. (1993)
	–0.32	Takeda (2007)

Table B.3. Literature compilation for calcium.

Star	[Ca/H]	Reference
psiPhe	–	–
alfCet	–	–
gamSge	0.05	Boyarchuk et al. (1995)
alfTau	–0.36	Alves-Brito et al. (2010)
	–0.31	Alves-Brito et al. (2010)
	–0.1	Thevenin (1998)
61CygB	–0.12	Luck & Heiter (2005)
betAra	1.15	Luck (1979)
Arcturus	–0.41	Ramírez & Allende Prieto (2011)
	–0.42	Worley et al. (2009)
	–0.28	Fulbright et al. (2007)
	–0.32	Britavskiy et al. (2012)
	–0.19	Britavskiy et al. (2012)
	–0.32	Mishenina & Kovtyukh (2001)
	–0.2	Thevenin (1998)
	–0.56	Luck & Heiter (2005)
HD 220009	–0.57	Smiljanic et al. (2007)
	–0.6	McWilliam (1990)
61CygA	–0.36	Mishenina et al. (2008)
	–0.32	Affer et al. (2005)
	–0.05	Luck & Heiter (2005)
	–5.9	Zboril & Byrne (1998)
muLeo	0.21	McWilliam (1990)
	0.05	Luck & Heiter (2007)
	0.32	Smith & Ruck (2000)
	0.2	Thevenin (1998)
HD 107328	–0.47	McWilliam (1990)
	–0.42	Luck & Heiter (2007)
	–0.23	Thevenin (1998)
HD 122563	–2.46	Fulbright (2000)
	–2.6	Hollek et al. (2011)
	–2.59	Hollek et al. (2011)
	–2.45	Westin et al. (2000)
	–2.32	Mashonkina et al. (2008)
	–2.52	Mashonkina et al. (2008)
Gmb1830	–0.99	Takeda (2007)
	–1.09	Luck & Heiter (2005)
	–1.16	Fulbright (2000)
	–1.07	Clementini et al. (1999)
	–1.02	Kotoneva et al. (2006)
	–1.04	Gratton et al. (2003)

Table B.3. continued.

Star	[Ca/H]	Reference
	–1.1	Thevenin (1998)
betGem	0.3	Allende Prieto et al. (2004)
	–0.01	McWilliam (1990)
	0.09	Luck & Heiter (2007)
	0.08	Luck & Heiter (2005)
	0.03	Thevenin (1998)
epsVir	0.06	McWilliam (1990)
	0.09	Luck & Heiter (2007)
	0.2	Thevenin (1998)
ksiHya	–0.22	McWilliam (1990)
	0.22	Bruntt et al. (2010)
delEri	0.19	Allende Prieto et al. (2004)
	0.101	Adibekyan et al. (2012)
	0.18	Bruntt et al. (2010)
	0.30	Bensby et al. (2014)
	0.14	Luck & Heiter (2005)
	0.13	Affer et al. (2005)
	0.2	Bensby et al. (2003)
	–0.07	Thevenin (1998)
	0.1	Bodaghee et al. (2003)
	0.2	Bensby et al. (2005)
	–0.02	Gilli et al. (2006)
	0.09	Neves et al. (2009)
epsEri	–0.01	Allende Prieto et al. (2004)
	–0.035	Adibekyan et al. (2012)
	0.06	Takeda (2007)
	0	Luck & Heiter (2005)
	–0.11	Zhao et al. (2002)
	–0.1	Bodaghee et al. (2003)
	–0.19	Gonzalez et al. (2001)
	–0.2	Gilli et al. (2006)
	–0.01	Gonzalez & Laws (2007)
	–0.04	Neves et al. (2009)
epsFor	–0.15	Bensby et al. (2014)
	–0.44	Fulbright (2000)
	–0.42	Bond et al. (2006)
	–0.46	Reddy et al. (2006)
	–0.1	Thorén et al. (2004)
	–0.31	Bensby et al. (2003)
	–0.55	Gratton et al. (2003)
	–0.31	Bensby et al. (2005)
	–0.42	Bond et al. (2008)
alfCenB	0.47	Allende Prieto et al. (2004)
	0	Gilli et al. (2006)
	0.21	Neuforge-Verheecke & Magain (1997)
	0.34	Porto de Mello et al. (2008)
muCas	–0.65	Allende Prieto et al. (2004)
	–0.55	Takeda (2007)
	–0.64	Reddy et al. (2006)
	–0.72	Luck & Heiter (2005)
	–0.7	Fulbright (2000)
	–0.59	Gratton et al. (2003)
tauCet	–0.36	Allende Prieto et al. (2004)
	–5.942	Pavlenko et al. (2012)
	–0.363	Adibekyan et al. (2012)
	–0.3	Bruntt et al. (2010)
	–0.27	Takeda (2007)
	–0.38	Bond et al. (2006)
	–0.44	Luck & Heiter (2005)
	–0.4	Thevenin (1998)
	–0.41	Bodaghee et al. (2003)
	–0.52	Gilli et al. (2006)
	–0.38	Bond et al. (2008)
	–0.35	Neves et al. (2009)
HD 140283	–2.1	Thevenin (1998)
	–2.25	Gratton et al. (2003)

Table B.3. continued.

Star	[Ca/H]	Reference
	–2.14	Fulbright (2000)
	–2.28	Jonsell et al. (2005)
	–2.24	Bensby et al. (2014)
18Sco	0.05	Thevenin (1998)
	0.06	Neves et al. (2009)
	0.03	Allende Prieto et al. (2004)
	0.052	Ramírez et al. (2009)
	0.04	Luck & Heiter (2005)
	0.11	Galeev et al. (2004)
	–0.01	Gilli et al. (2006)
	0.07	da Silva et al. (2012)
	0.07	González Hernández et al. (2010)
Sun	–	–
alfCenA	0.3	Thevenin (1998)
	0.16	Edvardsson et al. (1993)
	0.08	Bond et al. (2008)
	0.4	Allende Prieto et al. (2004)
	0.17	Gilli et al. (2006)
	0.29	da Silva et al. (2012)
	0.22	Neuforge-Verheecke & Magain (1997)
	0.27	Porto de Mello et al. (2008)
HD 22879	–0.5	Thevenin (1998)
	–0.58	Bensby et al. (2005)
	–0.65	Edvardsson et al. (1993)
	–0.66	Reddy et al. (2006)
	–0.56	Neves et al. (2009)
	–0.55	Gratton et al. (2003)
	–0.65	Fulbright (2000)
	–0.55	Nissen & Schuster (2010)
	–0.58	Zhang & Zhao (2006)
	–0.63	Nissen & Schuster (1997)
	–0.46	Bensby et al. (2014)
betHyi	–0.05	Thevenin (1998)
	0.02	Allende Prieto et al. (2004)
	0.07	Bensby et al. (2014)
muAra	0.3	Bensby et al. (2005)
	0.24	Neves et al. (2009)
	0.18	Bond et al. (2008)
	0.12	Gonzalez et al. (2001)
	0.17	Gonzalez & Laws (2007)
	0.13	Gilli et al. (2006)
	0.22	Bodaghee et al. (2003)
	0.33	da Silva et al. (2012)
	0.25	González Hernández et al. (2010)
	0.37	Bensby et al. (2014)
betVir	0.26	Thevenin (1998)
	0.11	Edvardsson et al. (1993)
	0.13	Allende Prieto et al. (2004)
	0.12	Takeda (2007)
	0.11	Luck & Heiter (2005)
etaBoo	0.42	Thevenin (1998)
	0.23	Edvardsson et al. (1993)
	0.25	Allende Prieto et al. (2004)
	0.23	Takeda (2007)
	0.21	Luck & Heiter (2005)
HD 84937	–1.7	Thevenin (1998)
	–1.78	Gratton et al. (2003)
	–1.69	Fulbright (2000)
	–1.69	Jonsell et al. (2005)
Procyon	–0.07	Thevenin (1998)
	–0.04	Edvardsson et al. (1993)
	0.25	Allende Prieto et al. (2004)
	0.03	Takeda (2007)
	–0.01	Luck & Heiter (2005)
HD 49933	–0.4	Thevenin (1998)
	–0.39	Edvardsson et al. (1993)
	–0.38	Takeda (2007)

Table B.4. Literature compilation for titanium.

Star	[Ti/H]	Reference
psiPhe	–	–
alfCet	–	–
gamSge	0	Boyarchuk et al. (1995)
alfTau	0.01	Alves-Brito et al. (2010)
	0.05	Alves-Brito et al. (2010)
	0	Thevenin (1998)
61CygB	–0.05	Luck & Heiter (2005)
betAra	0.34	Luck (1979)
	0.43	Luck (1979)
Arcturus	–0.25	Ramírez & Allende Prieto (2011)
	–0.31	Ramírez & Allende Prieto (2011)
	–0.26	Worley et al. (2009)
	–0.28	Worley et al. (2009)
	–0.2	Fulbright et al. (2007)
	–0.31	Fulbright et al. (2007)
	–0.36	Chou et al. (2010)
	–0.28	Britavskiy et al. (2012)
	–0.2	Thevenin (1998)
	–0.39	Luck & Heiter (2005)
HD 220009	–0.33	Smiljanic et al. (2007)
	–0.45	McWilliam (1990)
61CygA	–0.18	Mishenina et al. (2008)
	–0.25	Affer et al. (2005)
	–0.08	Luck & Heiter (2005)
muLeo	0.09	McWilliam (1990)
	0.49	McWilliam (1990)
	0.3	Luck & Heiter (2007)
	0.35	Smith & Ruck (2000)
	0.12	Thevenin (1998)
HD 107328	–0.44	McWilliam (1990)
	–0.29	Luck & Heiter (2007)
	–0.2	Thevenin (1998)
HD 122563	–2.57	Fulbright (2000)
	–2.83	Hollek et al. (2011)
	–2.71	Hollek et al. (2011)
	–2.82	Hollek et al. (2011)
	–2.55	Westin et al. (2000)
	–2.46	Westin et al. (2000)
Gmb1830	–0.86	Takeda (2007)
	–0.95	Takeda (2007)
	–1.16	Fulbright (2000)
	–0.93	Luck & Heiter (2005)
	–0.95	Clementini et al. (1999)
	–0.93	Kotoneva et al. (2006)
	–1.04	Valenti & Fischer (2005)
	–1.08	Gratton et al. (2003)
	–1.33	Gratton et al. (2003)
	–0.85	Thevenin (1998)
betGem	0.32	Allende Prieto et al. (2004)
	–0.02	McWilliam (1990)
	0.16	McWilliam (1990)
	0.16	Luck & Heiter (2007)
	0.11	Luck & Heiter (2005)
	–0.02	Thevenin (1998)
epsVir	0.17	McWilliam (1990)
	0.29	McWilliam (1990)
	0.09	Luck & Heiter (2007)
	0.06	Thevenin (1998)
ksiHya	–0.09	McWilliam (1990)
	0.16	McWilliam (1990)
	0.11	Bruntt et al. (2010)
	0.2	Bruntt et al. (2010)
	–0.05	Thevenin (1998)
delEri	0.37	Allende Prieto et al. (2004)
	0.09	Valenti & Fischer (2005)
	0.37	Bensby et al. (2014)

Table B.4. continued.

Star	[Ti/H]	Reference
	0.28	Luck & Heiter (2005)
	0.12	Affer et al. (2005)
	0.165	Adibekyan et al. (2012)
	0.277	Adibekyan et al. (2012)
	0.15	Bruntt et al. (2010)
	0.12	Bruntt et al. (2010)
	0.32	Bensby et al. (2003)
	0.32	Bensby et al. (2003)
	–0.05	Thevenin (1998)
	0.25	Bodaghee et al. (2003)
	0.32	Bensby et al. (2005)
	0.17	Gilli et al. (2006)
	0.26	Neves et al. (2009)
	0.25	Neves et al. (2009)
epsEri	0.01	Allende Prieto et al. (2004)
	–0.05	Valenti & Fischer (2005)
	0.06	Luck & Heiter (2005)
	–0.061	Adibekyan et al. (2012)
	–0.134	Adibekyan et al. (2012)
	0.12	Takeda (2007)
	0.05	Takeda (2007)
	–0.07	Zhao et al. (2002)
	0	Bodaghee et al. (2003)
	–0.05	Gonzalez et al. (2001)
	–0.05	Gilli et al. (2006)
	–0.09	Gonzalez & Laws (2007)
	0.03	Neves et al. (2009)
	–0.17	Neves et al. (2009)
epsFor	–0.38	Fulbright (2000)
	–0.08	Bond et al. (2006)
	–0.27	Bond et al. (2006)
	–0.07	Bensby et al. (2014)
	–0.38	Reddy et al. (2006)
	–0.27	Valenti & Fischer (2005)
	–0.08	Thorén et al. (2004)
	–0.23	Bensby et al. (2003)
	–0.31	Bensby et al. (2003)
	–0.65	Gratton et al. (2003)
	–0.64	Gratton et al. (2003)
	–0.23	Bensby et al. (2005)
	–0.08	Bond et al. (2008)
	–0.27	Bond et al. (2008)
alfCenB	0.12	Valenti & Fischer (2005)
	0.5	Allende Prieto et al. (2004)
	0.26	Gilli et al. (2006)
	0.27	Neuforge-Verheecke & Magain (1997)
	0.269	Porto de Mello et al. (2008)
muCas	–0.41	Allende Prieto et al. (2004)
	–0.46	Takeda (2007)
	–0.57	Takeda (2007)
	–0.6	Reddy et al. (2006)
	–0.52	Luck & Heiter (2005)
	–0.64	Fulbright (2000)
	–0.45	Thevenin (1998)
	–0.54	Gratton et al. (2003)
	–0.62	Gratton et al. (2003)
tauCet	–0.14	Allende Prieto et al. (2004)
	–0.31	Valenti & Fischer (2005)
	–0.37	Luck & Heiter (2005)
	–7.298	Pavlenko et al. (2012)
	–0.315	Adibekyan et al. (2012)
	–0.25	Bruntt et al. (2010)
	–0.14	Takeda (2007)
	–0.09	Bond et al. (2006)
	–7.29	Pavlenko et al. (2012)
	–0.35	Adibekyan et al. (2012)

Table B.4. continued.

Star	[Ti/H]	Reference
	–0.27	Bruntt et al. (2010)
	–0.21	Takeda (2007)
	–0.25	Bond et al. (2006)
	–0.32	Thevenin (1998)
	–0.23	Bodaghee et al. (2003)
	–0.27	Gilli et al. (2006)
	–0.09	Bond et al. (2008)
	–0.25	Bond et al. (2008)
	–0.24	Neves et al. (2009)
	–0.34	Neves et al. (2009)
HD 140283	–2.35	Thevenin (1998)
	–2.23	Gratton et al. (2003)
	–2.23	Gratton et al. (2003)
	–2.11	Fulbright (2000)
	–2.23	Bensby et al. (2014)
18Sco	0.03	Valenti & Fischer (2005)
	0.02	Thevenin (1998)
	0.08	Neves et al. (2009)
	0.04	Neves et al. (2009)
	0.16	Allende Prieto et al. (2004)
	0.086	Ramírez et al. (2009)
	0.04	Luck & Heiter (2005)
	0.04	Galeev et al. (2004)
	0.06	Gilli et al. (2006)
	0.06	da Silva et al. (2012)
	0.05	González Hernández et al. (2010)
Sun	–	–
alfCenA	0.18	Valenti & Fischer (2005)
	0.25	Thevenin (1998)
	0.18	Edvardsson et al. (1993)
	0.04	Bond et al. (2008)
	–0.01	Bond et al. (2008)
	0.36	Allende Prieto et al. (2004)
	0.28	Gilli et al. (2006)
	0.24	da Silva et al. (2012)
	0.25	Neuforge-Verheecke & Magain (1997)
	0.23	Porto de Mello et al. (2008)
HD 22879	–0.55	Valenti & Fischer (2005)
	–0.5	Thevenin (1998)
	–0.53	Bensby et al. (2005)
	–0.65	Edvardsson et al. (1993)
	–0.66	Reddy et al. (2006)
	–0.54	Neves et al. (2009)
	–0.52	Neves et al. (2009)
	–0.64	Gratton et al. (2003)
	–0.58	Gratton et al. (2003)
	–0.59	Fulbright (2000)
	–0.6	Nissen & Schuster (2010)
	–0.58	Zhang & Zhao (2006)
	–0.63	Nissen & Schuster (1997)
	–0.37	Bensby et al. (2014)
betHyi	–0.02	Valenti & Fischer (2005)
	–0.08	Thevenin (1998)
	0	Allende Prieto et al. (2004)
	0.06	Bensby et al. (2014)
muAra	0.26	Valenti & Fischer (2005)
	0.35	Bensby et al. (2005)
	0.31	Neves et al. (2009)
	0.32	Neves et al. (2009)
	0.18	Bond et al. (2008)
	0.12	Bond et al. (2008)
	0.27	Gonzalez et al. (2001)
	0.31	Gonzalez & Laws (2007)
	0.3	Gilli et al. (2006)
	0.31	Bodaghee et al. (2003)
	0.29	da Silva et al. (2012)

Table B.4. continued.

Star	[Ti/H]	Reference
	0.31	González Hernández et al. (2010)
	0.37	Bensby et al. (2014)
betVir	0.17	Valenti & Fischer (2005)
	0.2	Thevenin (1998)
	0.17	Edvardsson et al. (1993)
	0.18	Allende Prieto et al. (2004)
	0.13	Takeda (2007)
	0.12	Takeda (2007)
	0.08	Luck & Heiter (2005)
etaBoo	0.48	Thevenin (1998)
	0.32	Edvardsson et al. (1993)
	0.29	Allende Prieto et al. (2004)
	0.37	Takeda (2007)
	0.36	Takeda (2007)
	0.29	Luck & Heiter (2005)
HD 84937	–1.85	Thevenin (1998)
	–1.81	Gratton et al. (2003)
	–1.81	Gratton et al. (2003)
	–1.68	Fulbright (2000)
Procyon	0.08	Valenti & Fischer (2005)
	0.06	Thevenin (1998)
	0.12	Edvardsson et al. (1993)
	0.13	Allende Prieto et al. (2004)
	0.09	Takeda (2007)
	0	Takeda (2007)
	–0.07	Luck & Heiter (2005)
HD 49933	0.06	Takeda (2007)
	–0.47	Takeda (2007)

Table B.5. Literature compilation for scandium.

Star	[Sc/H]	Reference
psiPhe	–	–
alfCet	–	–
gamSge	–0.13	Boyarchuk et al. (1995)
alfTau	–0.1	Thevenin (1998)
61CygB	–0.3	Luck & Heiter (2005)
	–0.26	Luck & Heiter (2005)
betAra	0.3	Luck (1979)
	–0.02	Luck (1979)
Arcturus	–0.37	Ramírez & Allende Prieto (2011)
	–0.29	Ramírez & Allende Prieto (2011)
	–0.37	Worley et al. (2009)
	–0.1	Thevenin (1998)
	–0.67	Luck & Heiter (2005)
HD 220009	–0.62	Smiljanic et al. (2007)
	–0.56	McWilliam (1990)
61CygA	0.07	Mishenina et al. (2008)
	–0.25	Luck & Heiter (2005)
muLeo	0.09	McWilliam (1990)
	0.1	Luck & Heiter (2007)
	0.28	Thevenin (1998)
HD 107328	–0.62	Luck & Heiter (2007)
	–0.08	Thevenin (1998)
HD122563	–2.89	Hollek et al. (2011)
	–2.95	Hollek et al. (2011)
	–2.59	Westin et al. (2000)
Gmb1830	–0.68	Takeda (2007)
	–1.23	Takeda (2007)
	–0.84	Kotoneva et al. (2006)
	–1.07	Gratton et al. (2003)
	–1.2	Thevenin (1998)
betGem	0.29	Allende Prieto et al. (2004)
	–0.25	McWilliam (1990)
	0.03	Luck & Heiter (2007)

Table B.5. continued.

Star	[Sc/H]	Reference
	–0.16	Luck & Heiter (2005)
	–0.07	Thevenin (1998)
epsVir	–0.16	McWilliam (1990)
	0.05	Luck & Heiter (2007)
	0.1	Thevenin (1998)
ksiHya	–0.24	McWilliam (1990)
	0.01	Bruntt et al. (2010)
	0.13	Bruntt et al. (2010)
delEri	0.38	Allende Prieto et al. (2004)
	–0.02	Luck & Heiter (2005)
	0.3	Affer et al. (2005)
	0.193	Adibekyan et al. (2012)
	0.232	Adibekyan et al. (2012)
	0.13	Battistini & Bensby (2015)
	0.14	Bruntt et al. (2010)
	0	Thorén et al. (2004)
	0.05	Thevenin (1998)
	0.2	Bodaghee et al. (2003)
	0.1	Gilli et al. (2006)
	0.29	Neves et al. (2009)
	0.21	Neves et al. (2009)
epsEri	0.02	Allende Prieto et al. (2004)
	–0.095	Adibekyan et al. (2012)
	–0.1	Takeda (2007)
	–0.187	Adibekyan et al. (2012)
	–0.04	Takeda (2007)
	–0.08	Luck & Heiter (2005)
	–0.1	Zhao et al. (2002)
	–0.07	Bodaghee et al. (2003)
	–0.16	Gonzalez et al. (2001)
	–0.22	Gilli et al. (2006)
	–0.12	Gonzalez & Laws (2007)
	0.01	Neves et al. (2009)
	–0.19	Neves et al. (2009)
epsFor	–0.11	Thorén et al. (2004)
	–0.33	Thorén et al. (2004)
	–0.48	Battistini & Bensby (2015)
	–0.44	Reddy et al. (2006)
	–0.09	Thorén et al. (2004)
alfCenB	0.5	Allende Prieto et al. (2004)
	0.26	Gilli et al. (2006)
	0.26	Neuforge-Verheecke & Magain (1997)
	0.26	Porto de Mello et al. (2008)
muCas	–0.5	Allende Prieto et al. (2004)
	–0.52	Takeda (2007)
	–0.7	Takeda (2007)
	–0.68	Reddy et al. (2006)
tauCet	–0.22	Allende Prieto et al. (2004)
	–0.4	Luck & Heiter (2005)
	–0.371	Adibekyan et al. (2012)
	–0.33	Takeda (2007)
	–0.413	Adibekyan et al. (2012)
	–0.33	Bruntt et al. (2010)
	–0.25	Takeda (2007)
	–0.35	Bodaghee et al. (2003)
	–0.41	Gilli et al. (2006)
	–0.34	Neves et al. (2009)
	–0.39	Neves et al. (2009)
HD 140283	–2.6	Thevenin (1998)
18Sco	0	Thevenin (1998)
	0.08	Neves et al. (2009)
	0.04	Neves et al. (2009)
	0.15	Allende Prieto et al. (2004)
	0.064	Ramírez et al. (2009)
	0.05	Luck & Heiter (2005)
	0.04	Galeev et al. (2004)

Table B.5. continued.

Star	[Sc/H]	Reference
	0.05	Gilli et al. (2006)
	0.12	da Silva et al. (2012)
	0.05	González Hernández et al. (2010)
Sun	–	–
alfCenA	0.3	Thevenin (1998)
	0.32	Allende Prieto et al. (2004)
	0.37	Gilli et al. (2006)
	0.26	da Silva et al. (2012)
	0.25	Neuforge-Verheecke & Magain (1997)
	0.24	Porto de Mello et al. (2008)
HD 22879	–0.4	Thevenin (1998)
	–0.71	Reddy et al. (2006)
	–0.61	Neves et al. (2009)
	–0.63	Neves et al. (2009)
	–0.72	Zhang & Zhao (2006)
	–0.6	Battistini & Bensby (2015)
betHyi	0.07	Thevenin (1998)
	–0.05	Battistini & Bensby (2015)
	–0.03	Allende Prieto et al. (2004)
muAra	0.37	Neves et al. (2009)
	0.38	Neves et al. (2009)
	0.32	Gonzalez et al. (2001)
	0.39	Gonzalez & Laws (2007)
	0.32	Gilli et al. (2006)
	0.38	Bodaghee et al. (2003)
	0.27	da Silva et al. (2012)
	0.39	González Hernández et al. (2010)
betVir	0.25	Thevenin (1998)
	0.15	Allende Prieto et al. (2004)
	0.1	Takeda (2007)
	0.16	Takeda (2007)
	0.23	Luck & Heiter (2005)
etaBoo	0.26	Allende Prieto et al. (2004)
	0.47	Takeda (2007)
HD 84937	–2.05	Thevenin (1998)
	–2.18	Gratton et al. (2003)
Procyon	0.1	Thevenin (1998)
	0.07	Allende Prieto et al. (2004)
	–0.08	Takeda (2007)
	0.01	Takeda (2007)
HD 49933	–0.49	Takeda (2007)

Table B.6. Literature compilation for vanadium.

Star	[V/H]	Reference
psiPhe	–	–
alfCet	–	–
gamSge	0	Boyarchuk et al. (1995)
	0.08	Boyarchuk et al. (1995)
alfTau	0.1	Thevenin (1998)
61CygB	–	–
betAra	0.3	Luck (1979)
	0.4	Luck (1979)
Arcturus	–0.32	Ramírez & Allende Prieto (2011)
	–0.35	Thevenin (1998)
	–0.48	Luck & Heiter (2005)
HD 220009	–0.44	Smiljanic et al. (2007)
	–0.88	McWilliam (1990)
61CygA	–0.33	Luck & Heiter (2005)
muLeo	0.43	Luck & Heiter (2007)
HD 107328	–0.51	Luck & Heiter (2007)
HD 122563	–2.67	Westin et al. (2000)
	–2.6	Westin et al. (2000)
	–2.83	Fulbright (2000)
Gmb1830	–1.16	Kotoneva et al. (2006)

Table B.6. continued.

Star	[V/H]	Reference
	–1	Takeda (2007)
	–1.38	Fulbright (2000)
	–1.21	Gratton et al. (2003)
	–1.2	Thevenin (1998)
betGem	–0.13	Luck & Heiter (2005)
	0.12	Luck & Heiter (2007)
	–0.02	Thevenin (1998)
epsVir	–0.03	Luck & Heiter (2007)
	0.06	Thevenin (1998)
ksiHya	0.2	Bruntt et al. (2010)
delEri	0.519	Adibekyan et al. (2012)
	0.28	Battistini & Bensby (2015)
	0.24	Bruntt et al. (2010)
	0.1	Thevenin (1998)
	0.34	Bodaghee et al. (2003)
	0.33	Gilli et al. (2006)
	0.51	Neves et al. (2009)
epsEri	0.196	Adibekyan et al. (2012)
	–0.01	Luck & Heiter (2005)
	–0.04	Zhao et al. (2002)
	0.12	Takeda (2007)
	–0.13	Takeda (2007)
	0.07	Bodaghee et al. (2003)
	–0.04	Gilli et al. (2006)
	0.2	Neves et al. (2009)
epsFor	–0.15	Thorén et al. (2004)
	–0.32	Battistini & Bensby (2015)
	–0.45	Reddy et al. (2006)
	–0.54	Fulbright (2000)
	–0.85	Gratton et al. (2003)
alfCenB	0.44	Gilli et al. (2006)
	0.32	Neuforge-Verheecke & Magain (1997)
	0.46	Porto de Mello et al. (2008)
muCas	–0.57	Takeda (2007)
	–0.71	Takeda (2007)
	–0.71	Reddy et al. (2006)
	–0.85	Fulbright (2000)
	–0.5	Thevenin (1998)
	–0.72	Gratton et al. (2003)
tauCet	–0.308	Adibekyan et al. (2012)
	–0.3	Bruntt et al. (2010)
	–0.44	Luck & Heiter (2005)
	–0.21	Takeda (2007)
	–0.25	Takeda (2007)
	–0.31	Bodaghee et al. (2003)
	–0.33	Gilli et al. (2006)
	–0.3	Neves et al. (2009)
HD 140283	–	–
18Sco	0.1	Thevenin (1998)
	0.06	Neves et al. (2009)
	0.069	Ramírez et al. (2009)
	0.01	Luck & Heiter (2005)
	–0.07	Galeev et al. (2004)
	0.07	Gilli et al. (2006)
	0.12	da Silva et al. (2012)
	0.04	González Hernández et al. (2010)
Sun	–	–
alfCenA	0.3	Thevenin (1998)
	0.37	Gilli et al. (2006)
	0.3	da Silva et al. (2012)
	0.23	Neuforge-Verheecke & Magain (1997)
	0.26	Porto de Mello et al. (2008)
HD 22879	–0.68	Reddy et al. (2006)
	–0.74	Neves et al. (2009)
	–0.88	Gratton et al. (2003)
	–0.73	Fulbright (2000)

Table B.6. continued.

Star	[V/H]	Reference
	–0.77	Zhang & Zhao (2006)
	–0.61	Battistini & Bensby (2015)
betHyi	0.2	Thevenin (1998)
	–0.12	Battistini & Bensby (2015)
muAra	0.36	Neves et al. (2009)
	0.35	Gilli et al. (2006)
	0.33	Bodaghee et al. (2003)
	0.34	da Silva et al. (2012)
	0.35	González Hernández et al. (2010)
	0.22	Battistini & Bensby (2015)
betVir	0.2	Thevenin (1998)
	0.12	Takeda (2007)
	0.13	Takeda (2007)
etaBoo	0.43	Takeda (2007)
	0.51	Takeda (2007)
HD 84937	–	–
Procyon	0.1	Thevenin (1998)
	0.13	Takeda (2007)
	–0.02	Takeda (2007)
HD 49933	–	–

Table B.7. Literature compilation for chromium.

Star	[Cr/H]	Reference
psiPhe	–	–
alfCet	–	–
gamSge	–0.03	Boyarchuk et al. (1995)
alfTau	–0.1	Thevenin (1998)
61CygB	–0.26	Luck & Heiter (2005)
betAra	0.53	Luck (1979)
	0.64	Luck (1979)
Arcturus	–0.57	Ramírez & Allende Prieto (2011)
	–0.2	Thevenin (1998)
	–0.55	Luck & Heiter (2005)
HD 220009	–0.72	Smiljanic et al. (2007)
61CygA	–0.03	Mishenina et al. (2008)
	–0.17	Affer et al. (2005)
	–0.04	Luck & Heiter (2005)
muLeo	0.37	Luck & Heiter (2007)
	0.1	Thevenin (1998)
HD 107328	–0.46	Luck & Heiter (2007)
	–0.1	Thevenin (1998)
HD 122563	–3.04	Fulbright (2000)
	–3.19	Hollek et al. (2011)
	–2.71	Hollek et al. (2011)
	–3.24	Hollek et al. (2011)
	–3.13	Westin et al. (2000)
Gmb1830	–1.2	Takeda (2007)
	–0.95	Takeda (2007)
	–1.41	Fulbright (2000)
	–1.38	Clementini et al. (1999)
	–1.04	Kotoneva et al. (2006)
	–1.13	Luck & Heiter (2005)
	–1.39	Gratton et al. (2003)
	–1.26	Gratton et al. (2003)
	–1.2	Thevenin (1998)
betGem	0.16	Luck & Heiter (2007)
	0.14	Luck & Heiter (2005)
	–0.02	Thevenin (1998)
epsVir	0.15	Luck & Heiter (2007)
	0.08	Thevenin (1998)
ksiHya	0.16	Bruntt et al. (2010)
	0.14	Bruntt et al. (2010)
	–0.05	Thevenin (1998)
delEri	0.156	Adibekyan et al. (2012)

Table B.7. continued.

Star	[Cr/H]	Reference
	0.31	Bensby et al. (2014)
	0.137	Adibekyan et al. (2012)
	0.11	Bruntt et al. (2010)
	0.2	Luck & Heiter (2005)
	0.03	Affer et al. (2005)
	0.25	Bensby et al. (2003)
	0.24	Bensby et al. (2003)
	0	Thevenin (1998)
	0.07	Bodaghee et al. (2003)
	0.25	Bensby et al. (2005)
	–0.01	Gilli et al. (2006)
	0.17	Neves et al. (2009)
	0.14	Neves et al. (2009)
epsEri	–0.065	Adibekyan et al. (2012)
	0.03	Takeda (2007)
	–0.147	Adibekyan et al. (2012)
	0.08	Takeda (2007)
	0.03	Luck & Heiter (2005)
	–0.01	Zhao et al. (2002)
	–0.09	Bodaghee et al. (2003)
	–0.16	Gilli et al. (2006)
	–0.18	Gonzalez & Laws (2007)
	–0.06	Neves et al. (2009)
	–0.16	Neves et al. (2009)
epsFor	–0.67	Fulbright (2000)
	–0.64	Reddy et al. (2006)
	–0.43	Bensby et al. (2014)
	–0.4	Thorén et al. (2004)
	–0.22	Thorén et al. (2004)
	–0.51	Bensby et al. (2003)
	–0.64	Bensby et al. (2003)
	–0.95	Gratton et al. (2003)
	–0.51	Bensby et al. (2005)
alfCenB	0.13	Gilli et al. (2006)
	0.27	Neuforge-Verheecke & Magain (1997)
	0.26	Neuforge-Verheecke & Magain (1997)
	0.31	Porto de Mello et al. (2008)
muCas	–0.79	Takeda (2007)
	–0.74	Takeda (2007)
	–0.96	Fulbright (2000)
	–0.86	Reddy et al. (2006)
	–0.78	Luck & Heiter (2005)
	–0.87	Gratton et al. (2003)
tauCet	–0.5	Adibekyan et al. (2012)
	–6.837	Pavlenko et al. (2012)
	–0.48	Bruntt et al. (2010)
	–0.43	Takeda (2007)
	–0.523	Adibekyan et al. (2012)
	–0.52	Bruntt et al. (2010)
	–0.42	Takeda (2007)
	–0.56	Luck & Heiter (2005)
	–0.55	Thevenin (1998)
	–0.51	Bodaghee et al. (2003)
	–0.58	Gilli et al. (2006)
	–0.49	Neves et al. (2009)
	–0.49	Neves et al. (2009)
HD 140283	–2.3	Thevenin (1998)
	–2.75	Gratton et al. (2003)
	–2.44	Gratton et al. (2003)
	–2.68	Fulbright (2000)
	–2.76	Bergemann & Cescutti (2010)
	–2.46	Bergemann & Cescutti (2010)
	–2.48	Bensby et al. (2014)
18Sco	0.02	Thevenin (1998)
	0.06	Neves et al. (2009)
	0.02	Neves et al. (2009)

Table B.7. continued.

Star	[Cr/H]	Reference
	0.085	Ramírez et al. (2009)
	0.03	Luck & Heiter (2005)
	–0.02	Galeev et al. (2004)
	–0.01	Gilli et al. (2006)
	0.06	da Silva et al. (2012)
	0.06	González Hernández et al. (2010)
Sun	–	–
alfCenA	0.25	Thevenin (1998)
	0.01	Bond et al. (2008)
	0.21	Gilli et al. (2006)
	0.24	da Silva et al. (2012)
	0.24	Neuforge-Verheecke & Magain (1997)
	0.26	Neuforge-Verheecke & Magain (1997)
	0.24	Porto de Mello et al. (2008)
HD 22879	–0.4	Thevenin (1998)
	–0.75	Bensby et al. (2005)
	–0.9	Reddy et al. (2006)
	–0.83	Neves et al. (2009)
	–0.77	Neves et al. (2009)
	–0.88	Gratton et al. (2003)
	–0.82	Gratton et al. (2003)
	–0.88	Fulbright (2000)
	–0.89	Zhang & Zhao (2006)
	–0.7	Bensby et al. (2014)
betHyi	0	Thevenin (1998)
	0.05	Bensby et al. (2014)
muAra	0.33	Bensby et al. (2005)
	0.3	Neves et al. (2009)
	0.27	Neves et al. (2009)
	0.14	Bond et al. (2008)
	0.21	Gilli et al. (2006)
	0.28	Bodaghee et al. (2003)
	0.3	da Silva et al. (2012)
	0.31	González Hernández et al. (2010)
	0.38	Bensby et al. (2014)
betVir	0.2	Thevenin (1998)
	0.17	Takeda (2007)
	0.12	Takeda (2007)
	0.09	Luck & Heiter (2005)
etaBoo	0.37	Takeda (2007)
	0.45	Takeda (2007)
	0.32	Luck & Heiter (2005)
HD 84937	–1.95	Thevenin (1998)
	–2.31	Gratton et al. (2003)
	–2.33	Gratton et al. (2003)
	–2.07	Fulbright (2000)
	–2.4	Bergemann & Cescutti (2010)
	–2.24	Bergemann & Cescutti (2010)
Procyon	0	Thevenin (1998)
	–0.04	Takeda (2007)
	0.03	Takeda (2007)
	–0.05	Luck & Heiter (2005)
HD 49933	–0.56	Takeda (2007)
	–0.36	Takeda (2007)

Table B.8. Literature compilation for manganese.

Star	[Mn/H]	Reference
psiPhe	–	–
alfCet	–	–
gamSge	–	–
alfTau	–	–
61CygB	0	Luck & Heiter (2005)
betAra	0.36	Luck (1979)
Arcturus	–0.73	Ramírez & Allende Prieto (2011)

Table B.8. continued.

Star	[Mn/H]	Reference
	–0.4	Thevenin (1998)
	–0.66	Luck & Heiter (2005)
HD 220009	–0.95	Allen & Porto de Mello (2011)
	–0.91	Smiljanic et al. (2007)
61CygA	–0.04	Luck & Heiter (2005)
muLeo	0.7	Luck & Heiter (2007)
HD 107328	–0.6	Luck & Heiter (2007)
	–0.1	Thevenin (1998)
HD 122563	–3.43	Hollek et al. (2011)
	–3.32	Hollek et al. (2011)
	–3	Westin et al. (2000)
	–3.1	Bergemann & Gehren (2008)
	–2.66	Bergemann & Gehren (2008)
Gmb1830	–1.57	Bergemann & Gehren (2008)
	–1.42	Bergemann & Gehren (2008)
	–1.52	Luck & Heiter (2005)
	–1.68	Gratton et al. (2003)
	–1.45	Thevenin (1998)
betGem	0.31	Luck & Heiter (2007)
	0.29	Luck & Heiter (2005)
	0.1	Thevenin (1998)
epsVir	0.22	Luck & Heiter (2007)
	–0.14	Allen & Porto de Mello (2011)
ksiHya	–	–
delEri	0.258	Adibekyan et al. (2012)
	0.13	Battistini & Bensby (2015)
	0.03	Battistini & Bensby (2015)
	0.44	Luck & Heiter (2005)
	0.17	Feltzing et al. (2007)
	–0.08	Thevenin (1998)
	0.28	Bodaghee et al. (2003)
	0.23	Gilli et al. (2006)
	0.28	Neves et al. (2009)
epsEri	–0.135	Adibekyan et al. (2012)
	–0.01	Luck & Heiter (2005)
	–0.17	Zhao et al. (2002)
	–0.09	Bodaghee et al. (2003)
	–0.21	Gilli et al. (2006)
	0.16	Gonzalez & Laws (2007)
	–0.12	Neves et al. (2009)
epsFor	–0.68	Battistini & Bensby (2015)
	0.09	Battistini & Bensby (2015)
	–0.88	Reddy et al. (2006)
	–0.76	Feltzing et al. (2007)
alfCenB	0.3	Gilli et al. (2006)
	0.26	Neuforge-Verheecke & Magain (1997)
	0.44	Porto de Mello et al. (2008)
muCas	–0.93	Takeda (2007)
	–1.09	Reddy et al. (2006)
	–1.12	Luck & Heiter (2005)
tauCet	–0.673	Adibekyan et al. (2012)
	–0.78	Luck & Heiter (2005)
	–0.73	Bodaghee et al. (2003)
	–0.6	Gilli et al. (2006)
	–0.66	Neves et al. (2009)
HD 140283	–2.65	Thevenin (1998)
	–3.22	Gratton et al. (2003)
18Sco	0	Thevenin (1998)
	0.05	Neves et al. (2009)
	0.046	Ramírez et al. (2009)
	–0.01	Luck & Heiter (2005)
	0.02	Galeev et al. (2004)
	0.08	Gilli et al. (2006)
	0.06	da Silva et al. (2012)
	0.04	González Hernández et al. (2010)
Sun	–	–

Table B.8. continued.

Star	[Mn/H]	Reference
alfCenA	0.34	Gilli et al. (2006)
	0.3	da Silva et al. (2012)
	0.23	Neuforge-Verheecke & Magain (1997)
	0.31	Porto de Mello et al. (2008)
HD 22879	–1.26	Reddy et al. (2006)
	–1.2	Neves et al. (2009)
	–1.02	Feltzing et al. (2007)
	–1.19	Zhang & Zhao (2006)
	–1.12	Nissen & Schuster (2011)
	–1.11	Battistini & Bensby (2015)
	0.16	Battistini & Bensby (2015)
betHyi	0	Thevenin (1998)
	–0.14	Battistini & Bensby (2015)
	0.04	Battistini & Bensby (2015)
muAra	0.38	Neves et al. (2009)
	0.62	Gonzalez & Laws (2007)
	0.37	Gilli et al. (2006)
	0.36	Feltzing et al. (2007)
	0.37	Bodaghee et al. (2003)
	0.34	da Silva et al. (2012)
	0.4	González Hernández et al. (2010)
	0.29	Battistini & Bensby (2015)
	0	Battistini & Bensby (2015)
betVir	0.01	Luck & Heiter (2005)
etaBoo	0.27	Luck & Heiter (2005)
HD 84937	–2.72	Gratton et al. (2003)
Procyon	0	Thevenin (1998)
	–0.17	Luck & Heiter (2005)
HD 49933	–	–

Table B.9. Literature compilation for cobalt.

Star	[Co/H]	Reference
psiPhe	–	–
alfCet	–	–
gamSge	–0.05	Boyarchuk et al. (1995)
alfTau	–0.05	Thevenin (1998)
61CygB	–0.14	Luck & Heiter (2005)
betAra	0.37	Luck (1979)
Arcturus	–0.43	Ramírez & Allende Prieto (2011)
	–0.2	Thevenin (1998)
	–0.36	Luck & Heiter (2005)
HD 220009	–0.6	Smiljanic et al. (2007)
	–0.49	McWilliam (1990)
61CygA	0.15	Mishenina et al. (2008)
	–0.14	Luck & Heiter (2005)
muLeo	0.45	McWilliam (1990)
	0.59	Luck & Heiter (2007)
HD 107328	–0.23	Luck & Heiter (2007)
	0	Thevenin (1998)
HD 122563	–2.79	Hollek et al. (2011)
	–2.42	Westin et al. (2000)
Gmb1830	–1.17	Takeda (2007)
	–1.45	Luck & Heiter (2005)
	–1.22	Thevenin (1998)
betGem	0.28	Allende Prieto et al. (2004)
	–0.06	McWilliam (1990)
	0.22	Luck & Heiter (2007)
	0.22	Luck & Heiter (2005)
	0	Thevenin (1998)
epsVir	0.14	McWilliam (1990)
	0.11	Luck & Heiter (2007)
	0.1	Thevenin (1998)
ksiHya	0	McWilliam (1990)
delEri	0.33	Allende Prieto et al. (2004)

Table B.9. continued.

Star	[Co/H]	Reference
	0.319	Adibekyan et al. (2012)
	0.34	Luck & Heiter (2005)
	0.21	Affer et al. (2005)
	0.36	Bodaghee et al. (2003)
	0.27	Gilli et al. (2006)
	0.33	Neves et al. (2009)
epsEri	–0.08	Allende Prieto et al. (2004)
	–0.173	Adibekyan et al. (2012)
	–0.06	Takeda (2007)
	–0.02	Luck & Heiter (2005)
	–0.09	Bodaghee et al. (2003)
	–0.19	Gilli et al. (2006)
	–0.11	Neves et al. (2009)
epsFor	–0.44	Battistini & Bensby (2015)
	0.08	Battistini & Bensby (2015)
	–0.51	Reddy et al. (2006)
	–0.3	Thorén et al. (2004)
alfCenB	0.5	Allende Prieto et al. (2004)
	0.4	Gilli et al. (2006)
	0.26	Neuforge-Verheecke & Magain (1997)
	0.31	Porto de Mello et al. (2008)
muCas	–0.65	Allende Prieto et al. (2004)
	–0.71	Takeda (2007)
	–0.68	Reddy et al. (2006)
	–0.7	Luck & Heiter (2005)
tauCet	–0.37	Allende Prieto et al. (2004)
	–0.447	Adibekyan et al. (2012)
	–0.33	Takeda (2007)
	–0.45	Luck & Heiter (2005)
	–0.4	Bodaghee et al. (2003)
	–0.41	Gilli et al. (2006)
	–0.41	Neves et al. (2009)
HD 140283	–2.3	Thevenin (1998)
18Sco	0.05	Neves et al. (2009)
	0	Allende Prieto et al. (2004)
	–0.01	Luck & Heiter (2005)
	–0.03	Galeev et al. (2004)
	0.05	Gilli et al. (2006)
	0.07	da Silva et al. (2012)
	0.03	González Hernández et al. (2010)
Sun	–	–
alfCenA	0.35	Thevenin (1998)
	0.2	Allende Prieto et al. (2004)
	0.38	Gilli et al. (2006)
	0.3	da Silva et al. (2012)
	0.28	Neuforge-Verheecke & Magain (1997)
	0.24	Porto de Mello et al. (2008)
HD 22879	–0.76	Reddy et al. (2006)
	–0.79	Neves et al. (2009)
	–0.68	Battistini & Bensby (2015)
	0.15	Battistini & Bensby (2015)
betHyi	–0.12	Allende Prieto et al. (2004)
	–0.04	Battistini & Bensby (2015)
	0.08	Battistini & Bensby (2015)
muAra	0.39	Neves et al. (2009)
	0.41	Gilli et al. (2006)
	0.39	Bodaghee et al. (2003)
	0.3	da Silva et al. (2012)
	0.38	González Hernández et al. (2010)
	0.28	Battistini & Bensby (2015)
	0.03	Battistini & Bensby (2015)
betVir	0.1	Allende Prieto et al. (2004)
	0.13	Takeda (2007)
	0.08	Luck & Heiter (2005)
etaBoo	0.35	Allende Prieto et al. (2004)
	0.39	Takeda (2007)

Table B.9. continued.

Star	[Co/H]	Reference
	0.36	Luck & Heiter (2005)
HD 84937	–	–
Procyon	0.15	Thevenin (1998)
	0.05	Allende Prieto et al. (2004)
	0	Takeda (2007)
	–0.08	Luck & Heiter (2005)
HD 49933	–0.54	Takeda (2007)

Table B.10. Literature compilation for nickel.

Star	[Ni/H]	Reference
psiPhe	–	–
alfCet	–	–
gamSge	–0.01	Boyarchuk et al. (1995)
alfTau	–0.1	Thevenin (1998)
61CygB	–0.15	Luck & Heiter (2005)
betAra	0.34	Luck (1979)
Arcturus	–0.46	Ramírez & Allende Prieto (2011)
	–0.35	Thevenin (1998)
	–0.48	Luck & Heiter (2005)
HD 220009	–0.73	Smiljanic et al. (2007)
	–0.82	McWilliam (1990)
61CygA	0.04	Mishenina et al. (2008)
	–0.47	Affer et al. (2005)
	–0.19	Luck & Heiter (2005)
muLeo	0.04	McWilliam (1990)
	0.37	Luck & Heiter (2007)
	0.35	Smith & Ruck (2000)
	0.3	Thevenin (1998)
HD 107328	–0.77	McWilliam (1990)
	–0.38	Luck & Heiter (2007)
	–0.2	Thevenin (1998)
HD 122563	–2.67	Fulbright (2000)
	–2.79	Hollek et al. (2011)
	–2.7	Westin et al. (2000)
Gmb1830	–1.32	Takeda (2007)
	–1.52	Fulbright (2000)
	–1.36	Clementini et al. (1999)
	–1.35	Kotoneva et al. (2006)
	–1.47	Valenti & Fischer (2005)
	–1.28	Luck & Heiter (2005)
	–1.41	Gratton et al. (2003)
	–1.35	Thevenin (1998)
betGem	0.22	Allende Prieto et al. (2004)
	–0.3	McWilliam (1990)
	0.16	Luck & Heiter (2007)
	0.15	Luck & Heiter (2005)
	–0.07	Thevenin (1998)
epsVir	–0.15	McWilliam (1990)
	0.13	Luck & Heiter (2007)
	0.1	Thevenin (1998)
ksiHya	–0.22	McWilliam (1990)
	0.18	Bruntt et al. (2010)
delEri	0.25	Allende Prieto et al. (2004)
	0.152	Adibekyan et al. (2012)
	0.21	Bruntt et al. (2010)
	0.14	Valenti & Fischer (2005)
	0.25	Luck & Heiter (2005)
	0.12	Affer et al. (2005)
	0.31	Bensby et al. (2014)
	–0.01	Thorén et al. (2004)
	0.31	Bensby et al. (2003)
	0.02	Thevenin (1998)
	0.21	Bodaghee et al. (2003)

Table B.10. continued.

Star	[Ni/H]	Reference
	0.31	Bensby et al. (2005)
	0.13	Gilli et al. (2006)
	0.16	Neves et al. (2009)
	0.16	Delgado Mena et al. (2010)
epsEri	–0.06	Allende Prieto et al. (2004)
	–0.156	Adibekyan et al. (2012)
	–0.02	Takeda (2007)
	–0.11	Valenti & Fischer (2005)
	–0.07	Luck & Heiter (2005)
	–0.15	Mishenina et al. (2004)
	–0.2	Zhao et al. (2002)
	–0.16	Bodaghee et al. (2003)
	–0.19	Gonzalez et al. (2001)
	–0.25	Gilli et al. (2006)
	–0.13	Gonzalez & Laws (2007)
	–0.15	Neves et al. (2009)
	–0.15	Delgado Mena et al. (2010)
epsFor	–0.65	Fulbright (2000)
	–0.51	Bond et al. (2006)
	–0.6	Reddy et al. (2006)
	–0.43	Bensby et al. (2014)
	–0.52	Valenti & Fischer (2005)
	–0.35	Thorén et al. (2004)
	–0.53	Bensby et al. (2003)
	–0.88	Gratton et al. (2003)
	–0.53	Bensby et al. (2005)
	–0.51	Bond et al. (2008)
alfCenB	0.25	Valenti & Fischer (2005)
	0.4	Allende Prieto et al. (2004)
	0.24	Gilli et al. (2006)
	0.3	Neuforge-Verheecke & Magain (1997)
	0.36	Porto de Mello et al. (2008)
muCas	–0.75	Allende Prieto et al. (2004)
	–0.81	Takeda (2007)
	–0.9	Fulbright (2000)
	–0.74	Reddy et al. (2006)
	–0.83	Luck & Heiter (2005)
	–0.94	Mishenina et al. (2004)
	–0.93	Gratton et al. (2003)
tauCet	–0.44	Allende Prieto et al. (2004)
	–6.254	Pavlenko et al. (2012)
	–0.513	Adibekyan et al. (2012)
	–0.46	Bruntt et al. (2010)
	–0.4	Takeda (2007)
	–0.43	Bond et al. (2006)
	–0.49	Valenti & Fischer (2005)
	–0.55	Luck & Heiter (2005)
	–0.5	Bodaghee et al. (2003)
	–0.55	Gilli et al. (2006)
	–0.43	Bond et al. (2008)
	–0.5	Neves et al. (2009)
	–0.5	Delgado Mena et al. (2010)
HD 140283	–2.45	Thevenin (1998)
	–2.5	Gratton et al. (2003)
	–2.37	Fulbright (2000)
	–2.48	Bensby et al. (2014)
18Sco	0.01	Valenti & Fischer (2005)
	0.08	Thevenin (1998)
	0.04	Neves et al. (2009)
	0.04	Allende Prieto et al. (2004)
	0.04	Mishenina et al. (2004)
	0.029	Ramírez et al. (2009)
	0.02	Luck & Heiter (2005)
	–0.02	Galeev et al. (2004)
	0.02	Gilli et al. (2006)

Table B.10. continued.

Star	[Ni/H]	Reference
	0.06	da Silva et al. (2012)
	0.04	Delgado Mena et al. (2010)
	0.04	González Hernández et al. (2010)
Sun	–	–
alfCenA	0.26	Valenti & Fischer (2005)
	0.28	Thevenin (1998)
	0.2	Edvardsson et al. (1993)
	0.06	Bond et al. (2008)
	0.2	Allende Prieto et al. (2004)
	0.31	Gilli et al. (2006)
	0.27	da Silva et al. (2012)
	0.3	Neuforge-Verheecke & Magain (1997)
	0.34	Porto de Mello et al. (2008)
HD 22879	–0.95	Valenti & Fischer (2005)
	–0.75	Thevenin (1998)
	–0.83	Bensby et al. (2005)
	–0.83	Edvardsson et al. (1993)
	–0.89	Reddy et al. (2006)
	–0.83	Neves et al. (2009)
	–0.84	Gratton et al. (2003)
	–0.75	Mishenina et al. (2004)
	–0.89	Fulbright (2000)
	–0.88	Zhang & Zhao (2006)
	–0.83	Nissen & Schuster (1997)
	–0.7	Bensby et al. (2014)
betHyi	–0.08	Valenti & Fischer (2005)
	–0.08	Thevenin (1998)
	–0.12	Allende Prieto et al. (2004)
	0.05	Bensby et al. (2014)
muAra	0.34	Valenti & Fischer (2005)
	0.4	Bensby et al. (2005)
	0.35	Neves et al. (2009)
	0.18	Bond et al. (2008)
	0.31	Gonzalez et al. (2001)
	0.35	Gonzalez & Laws (2007)
	0.3	Gilli et al. (2006)
	0.34	Bodaghee et al. (2003)
	0.3	da Silva et al. (2012)
	0.35	Delgado Mena et al. (2010)
	0.33	González Hernández et al. (2010)
	0.38	Bensby et al. (2014)
betVir	0.19	Valenti & Fischer (2005)
	0.25	Thevenin (1998)
	0.16	Edvardsson et al. (1993)
	0.15	Allende Prieto et al. (2004)
	0.17	Mishenina et al. (2004)
	0.14	Takeda (2007)
	0.1	Luck & Heiter (2005)
etaBoo	0.4	Thevenin (1998)
	0.3	Edvardsson et al. (1993)
	0.3	Allende Prieto et al. (2004)
	0.35	Takeda (2007)
	0.34	Luck & Heiter (2005)
HD 84937	–2.1	Thevenin (1998)
	–2.21	Gratton et al. (2003)
	–2.05	Fulbright (2000)
Procyon	–0.05	Valenti & Fischer (2005)
	0.08	Thevenin (1998)
	0.02	Edvardsson et al. (1993)
	0.07	Allende Prieto et al. (2004)
	–0.01	Takeda (2007)
	–0.05	Luck & Heiter (2005)
HD 49933	–0.38	Thevenin (1998)
	–0.41	Edvardsson et al. (1993)
	–0.51	Takeda (2007)

References

Adibekyan, V. Z., Sousa, S. G., Santos, N. C., et al. 2012, A&A, 545, A32
Affer, L., Micela, G., Morel, T., Sanz-Forcada, J., & Favata, F. 2005, A&A, 433, 647
Allen, D. M., & Porto de Mello, G. F. 2011, A&A, 525, A63
Allende Prieto, C., Barklem, P. S., Lambert, D. L., & Cunha, K. 2004, A&A, 420, 183
Allende Prieto, C., Majewski, S. R., Schiavon, R., et al. 2008, Astron. Nachr., 329, 1018
Alvarez, R., & Plez, B. 1998, A&A, 330, 1109
Alves-Brito, A., Meléndez, J., Asplund, M., Ramírez, I., & Yong, D. 2010, A&A, 513, A35
Asplund, M., Grevesse, N., Sauval, A. J., & Scott, P. 2009, ARA&A, 47, 481
Bai, G. S., Zhao, G., Chen, Y. Q., et al. 2004, A&A, 425, 671
Bailer-Jones, C. A. L., Andrae, R., Arcay, B., et al. 2013, A&A, 559, A74
Barbuy, B., Hill, V., Zoccali, M., et al. 2013, A&A, 559, A5
Battistini, C., & Bensby, T. 2015, A&A, 577, A9
Bensby, T., Feltzing, S., & Lundström, I. 2003, A&A, 410, 527
Bensby, T., Feltzing, S., Lundström, I., & Ilyin, I. 2005, A&A, 433, 185
Bensby, T., Feltzing, S., & Oey, M. S. 2014, A&A, 562, A71
Bergemann, M., & Cescutti, G. 2010, A&A, 522, A9
Bergemann, M., & Gehren, T. 2008, A&A, 492, 823
Bergemann, M., Pickering, J. C., & Gehren, T. 2010, MNRAS, 401, 1334
Bergemann, M., Kudritzki, R.-P., Würl, M., et al. 2013, ApJ, 764, 115
Bergemann, M., Ruchti, G. R., Serenelli, A., et al. 2014, A&A, 565, A89
Bijaoui, A., Recio-Blanco, A., de Laverny, P., & Ordenovic, C. 2012, Stat. Met., 9, 55
Blanco-Cuaresma, S., Soubiran, C., Heiter, U., & Jofré, P. 2014a, A&A, 569, A111
Blanco-Cuaresma, S., Soubiran, C., Jofré, P., & Heiter, U. 2014b, A&A, 566, A98
Bodaghee, A., Santos, N. C., Israelian, G., & Mayor, M. 2003, A&A, 404, 715
Boeche, C., Siebert, A., Piffl, T., et al. 2014, A&A, 568, A71
Bond, J. C., Tinney, C. G., Butler, R. P., et al. 2006, MNRAS, 370, 163
Bond, J. C., Lauretta, D. S., Tinney, C. G., et al. 2008, ApJ, 682, 1234
Boyarchuk, A. A., Antipova, L. I., Boyarchuk, M. E., & Savanov, I. S. 1995, AZh, 72, 864
Bravo, E., & Martínez-Pinedo, G. 2012, Phys. Rev. C, 85, 055805
Britavskiy, N. E., Andrievsky, S. M., Tsymbal, V. V., et al. 2012, A&A, 542, A104
Brown, J. A., Tomkin, J., & Lambert, D. L. 1983, ApJ, 265, L93
Bruntt, H., Bedding, T. R., Quirion, P.-O., et al. 2010, MNRAS, 405, 1907
Cantat-Gaudin, T., Donati, P., Pancino, E., et al. 2014, A&A, 562, A10
Carretta, E., Gratton, R. G., & Sneden, C. 2000, A&A, 356, 238
Cayrel, R., Depagne, E., Spite, M., et al. 2004, A&A, 416, 1117
Chieffi, A., & Limongi, M. 2002, ApJ, 577, 281
Chou, M.-Y., Cunha, K., Majewski, S. R., et al. 2010, ApJ, 708, 1290
Clementini, G., Gratton, R. G., Carretta, E., & Sneden, C. 1999, MNRAS, 302, 22
Creevey, O. L., Thévenin, F., Berio, P., et al. 2015, A&A, 575, A26
da Silva, R., Porto de Mello, G. F., Milone, A. C., et al. 2012, A&A, 542, A84
de Laverny, P., Recio-Blanco, A., Worley, C. C., & Plez, B. 2012, A&A, 544, A126
de Laverny, P., Recio-Blanco, A., Worley, C. C., et al. 2013, The Messenger, 153, 18
Delgado Mena, E., Israelian, G., González Hernández, J. I., et al. 2010, ApJ, 725, 2349
De Pascale, M., Worley, C. C., de Laverny, P., et al. 2014, A&A, 570, A68
De Silva, G. M., Freeman, K. C., Bland-Hawthorn, J., et al. 2015, MNRAS, 449, 2604
Drawin, H.-W. 1968, Z. Phys., 211, 404
Edvardsson, B., Andersen, J., Gustafsson, B., et al. 1993, A&A, 275, 101
Feltzing, S., & Chiba, M. 2013, New Astron. Rev., 57, 80
Feltzing, S., Fohlman, M., & Bensby, T. 2007, A&A, 467, 665
Fernández-Alvar, E., Allende Prieto, C., Schlesinger, K. J., et al. 2015, A&A, 577, A81
Francois, P. 1986, A&A, 160, 264
Fuhrmann, K. 2011, MNRAS, 414, 2893
Fulbright, J. P. 2000, AJ, 120, 1841
Fulbright, J. P., McWilliam, A., & Rich, R. M. 2007, ApJ, 661, 1152
Galeev, A. I., Bikmaev, I. F., Musaev, F. A., & Galazutdinov, G. A. 2004, Astron. Rep., 48, 492
Gehren, T., Shi, J. R., Zhang, H. W., Zhao, G., & Korn, A. J. 2006, A&A, 451, 1065
Gilli, G., Israelian, G., Ecuvillon, A., Santos, N. C., & Mayor, M. 2006, A&A, 449, 723

Gilmore, G., Randich, S., Asplund, M., et al. 2012, The Messenger, 147, 25
Gonzalez, G., & Laws, C. 2007, MNRAS, 378, 1141
Gonzalez, G., Laws, C., Tyagi, S., & Reddy, B. E. 2001, AJ, 121, 432
González Hernández, J. I., Israelian, G., Santos, N. C., et al. 2010, ApJ, 720, 1592
Gratton, R. G. 1989, A&A, 208, 171
Gratton, R. G., & Sneden, C. 1991, A&A, 241, 501
Gratton, R. G., Carretta, E., Eriksson, K., & Gustafsson, B. 1999, A&A, 350, 955
Gratton, R. G., Carretta, E., Claudi, R., Lucatello, S., & Barbieri, M. 2003, A&A, 404, 187
Gray, D. F. 1992, The observation and analysis of stellar photospheres (Cambridge Univ. Press)
Grevesse, N., Asplund, M., & Sauval, A. J. 2007, Space Sci. Rev., 130, 105
Gustafsson, B., Edvardsson, B., Eriksson, K., et al. 2008, A&A, 486, 951
Hawkins, K., Jofré, P., Gilmore, G., & Masseron, T. 2014, MNRAS, 445, 2575
Hawkins, K., Jofré, P., Masseron, T., & Gilmore, G. 2015, MNRAS, 453, 758
Heiter, U., Jofré, P., Gustafsson, B., et al. 2015a, A&A, 582, A49
Heiter, U., Lind, K., Asplund, M., et al. 2015b, Phys. Scr., 90, 054010
Hinkle, K., Wallace, L., Valenti, J., & Harmer, D. 2000, Visible and Near Infrared Atlas of the Arcturus Spectrum 3727–9300 Å
Hinkel, N. R., Timmes, F. X., Young, P. A., Pagano, M. D., & Turnbull, M. C. 2014, AJ, 148, 54
Hollek, J. K., Frebel, A., Roederer, I. U., et al. 2011, ApJ, 742, 54
Holtzman, J. A., Shetrone, M., Johnson, J. A., et al. 2015, AJ, submitted [arXiv:1501.04110]
Ishigaki, M. N., Aoki, W., & Chiba, M. 2013, ApJ, 771, 67
Ivezić, Ž., Beers, T. C., & Jurić, M. 2012, ARA&A, 50, 251
Jackson-Jones, R., Jofré, P., Hawkins, K., et al. 2014, A&A, 571, L5
Jofré, P., Panter, B., Hansen, C. J., & Weiss, A. 2010, A&A, 517, A57
Jofré, P., Heiter, U., Blanco-Cuaresma, S., & Soubiran, C. 2014a, Astron. Soc. India Conf. Ser., 11, 159
Jofré, P., Heiter, U., Soubiran, C., et al. 2014b, A&A, 564, A133
Jonsell, K., Edvardsson, B., Gustafsson, B., et al. 2005, A&A, 440, 321
Kang, W., & Lee, S.-G. 2012, MNRAS, 425, 3162
Kobayashi, C., & Nakasato, N. 2011, ApJ, 729, 16
Kordopatis, G. 2014, in SF2A-2014: Proc. of the Annual meeting of the French Society of Astronomy and Astrophysics, eds. J. Ballet, F. Martins, F. Bournaud, R. Monier, & C. Reylé, 431
Kordopatis, G., Recio-Blanco, A., de Laverny, P., et al. 2011, A&A, 535, A106
Kotoneva, E., Shi, J. R., Zhao, G., & Liu, Y. J. 2006, A&A, 454, 833
Kurucz, R. L. 2005, Mem. Soc. Astron. It. Suppl., 8, 14
Lai, D. K., Bolte, M., Johnson, J. A., et al. 2008, ApJ, 681, 1524
Lawler, J. E., Wood, M. P., Den Hartog, E. A., et al. 2014, ApJS, 215, 20
Lee, Y. S., Beers, T. C., Sivarani, T., et al. 2008, AJ, 136, 2022
Lee, Y. S., Beers, T. C., Allende Prieto, C., et al. 2011, AJ, 141, 90
Li, X., Wu, Q. M. J., Luo, A., et al. 2014, ApJ, 790, 105
Lind, K., Melendez, J., Asplund, M., Collet, R., & Magic, Z. 2013, A&A, 554, A96
Liu, C., Ruchti, G., Feltzing, S., et al. 2015, A&A, 575, A51
Luck, R. E. 1979, ApJ, 232, 797
Luck, R. E., & Heiter, U. 2005, AJ, 129, 1063
Luck, R. E., & Heiter, U. 2007, AJ, 133, 2464
Magrini, L., Randich, S., Friel, E., et al. 2013, A&A, 558, A38
Magrini, L., Randich, S., Romano, D., et al. 2014, A&A, 563, A44
Mashonkina, L., Zhao, G., Gehren, T., et al. 2008, A&A, 478, 529
McWilliam, A. 1990, ApJS, 74, 1075
Meléndez, J., Bergemann, M., Cohen, J. G., et al. 2012, A&A, 543, A29
Meléndez, J., Ramírez, I., Karakas, A. I., et al. 2014, ApJ, 791, 14
Mikolaitis, Š., Hill, V., Recio-Blanco, A., et al. 2014, A&A, 572, A33
Milone, A. D. C., Sansom, A. E., & Sánchez-Blázquez, P. 2011, MNRAS, 414, 1227
Mishenina, T. V., & Kovtyukh, V. V. 2001, A&A, 370, 951
Mishenina, T. V., Soubiran, C., Kovtyukh, V. V., & Korotin, S. A. 2004, A&A, 418, 551
Mishenina, T. V., Soubiran, C., Bienaymé, O., et al. 2008, A&A, 489, 923
Mucciarelli, A., Pancino, E., Lovisi, L., Ferraro, F. R., & Lapenna, E. 2013, ApJ, 766, 78
Neuforge-Verheecke, C., & Magain, P. 1997, A&A, 328, 261
Neves, V., Santos, N. C., Sousa, S. G., Correia, A. C. M., & Israelian, G. 2009, A&A, 497, 563
Nidever, D. L., Bovy, J., Bird, J. C., et al. 2014, ApJ, 796, 38
Nissen, P. E. 2015, A&A, 579, A52
Nissen, P. E., & Schuster, W. J. 1997, A&A, 326, 751
Nissen, P. E., & Schuster, W. J. 2010, A&A, 511, L10
Nissen, P. E., & Schuster, W. J. 2011, A&A, 530, A15
Nomoto, K., Kobayashi, C., & Tominaga, N. 2013, ARA&A, 51, 457
North, P., Cescutti, G., Jablonka, P., et al. 2012, A&A, 541, A45
Osorio, Y., Barklem, P. S., Lind, K., et al. 2015, A&A, 579, A53
Pagel, B. E. J. 1997, Nucleosynthesis and Chemical Evolution of Galaxies (Cambridge Univ. Press)
Pavlenko, Y. V., Jenkins, J. S., Jones, H. R. A., Ivanyuk, O., & Pinfield, D. J. 2012, MNRAS, 422, 542
Petit, P., Louge, T., Théado, S., et al. 2014, PASP, 126, 469
Plez, B. 2012, Astrophysics Source Code Library [record ascl:1205.004]
Porto de Mello, G. F., Lyra, W., & Keller, G. R. 2008, A&A, 488, 653
Preston, G. W., & Sneden, C. 2000, AJ, 120, 1014
Prochaska, J. X., & McWilliam, A. 2000, ApJ, 537, L57
Ramírez, I., & Allende Prieto, C. 2011, ApJ, 743, 135
Ramírez, I., Meléndez, J., & Asplund, M. 2009, A&A, 508, L17
Ramírez, I., Allende Prieto, C., & Lambert, D. L. 2013, ApJ, 764, 78
Randich, S., Gilmore, G., & Gaia-ESO Consortium. 2013, The Messenger, 154, 47
Reddy, B. E., Lambert, D. L., & Allende Prieto, C. 2006, MNRAS, 367, 1329
Schönrich, R., & Bergemann, M. 2014, MNRAS, 443, 698
Scott, P., Asplund, M., Grevesse, N., Bergemann, M., & Sauval, A. J. 2015, A&A, 573, A26
Shi, J. R., Takada-Hidai, M., Takeda, Y., et al. 2012, ApJ, 755, 36
Smiljanic, R., Porto de Mello, G. F., & da Silva, L. 2007, A&A, 468, 679
Smiljanic, R., Korn, A. J., Bergemann, M., et al. 2014, A&A, 570, A122
Smith, G., & Ruck, M. J. 2000, A&A, 356, 570
Sneden, C. A. 1973, Ph.D. Thesis, The University of Texas at Austin
Sousa, S. G., Santos, N. C., Israelian, G., Mayor, M., & Monteiro, M. J. P. F. G. 2007, A&A, 469, 783
Steinmetz, M., Zwitter, T., Siebert, A., et al. 2006, AJ, 132, 1645
Stetson, P. B., & Pancino, E. 2008, PASP, 120, 1332
Tabernero, H. M., Montes, D., & González Hernández, J. I. 2012, A&A, 547, A13
Takeda, Y. 2007, PASJ, 59, 335
Thevenin, F. 1998, VizieR Online Data Catalog, III/193
Thorén, P., Edvardsson, B., & Gustafsson, B. 2004, A&A, 425, 187
Timmes, F. X., Woosley, S. E., & Weaver, T. A. 1995, ApJS, 98, 617
Tsujimoto, T., Nomoto, K., Yoshii, Y., et al. 1995, MNRAS, 277, 945
Valenti, J. A., & Fischer, D. A. 2005, ApJS, 159, 141
VandenBerg, D. A., Bond, H. E., Nelan, E. P., et al. 2014, ApJ, 792, 110
Venn, K. A., Irwin, M., Shetrone, M. D., et al. 2004, AJ, 128, 1177
Vieytes, M. C., & Fontenla, J. M. 2013, ApJ, 769, 103
Westin, J., Sneden, C., Gustafsson, B., & Cowan, J. J. 2000, ApJ, 530, 783
Woosley, S. E., & Weaver, T. A. 1995, ApJS, 101, 181
Worley, C. C., Cottrell, P. L., Freeman, K. C., & Wylie-de Boer, E. C. 2009, MNRAS, 400, 1039
Zboril, M., & Byrne, P. B. 1998, MNRAS, 299, 753
Zhang, H. W., & Zhao, G. 2006, A&A, 449, 127
Zhang, H. W., Gehren, T., & Zhao, G. 2008, A&A, 481, 489
Zhao, G., & Gehren, T. 2000, A&A, 362, 1077
Zhao, G., Chen, Y. Q., Qiu, H. M., & Li, Z. W. 2002, AJ, 124, 2224